University of Pennsylvania
ScholarlyCommons

Publicly Accessible Penn Dissertations

Fall 12-22-2010

The Development, Characterization and Implementation of a Reactive Oxygen Species-Responsive Ratiometric Bioluminescent Reporter and Its Use As A Sensor for Programmed Cell Death

Julie Czupryna
University of Pennsylvania, czupryna@seas.upenn.edu

Follow this and additional works at: http://repository.upenn.edu/edissertations

 Part of the Bioimaging and Biomedical Optics Commons

Recommended Citation
Czupryna, Julie, "The Development, Characterization and Implementation of a Reactive Oxygen Species-Responsive Ratiometric Bioluminescent Reporter and Its Use As A Sensor for Programmed Cell Death" (2010). *Publicly Accessible Penn Dissertations*. 461.
http://repository.upenn.edu/edissertations/461

This paper is posted at ScholarlyCommons. http://repository.upenn.edu/edissertations/461
For more information, please contact libraryrepository@pobox.upenn.edu.

The Development, Characterization and Implementation of a Reactive Oxygen Species-Responsive Ratiometric Bioluminescent Reporter and Its Use As A Sensor for Programmed Cell Death

Abstract
The process of programmed cell death (PCD) is a prevalent area of scientific research and is characterized by a highly complex proteolytic cascade. PCD is involved in development, homeostasis and the immune response. Further, unregulated PCD has been implicated in various, often, devastating pathologies including cancer, autoimmune diseases and neurodegenerative disorders. The importance of PCD in human health and disease has led to the widespread utilization of genetically encoded reporters for the non-invasive imaging of PCD in vitro and in vivo; however, it is currently not well understood whether the reporters themselves are susceptible to inactivation and/or degradation during PCD. Molecular reporters that do exhibit an unexpected sensitivity to their environment could lead to ambiguous findings and/or inaccurate conclusions. Interestingly, we have found that the commonly used bioluminescent reporter protein, Firefly Luciferase (fLuc), exhibits a rapid loss in activity in cells undergoing PCD. In contrast, a variant of Renilla Luciferase, RLuc8, demonstrated quite stable activity under the same conditions. Following extensive inhibition analyses, it was determined that reactive oxygen species (ROS), particularly hydrogen peroxide (H2O2), play a large role in the disparity between fLuc and RLuc8 activity, in cells undergoing PCD. ROS are natural byproducts of oxygen metabolism that are normally regulated by antioxidants; if the balance between ROS and antioxidants becomes skewed, cells can enter a state of 'oxidative stress.' It has been reported that many cases of PCD are associated with elevated levels of ROS. Consistent with these reports, when fLuc and RLuc8 were intracellularly coexpressed, it was found that the bioluminescence ratio, RLuc8:fLuc, served as a useful metric to report on caspase-dependent and –independent PCD in vitro and in vivo in an ROS-mediated manner. It is envisioned that this ratiometric reporter could have widespread impact on research endeavors involving the aforementioned maladies, including therapeutic development and evaluation.

Degree Type
Dissertation

Degree Name
Doctor of Philosophy (PhD)

Graduate Group
Bioengineering

First Advisor
Andrew Tsourkas

Keywords
bioluminescence, ROS, PCD

This dissertation is available at ScholarlyCommons: http://repository.upenn.edu/edissertations/461

Subject Categories
Bioimaging and Biomedical Optics | Biomedical Engineering and Bioengineering

This dissertation is available at ScholarlyCommons: http://repository.upenn.edu/edissertations/461

THE DEVELOPMENT, CHARACTERIZATION AND IMPLEMENTATION OF A REACTIVE OXYGEN SPECIES-RESPONSIVE RATIOMETRIC BIOLUMINESCENT REPORTER AND ITS USE AS A SENSOR FOR PROGRAMMED CELL DEATH

Julie Czupryna

A DISSERTATION

in

Bioengineering

Presented to the Faculties of the University of Pennsylvania

in

Partial Fulfillment of the Requirements for the

Degree of Doctor of Philosophy

2010

_____

Andrew Tsourkas, Ph.D. – Dissertation Supervisor

_____

Susan S. Margulies, Ph.D. – Graduate Group Chairperson

Dissertation Committee

Casim A. Sarkar, Ph.D. – Committee Chair

Jason A. Burdick, Ph.D.

Jim Delikatny, Ph.D.

This thesis is dedicated to my Babci, Eleanor Czupryna

&

to my sister-in-law Kirsten Czupryna

These two women have inspired me more than they ever knew and I can only hope that they are as proud of me as I am of them….

Acknowledgements

First, I would like to thank my thesis advisor, Dr. Andrew Tsourkas, who has provided me with the knowledge, encouragement and skill set required for this rigorous endeavor. His enthusiasm for molecular imaging has never waned since my first day in the lab and because of that, I have been inspired to become a better scientist and to continue performing research in this field. Throughout my time here, Dr. Tsourkas has been a constant source of academic, personal and professional support and I cannot express how much it is appreciated.

I would also like to thank the members of my thesis committee: Dr. Casim Sarkar, Dr. Jason Burdick and Dr. Jim Delikatny. Dr. Sarkar has been especially helpful regarding many of the protein studies involved in this work. Dr. Burdick was a member of my qualifier committee, and has been a great source of guidance since (way back) then. Dr. Delikatny is a relatively new member of my committee, but experiences with him at molecular imaging conferences have helped me gain new perspectives on the field of molecular imaging.

There are many members of the Tsourkas Lab that I have to thank. I would especially like to thank Dr. Daniel Thorek, my desk buddy from day one, who became one of my best friends here and who I can honestly say I probably could not have gotten through grad school without. Dr. Antony Chen was the third member of the original three who started in the Tsourkas lab and his work ethic was inspiring. I would also like to thank Drew Elias, Sam Crayton, Rob Warden, Zhiliang Cheng, Ching-Hui Huang, Ajlan Al-Zaki and Xuemei Zhang. Also, I would like to thank members of the Hammer

lab who have provided a source of enjoyment both in and out of the lab, Dalia Levine, Randi Saunders and Aaron Dominguez.

My friends from high school, college and here at Penn have been such a blessing and I cannot thank them enough. The friendships of Mary Lynn and Renee, both of whom I've known since kindergarten, and Shelly, Andrea and Katrina from college have provided a constant supply of support and laughter. My friends from Penn, Annie, Cathy, Steph and Derek deserve many thanks for all of the enjoyable experiences I've been lucky enough to have with them, especially cookouts, tailgating and Phillies games. Thanks to my knitting club (wine drinking club?) friends, Jamie, Elena, April, Shannon, Lara and Heather. I would especially like to thank Ross for sharing my sense of humor and quirkiness, for being a guinea pig during my cooking adventures and most importantly for his unwavering encouragement throughout my final year of grad school.

Finally, I would like to thank my amazing family for their support, love, generosity and encouragement during this process. Thanks to my godmother Aunt Doreen, Aunt Debby, Uncle Rob, Aunt Nancy, Uncle Kenny, cousins Kim and Missi and nephew Michael. I have shared many fun times in Philly with my Uncle Nick, Aunt Patti and cousin Andy and I thank them for everything they've done for me. Thank you to my brother Steve, who has been there for me no matter what. Finally, the unconditional love and support of my parents, Tim and Paula, are the reasons why I am where I am today, and I am eternally grateful. I love you all.

ABSTRACT

THE DEVELOPMENT, CHARACTERIZATION AND IMPLEMENTATION OF A REACTIVE OXYGEN SPECIES-RESPONSIVE RATIOMETRIC BIOLUMINESCENT REPORTER AND ITS USE AS A SENSOR FOR PROGRAMMED CELL DEATH

Julie Czupryna

Advisor: Andrew Tsourkas, Ph.D.

The process of programmed cell death (PCD) is a prevalent area of scientific research and is characterized by a highly complex proteolytic cascade. PCD is involved in development, homeostasis and the immune response. Further, unregulated PCD has been implicated in various, often, devastating pathologies including cancer, autoimmune diseases and neurodegenerative disorders. The importance of PCD in human health and disease has led to the widespread utilization of genetically encoded reporters for the non-invasive imaging of PCD *in vitro* and *in vivo*; however, it is currently not well understood whether the reporters themselves are susceptible to inactivation and/or degradation during PCD. Molecular reporters that do exhibit an unexpected sensitivity to their environment could lead to ambiguous findings and/or inaccurate conclusions. Interestingly, we have found that the commonly used bioluminescent reporter protein, Firefly Luciferase (fLuc),

exhibits a rapid loss in activity in cells undergoing PCD. In contrast, a variant of Renilla Luciferase, RLuc8, demonstrated quite stable activity under the same conditions. Following extensive inhibition analyses, it was determined that reactive oxygen species (ROS), particularly hydrogen peroxide (H_2O_2), play a large role in the disparity between fLuc and RLuc8 activity, in cells undergoing PCD. ROS are natural byproducts of oxygen metabolism that are normally regulated by antioxidants; if the balance between ROS and antioxidants becomes skewed, cells can enter a state of 'oxidative stress.' It has been reported that many cases of PCD are associated with elevated levels of ROS. Consistent with these reports, when fLuc and RLuc8 were intracellularly coexpressed, it was found that the bioluminescence ratio, RLuc8:fLuc, served as a useful metric to report on caspase-dependent and –independent PCD *in vitro* and *in vivo* in an ROS-mediated manner. It is envisioned that this ratiometric reporter could have widespread impact on research endeavors involving the aforementioned maladies, including therapeutic development and evaluation.

TABLE OF CONTENTS

Chapter 1: Introduction to bioluminescence imaging, programmed cell death and reactive oxygen species 1

1.1 Introduction 1

1.2 Background 2

1.2.1 Bioluminescence Imaging 2

1.2.1a Overview 2

1.2.1b Types of luciferases and their substrates 3

1.2.1c BLI: general considerations 5

1.2.2 Programmed Cell Death 8

1.2.2a Overview 8

1.2.2b Current Sensors for Apoptosis 12

1.2.2c Current Sensors for Caspase-Independent PCD 22

1.2.3 Reactive Oxygen Species, Oxidative Stress and Cell Death 23

1.2.3a Overview 23

1.2.3b Protein modification, damage and degradation by ROS 24

1.2.3c Common Probes for Imaging ROS/Oxidative Stress 28

1.2.4 The Role of ROS/Oxidative Stress in PCD 31

1.3 References 32

Chapter 2: Proposed Strategy and Experimental Methods 53

2.1 Proposed Strategy 53

2.2 Materials and Methods 55

2.2.1 Preliminary transient transfection studies 55

2.2.2 RBS plasmid vector construction 56
2.2.3 Reverse RBS plasmid vector construction 57
2.2.4 Cell culture 58
2.2.5 Lentiviral particle production and stable cell line creation 59
2.2.6 Cellular stress and inhibition assays 59
2.2.7 Cellular bioluminescence assays 60
2.2.8 Cellular bioluminescence imaging 61
2.2.9 Cellular bioluminescence image analysis 61
2.2.10 Cell death assays 62
2.2.11 Proteasome inhibition control assay 62
2.2.12 Protease inhibition control assays 63
2.2.13 Superoxide ($O_2^{\bullet-}$) scavenger control assay 64
2.2.14 Hydroxyl Radical ($^{\bullet}OH$) scavenger/inhibitor control assay 64
2.2.15 Hydrogen peroxide (H_2O_2)-related inhibitor control assays 65
2.2.16 Quantitative real-time PCR (qRT-PCR) 66
2.2.17 Western blot analysis 66
2.2.18 Intracellular hydrogen peroxide detection 67
2.2.19 RLuc8 and fLuc protein purification 68
2.2.20 *In vitro* bioluminescence assays on purified proteins 69
2.2.21 SDS-PAGE gels on purified proteins treated with H_2O_2 70
2.2.22 Cellular protein carbonylation detection 70
2.2.23 Purified protein carbonylation detection 71
2.2.24 Animal imaging 72

2.2.25 Animal image analysis 73
2.3 References 74
Chapter 3: Development of the Ratiometric Bioluminescent Sensor (RBS) and its response to cellular stress in HeLa cells 75
3.1 Abstract 75
3.2 Introduction 75
3.3 Results 77
3.4 Discussion 88
3.5 References 90
Chapter 4: The RBS mechanism relies on hydrogen peroxide 95
4.1 Abstract 95
4.2 Introduction 95
4.3 Results 97
4.4 Discussion 114
4.5 References 120
Chapter 5: The RBS can detect caspase-dependent PCD in multiple cell lines using multiple inducers 128
5.1 Abstract 128
5.2 Introduction 128
5.3 Results 130
5.4 Discussion 143
5.5 References 146

Chapter 6: The RBS can detect caspase-independent PCD through pathways involving ROS production, Bcl-2 downregulation and mitochondrial membrane permeabilization 151

6.1 Abstract 151

6.2 Introduction 151

6.3 Results 153

6.4 Discussion 162

6.5 References 164

Chapter 7: The RBS detects programmed cell death *in vivo* 168

7.1 Abstract 168

7.2 Introduction 168

7.3 Results 170

7.4 Discussion 172

7.5 References 174

Chapter 8: Overall discussion, future directions and concluding remarks 178

8.1 Overall Discussion 178

8.1.1 Development of the Ratiometric Bioluminescent Sensor (RBS) and its response to cellular stress in HeLa cells 178

8.1.2 The RBS mechanism relies on ROS, particularly H_2O_2 182

8.1.3 The RBS can detect caspase-dependent PCD in multiple cell lines using multiple inducers 190

8.1.4 The RBS can detect caspase-independent PCD through pathways involving ROS production, Bcl-2 downregulation and mitochondrial membrane permeabilization 193

8.1.5 The RBS detects programmed cell death *in vivo* 196

8.2 Future Directions 197

8.3 Concluding remarks 200

8.4 References 201

LIST OF TABLES

Table 1.1. Common luciferases and selected characteristics. 4
Table 1.2. Pathogenic conditions related to PCD..... 12
Table 1.3. Summary of leuco dyes and fluorescein derivatives for ROS detection..... 29
Table 2.1. Summary of reagents..... 60
Table 3.1. Luciferase mutations and their reported effects. 80

LIST OF FIGURES

Figure 1.1. Emission spectra of various bioluminescent proteins..... 5
Figure 1.2. Illustration of caspase-dependent and caspase-independent PCD pathways.11
Figure 1.3. Schematic of a fluorogenic peptide probe for caspase-3. 14
Figure 1.4. Schematic of FRET and its use in a reporter for caspase-3 activity. 16
Figure 1.5. Schematic of ER-fLuc-ER sensor for caspase-3. 17
Figure 1.6. Schematic of split fLuc reporter for caspase-3 19
Figure 1.7. Schematic representing potential pathways for intracellular protein modification and/or degradation 24
Figure 2.1. Schematic of RBS 54
Figure 2.2. Plasmid map of the RBS. 57
Figure 3.1. Effect of staurosporine on fLuc and RLuc bioluminescence. 78
Figure 3.2. Caspase-3 activity during a time course of STS treatment. 79
Figure 3.3. Response of fLuc to STS or STS + PBT treatment 80
Figure 3.4. Effect of STS on fLuc5 compared to wt fLuc 81
Figure 3.5. Effect of STS on RLuc8 compared to wt RLuc 82
Figure 3.6. Response of RBS-HeLa cells to STS 84
Figure 3.7. Analysis of RLuc8:fLuc ratio as a function of cell number and time 85
Figure 3.8. Response of reverse RBS-HeLa cells to STS 86
Figure 3.9. Commercial PCD assays on STS-treated RBS-HeLa cells. 87
Figure 4.1. Assessment of mRNA and protein levels in STS-treated RBS-HeLa cells... 98
Figure 4.2. RBS response to proteasome inhibition. 99
Figure 4.3. RBS response to various protease inhibitors 100
Figure 4.4. RBS response to O2·- scavengers. 101
Figure 4.5. RBS response to ·OH scavengers. 102
Figure 4.6. RBS response to H_2O_2 related scavengers. 103
Figure 4.7. RBS response to an ONOO- scavenger, uric acid 104
Figure 4.8. Dose response and Western blot analysis of STS-treated cells to H_2O_2-related scavengers 105
Figure 4.9. Analysis of intracellular H_2O_2, exogenous application of H_2O_2, and the hypoxanthine-xanthine oxidase reaction. 107
Figure 4.10. Summary of RBS-HeLa responses to allopurinol pretreatment 109
Figure 4.11. Response of purified fLuc and RLuc8 proteins to H_2O_2 visualized with SDS-PAGE 110
Figure 4.12. Bioluminescence response of purified fLuc and RLuc8 proteins to H_2O_2. 111
Figure 4.13. Analysis of protein carbonylation in STS-treated RBS-HeLa cells and H_2O_2-treated fLuc and RLuc8 proteins. 113
Figure 5.1. Response of RBS-MCF7 cells to increasing STS dosage. 131
Figure 5.2. Response of STS-treated RBS-MCF7 cells to allopurinol pretreatment 133
Figure 5.3. Response of RBS-MCF7 to treatment with PBS (untreated control) or 10 μM STS over the course of 24 hours 135
Figure 5.4. Response of 293T/17 cells to increasing STS dosage 136

Figure 5.5. Response of RBS-293T/17 to treatment with PBS (untreated control) or 10 μM STS over the course of 24 hours 138
Figure 5.6. Effect of allopurinol on PBS (-STS) and STS treated RBS-293T/17 cells. 139
Figure 5.7. Effects of DOX and Cpt on RBS-HeLa cells 140
Figure 5.8. Response of commercial cell death assays in RBS-HeLa cells treated with DOX or Cpt..... 141
Figure 5.9. Response of DOX and Cpt treated RBS-HeLa cells to allopurinol pretreatment 143
Figure 6.1. Response of RBS-HeLa cells to increasing doses of sodium selenite..... 154
Figure 6.2. Response of RBS-MCF7 cells to increasing doses of sodium selenite 156
Figure 6.3. Response of RBS-MCF7 cells to increasing doses of resveratrol 158
Figure 6.4. Effect of allopurinol on RBS-HeLa and RBS-MCF7 cells treated with SSe and RBS-MCF7 cells treated with Res 160
Figure 6.5. Extent of DNA fragmentation in RBS cells pretreated with allopurinol prior to the addition of SSe or Res..... 161
Figure 7.1. Assessment of RBS performance *in vivo* 171
Figure 7.2. Quantitative analysis of RBS in live animals 172

Chapter 1: Introduction to bioluminescence imaging, programmed cell death and reactive oxygen species

1.1 Introduction

Complete understanding of physiology and disease states requires the capability to monitor specific cellular and molecular phenomena over biologically relevant time scales. Molecular imaging technologies provide investigators with the ability to non-invasively examine a wide variety of biological processes, both *in vitro* and in animal models. Bioluminescence imaging (BLI) is a molecular imaging modality wherein luciferase enzymes oxidize a substrate to produce light. Attributes of BLI include high sensitivity, cost-effectiveness, simplicity, virtually non-existent background signals, high-throughput screening potential and ability to acquire temporal information in cells and in live animal models. While safety concerns regarding transgene expression preclude BLI usage in humans, it remains a powerful tool for pre-clinical *in vivo* imaging studies.

Luciferases and their substrates have been engineered to report on gene expression levels, promoter activity and various other molecular processes, including programmed cell death (PCD), which is known as an exquisitely regulated 'cell suicide' mechanism. PCD is the primary contributor to the removal of excessive and damaged cells and plays a role in development, aging and the immune response. However, many pathologies can result from unregulated PCD including cancer, Alzheimer's disease and autoimmune disorders. Thus, the ability to monitor aberrant PCD could have widespread impact on the development of therapeutics for diseases characterized by this process.

We have found that in cells undergoing PCD, the activity of wild-type Firefly Luciferase (fLuc) is rapidly lost, and under the same conditions the activity of a Renilla Luciferase variant (RLuc8) remains relatively stable (Chapter 3). Investigation into the mechanism behind this disparity suggested that reactive oxygen species (ROS), particularly hydrogen peroxide (H_2O_2), play a dominant role (Chapter 4). Therefore it was hypothesized that when fLuc and RLuc8 were coexpressed in cells, their activity differential could be used in a ratiometric manner (i.e. RLuc8:fLuc) to relay information on intracellular ROS levels. It is well established that certain chemotherapeutic agents can generate ROS in their induction of cell death and that ROS often serve as mediators in caspase-dependent and –independent pathways. Consistent with these findings, we have found that levels of intracellular H_2O_2 increased in multiple cell types treated with a variety of PCD inducers and that this increase correlated well with RLuc8:fLuc ratios (Chapter 5 and Chapter 6). The implementation of the ratiometric reporter in murine models demonstrated that it was capable of detecting PCD in drug-treated tumors and that this detection was related to intratumoral ROS levels (Chapter 7). In this chapter, extensive background is provided on BLI, PCD and ROS.

1.2 Background

1.2.1 Bioluminescence Imaging

1.2.1a Overview

In order to obtain comprehensive knowledge regarding normal and pathological physiology, it is important for biological processes related to these states to be monitored

in real-time and over biologically relevant time scales. Molecular imaging techniques can facilitate the ability of investigators to non-invasively scrutinize the spatiotemporal dynamics of specific biological processes without sacrificing cells or animals (see (1) for extensive review). The field of molecular imaging encompasses many modalities including magnetic resonance imaging (MRI), optical imaging, signal photon emission spectroscopy (SPECT), ultrasound, and positron emission tomography (PET). Bioluminescence imaging (BLI) is an optical molecular imaging modality that harnesses the light produced during enzyme (luciferase)-mediated oxidation of a substrate (e.g. luciferin or coelenterazine) when the enzyme is expressed in cells, tissues or animals (see (2) for review). BLI has been utilized in studies examining tumor growth and metastasis(3), gene therapy(4), cell tracking(5), infection progression(6), gene expression(7) and toxicology(8), among others.

1.2.1b Types of luciferases and their substrates

Various types of luciferases have been identified across diverse phyla; however, only a few of these have been characterized sufficiently for mammalian use. Even though structures, sizes, substrates and emission wavelengths of these enzymes are quite varied, their mechanisms of light production are generally similar: during the oxidation of luciferin or coelenterazine by luciferase, an excited intermediate is generated and upon its relaxation to ground state, it emits a photon of light(9). The most commonly used luciferases and key attributes are highlighted in Table 1.1.

Table 1.1. Common luciferases and selected characteristics. Adapted from (2).

Luciferase	Luciferin	Peak emission (nm)	Size (kDa)	Comments	Reference(s)
Firefly (fLuc)	D-luciferin	612	61	Codon-optimized for mammalian expression; requires ATP	(10)
Click beetle red (cbRed)	D-luciferin	611	61	Requires ATP	(10, 11)
Click beetle green (cbGreen)	D-luciferin	544	61	Requires ATP	(10, 11)
Renilla reniformis (RLuc)	Coelenterazine	480	36	Does not require ATP; codon-optimized for mammalian expression	(9, 11, 12)
Gaussia princes (gLuc)	Coelenterazine	480	36	Does not require ATP; naturally secreted from cells	(12)

The luciferases from Firefly (fLuc) and *Renilla reniformis* (RLuc) are two of the most widely used bioluminescent proteins in current research. Fluc emits light at ~600 nm making it more suitable for *in vivo* imaging compared with the ~480 nm light emitted by RLuc, as fLuc photons are less absorbed by animal tissue. To produce light, fLuc must react with its substrate, luciferin, in the presence of ATP, oxygen and magnesium. RLuc requires its substrate, coelenterazine, and oxygen to produce light. The emission spectra of the luciferases are depicted in Figure 1.1.

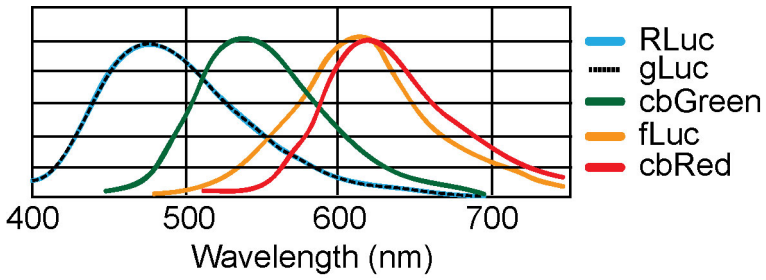

Figure 1.1. Emission spectra of various bioluminescent proteins. Adapted from (10).

Despite the low emission wavelength of RLuc, both fLuc and RLuc are commonly used together in both cell culture(13) and *in vivo*(14), with RLuc often serving as a transfection control for studies involving fLuc under the control of a specific promoter, and vice verse. The distinct substrates of these enzymes also allow for their use in this manner since after washing or clearance of the substrate for the first enzyme examined, a second substrate may be administered to specifically examine the second enzyme (see Table I). An alternative to washing/clearance involves using spectral separation to distinguish the signal from each protein. Each luciferase emits at a different wavelength of light; thus if the imaging equipment possesses emission filters appropriate for each enzyme, substrates can be administered at the same time, and each signal can be spectrally separated.

1.2.1c BLI: general considerations

There are many advantages of utilizing BLI as a molecular imaging modality. Since bioluminescent proteins are genetically encoded, once validated, they can be employed in a range of vectors to investigate a wide variety of intracellular pathways(15-17). A study using BLI to examine intracellular pathways involved heat shock proteins (HSPs), which are proteins utilized in cellular heat shock response. Heat shock response

occurs in cells undergoing thermal and other stresses and can abrogate resulting cellular damage and programmed cell death (see (18) for review). This group used transgenic mice expressing fLuc under the control of an HSP promoter to assess spatiotemporal patterns of HSP70 expression after thermal stress induced by laser irradiation(17). BLI has been used to investigate many other promoters in addition to HSP, including β-catenin promoters(19), insulin promoters(20), ubiquitin promoters(21) and hepatitis B virus promoters(22).

BLI has been used in conjunction with positron emission tomography (PET) to examine tumor hypoxia and related molecular events (15). Tumor hypoxia was monitored using a hypoxia-sensitive PET tracer, followed by investigation of hypoxia inducible factor (HIF), a transcription factor that helps tumor cells adapt to low oxygen environments(23), using BLI. Specifically, a fusion protein of HIF-1α-luciferase was monitored to assess the stability of HIF-1α, the subunit of HIF that is a target for degradation under normoxic conditions and stabilization under hypoxic conditions(24). In the same study, the gene encoding fLuc was placed downstream of a hypoxia response element (HRE) promoter to monitor HIF-driven gene expression.

The optical properties of some bioluminescent proteins allow for depths of up to a few centimeters to be imaged *in vivo*(25, 26). The emission wavelength of fLuc is ~600 nm, making it less likely than fluorescent light to be attenuated in animal tissue. Tumor cells expressing fLuc have been imaged in rat colon(25) and mouse lungs(26), illustrating the potential of BLI to image beyond superficial depths *in vivo.* Also, the intrinsically low bioluminescence of tissues allows for greater signal-to-background ratios compared

to fluorescence. For example, when using fluorescence imaging, the autofluorescence of tissues causes unwanted background signal, effectively reducing this ratio.

In addition to its cost-effectiveness, robustness and simplicity, BLI has recently proven to be quite useful in high-throughput screening assays(27-29). For example, malignant cells expressing fLuc were co-cultured with non-fLuc stromal cells and this co-culture was screened with anti-neoplastic candidates(27). Here, it was possible to specifically identify the effects of the compounds on malignant cells in an environment more representative of *in vivo* conditions as tumor-stroma interactions play key roles in tumor biology(30, 31). This ability to distinguish between cancerous and normal cells using this method holds an advantage over traditional viability assays (discussed later) where the high background of the stromal cells could skew information on malignant cell viability.

However, like any imaging modality, BLI possesses certain disadvantages that should be considered before its use in study design. Safety concerns preclude genetically encoded reporters (including bioluminescent proteins) from being used in humans, with the exception of gene therapy. Additionally, while the multi-centimeter depth penetration of bioluminescent proteins is greater than that of fluorescent molecular reporters, it nonetheless limits their *in vivo* application to small rodents. Another consideration regarding BLI is the potential for the proteins themselves to interfere with intracellular processes and possible phenotypic changes. Notably, it has been shown that colon cancer cells expressing fLuc were unable to grow into tumors in immunocompetent rats as opposed to parental colon cancer cells(32); it was hypothesized that the high expression levels of fLuc created unwanted immunogenecity and/or altered growth rates. Finally,

issues with substrate administration include altered substrate catalysis and pharmacokinetics due to disease states and cellular transporters, respectively. The tumor microenvironment is often hypoxic, and since the fLuc-luciferin reaction is oxygen dependent, this reaction may be impeded and resulting light output diminished. Additionally, the cellular membrane pumps ABCG2(29) and MDR1 P-glycoprotein(33) have been shown to transport luciferin and coelenterazine, respectively, out of cells, potentially hindering light output of the bioluminescent enzymes. Taken together, these issues can lead to inaccurate findings and ambiguous conclusions.

1.2.2 Programmed Cell Death

1.2.2a Overview

Programmed cell death (PCD) is a major contributor to the removal of excessive and damaged cells through an exquisitely regulated 'cell suicide' mechanism and is an essential process that is involved in development(34), aging(35), homeostasis(36) and the immune response(37). Apoptosis, or Type I PCD, is mechanistically characterized by a proteolytic cascade involving cysteine-aspartic proteases (caspases)(38); these caspases can be distinguished by the specific amino acid sequences wherein they cleave(39). Many types of caspases can be activated during apoptosis, however, the activation of caspase-3, an effector caspase, is required to complete the process (40); this necessity makes caspase-3 an often utilized target in studies assessing PCD. Additional characteristics of apoptosis include membrane blebbing, chromatin condensation, and nuclear fragmentation and the process ends with phagocytic engulfment of the dead cell and debris(36).

While apoptosis has been thoroughly characterized and is generally accepted as the most prevalent form of PCD, a number of alternative cell death pathways have been identified and are referred to as 'caspase-independent cell death pathways'. These pathways serve many purposes *in vivo* including embryonic removal of interdigital webs(41), the death of chondrocytes controlling bone growth(42), and the negative selection of lymphocytes(34, 35).

One form of caspase-independent PCD involves the mitochondria. Under certain stimuli the mitochondria release the apoptosis-inducing factor (AIF) from the intermembrane space(43); AIF enters the nucleus and eventually causes the degradation of chromatin into large (50 kb) chromatin fragments, in contrast to the oligonucleosomal DNA fragments that are formed when certain DNase's are activated by caspases(43, 44). The exact mechanism behind chromatin degradation by AIF remains unknown. Another mitochondrial-related PCD mechanism involves signaling from the tumor necrosis factor receptor 1 resulting in mitochondrial production of reactive oxygen species (ROS) and necrosis-like PCD(40).

Autophagy, or type II PCD, is a type of caspase-independent cell death that mechanistically manifests cellular metabolism through the cell's own lysosomal machinery (see (45) for review). In cells undergoing type II PCD, autophagic vesicles are formed to engulf various cytoplasmic components and these vesicles subsequently fuse with lysosomes to form autophagolysosomes. Various digestive enzymes are present in the lysosomal machinery, including aspartate, zinc and cysteine proteases (cathepsins), which are responsible for macromolecule breakdown. Autophagy can play

multiple roles as it can be a method for cells to adapt to cellular stresses and avoid apoptosis, or it can be an alternative method of PCD if apoptosis is inhibited(46).

Figure 1.2 illustrates pathways involved in both caspase-dependent and caspase-independent cell death. Caspase-dependent PCD can result from various onslaughts; however, regardless of induction method, this process is characterized by the activation of initiator caspases (e.g., caspases-2 and –8), eventually leading to the activation of effector caspases (e.g., caspase-3). Various stimuli can also induce caspase-independent PCD, however this type of cell death is usually characterized by increased proteolysis. ROS production and DNA damage can play prominent roles as well.

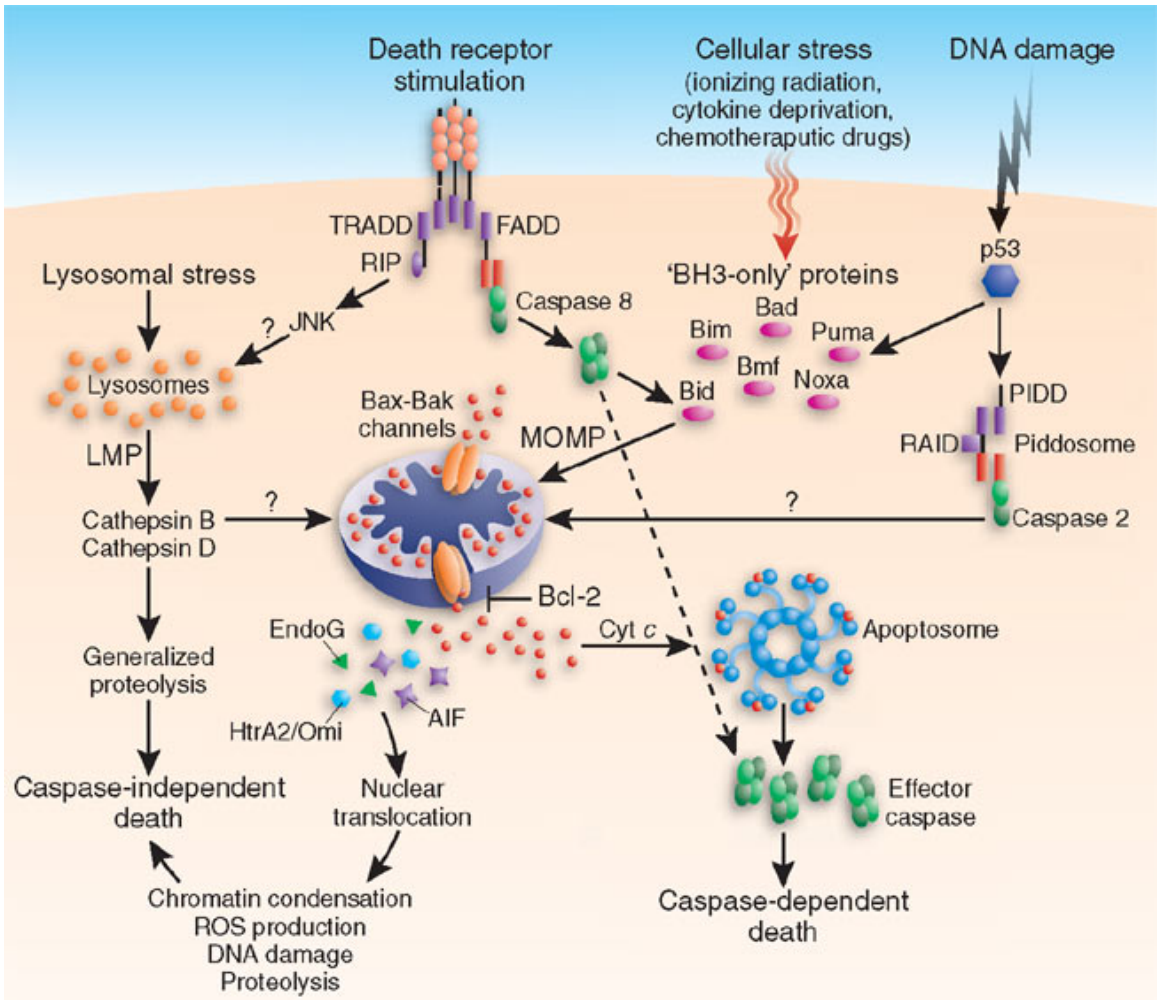

Figure 1.2. Illustration of caspase-dependent and caspase-independent PCD pathways. Reprinted with permission from (47).

Given the myriad processes in which PCD is involved, it is not surprising that unregulated PCD can result in various devastating pathologies, including autoimmune diseases, neurodegenerative disorders, and cancer (see (48) for review). Table 1.2 lists conditions that may result from either increased or inhibited PCD. Accordingly, many sensors have been developed to monitor and image PCD both *in vitro* and *in vivo* with the

impression that these sensors will aid in the development and evaluation of therapeutics designed to combat the many ailments associated with unregulated PCD.

Table 1.2. Pathogenic conditions related to PCD.

	Condition	Reference(s)
PCD inhibition	Cancer	
	Carcinomas with p53 mutations	(49, 50)
	Hormone-dependent tumors	
	Breast	(51)
	Prostate	(52)
	Autoimmune diseases	
	Lupus	(53)
	Viral Infection	
	Poxviruses	(54)
	Adenoviruses	(55, 56)
Increased PCD	AIDS	(49-51)
	Neurodegenerative disorders	
	Alzheimer's disease	(52-54)
	Huntington's disease	(55, 56)
	Ischemic Injury	
	Myocardial Infarction	(57, 58)
	Stroke	(57, 59)

1.2.2b Current Sensors for Apoptosis

Over the past decade, a large number of probes have been specifically developed for assessing apoptosis in cell culture and animal model studies. Since apoptosis occurs via a complex signaling cascade that is tightly regulated, these probes have been designed to take advantage of a number of different molecular targets to identify apoptosis. Some of the most commonly used agents involve measuring the level of caspase activity. These probes can generally be categorized as fluorogenic peptide probes, fluorescent molecular reporters, or bioluminescent reporters. However, not all sensors for apoptosis

rely on caspase activity. Phosphatidylserine (PS) targeting agents are designed to detect PS phospholipids that have flipped from the inner-leaflet to the outer-leaflet of membranes of cells undergoing apoptosis. Also, various commercial sensors are available to detect DNA fragmentation levels, dead-cell proteases and enzymes related to cellular viability. The following subsections will expand upon each of these types of sensors.

Fluorogenic Peptide Probes

Fluorogenic peptide probes for caspases are typically comprised of a peptidic protease substrate, e.g. a caspase recognition motif, intervening between two fluorophores or a fluorophore and a quencher(57-63). Peptidic cleavage by the target enzyme separates the fluorescent/quenching moieties and the subsequent change in the fluorescent emission spectrum is used to indicate enzymatic activity. Figure 1.3 represents a schematic of fluorogenic peptide probes for caspase-3; a quencher is attached to a fluorophore via a DEVD amino acid linkage, effectively quenching the fluorescence of the excited fluorophore. After caspase-3 cleavage of DEVD (its recognition sequence), the quencher is removed and the fluorophore emission is restored.

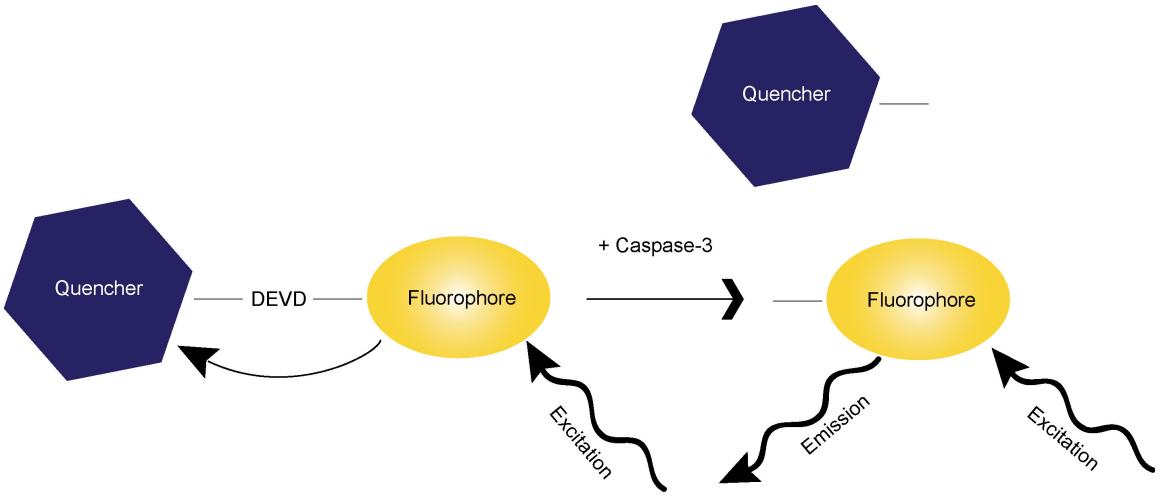

Figure 1.3. Schematic of a fluorogenic peptide probe for caspase-3. A fluorophore is conjugated to a quenching molecule via the DEVD amino acid sequence. Thus when excited, the fluorophore's emission is quenched. However upon caspase-3 mediated cleavage of its target sequence, DEVD, the quencher is released and the fluorophore emits light.

While fluorogenic peptide probes represent an important breakthrough in caspase activation detection, their sensitivity can be less than ideal, due to incomplete quenching before cleavage or spectral overlap of the two fluorophores in fluorescence resonance energy transfer (FRET)-based assays. Additional problems are manifested *in vivo* where autofluorescence of the living subject and/or pharmaceuticals can further reduce sensitivity. As both caspase activity and the biodistribution/pharmacokinetics of these probes affect the fluorescence intensity over time, imaging the temporal dynamics of apoptosis using these sensors can be challenging. Finally, cytoplasmic delivery of these probes can present additional issues as they may become non-specifically trapped and degraded in the lysosomes.

Fluorescent Molecular Reporters

Another category of fluorescent imaging sensors for apoptosis consists of fluorescent molecular reporters (64-66). These probes are defined by two fluorescent proteins with overlapping emission-excitation wavelengths that are linked by a protease-specific recognition sequence. For example, the emission spectrum of cyan fluorescent protein (CFP) significantly overlaps the excitation spectrum of yellow fluorescent protein (YFP). When these two proteins are in close proximity (i.e., connected by the amino acid sequence DEVD), the excitation of CFP results in emission from YFP, as a result of FRET. This phenomenon is depicted in Figure 1.4A. The tethering of YFP to CFP with DEVD effectively creates an activatable sensor for caspase-3; with increasing caspase-3 activation, the DEVD sequence is cleaved, the proteins separate, YFP emission decreases and CFP emission increases with CFP excitation(66). A summary of this mechanism is illustrated in Figure 1.4B.

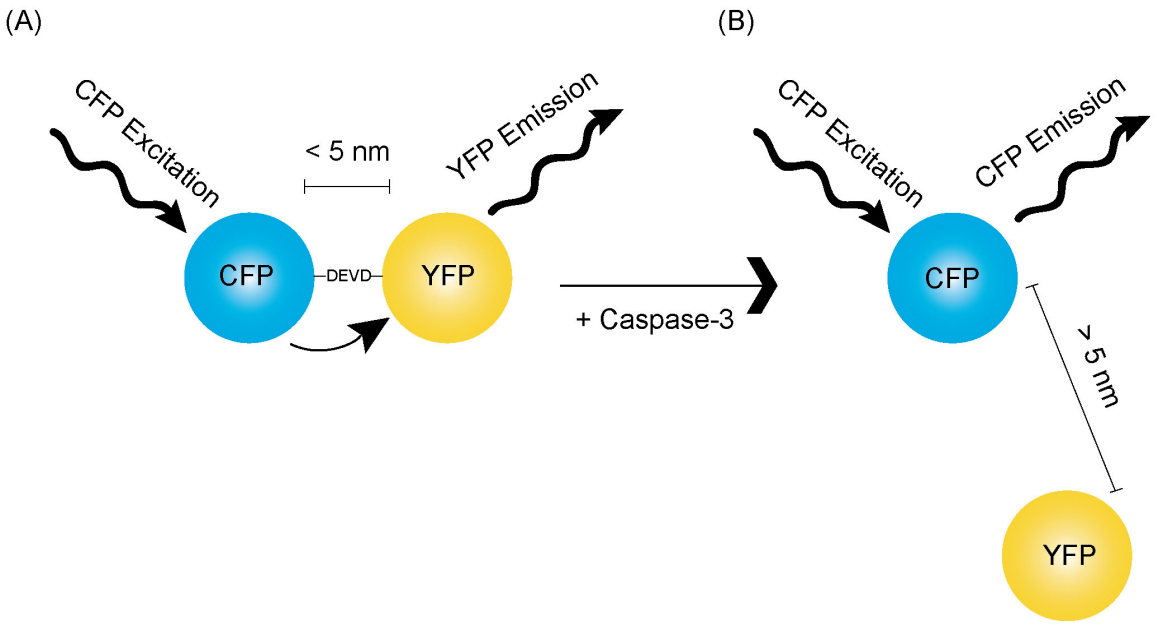

Figure 1.4. Schematic of FRET and its use in a reporter for caspase-3 activity. (A) In an activatable reporter for caspase-3 activity, CFP and YFP are fused together via the DEVD sequence, resulting in FRET. (B) Upon caspase-3 activation, its target DEVD sequence is cleaved, and CFP emission increases as the distance between the fluorophores increases (i.e., FRET is no longer occurring).

Fluorescent molecular reporters are genetically encoded, thus their synthesis costs are typically less than fluorogenic peptide probes. Another advantage of these reporters is their constitutive expression reduces their chances of lysosomal degradation and endosomal entrapment, two concerns of fluorogenic peptide probes. However fluorescent molecular reporters still suffer from similar background and autofluorescence issues, especially given the dearth of highly fluorescent near-infrared (NIR) molecular reporters available. It should be noted that very recently, an NIR fluorophore has been developed that could allow for much improvement on these sensors in regards to *in vivo* imaging capability(67).

Bioluminescent Reporters

To avoid sensitivity issues commonly associated with fluorogenic sensors, several groups have recently employed bioluminescent caspase reporter systems for PCD detection. One of these sensors utilized a recombinant Firefly luciferase (fLuc) reporter protein that was flanked on both sides by an estrogen receptor regulatory domain protein (ER)(68). The presence of these two large ER proteins (35 kDa each) effectively silenced the enzymatic activity of fLuc by ~90%. Additionally, a DEVD sequence was included between fLuc and each ER protein, which allowed for caspase-3 mediated removal of the silencing ER domains and thus restoration of fLuc activity. An illustration of this sensor is shown in Figure 1.5.

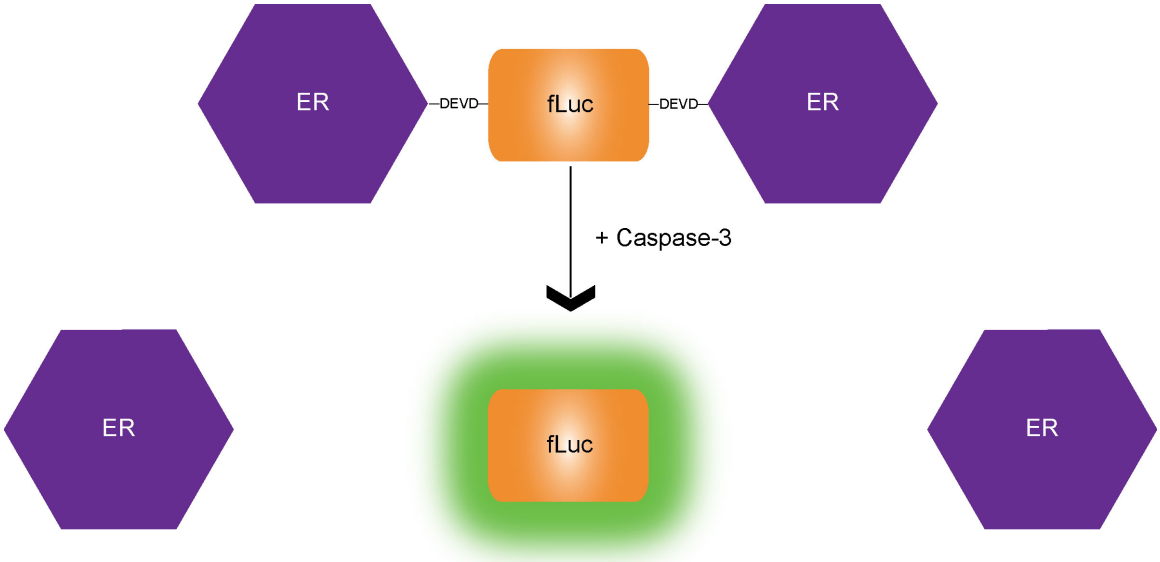

Figure 1.5. Schematic of ER-fLuc-ER sensor for caspase-3. Under normal cellular conditions, the large ER proteins flank the fLuc protein via DEVD linkages, hindering its enzymatic activity. When caspase-3 is activated in PCD inducing conditions, the DEVD sequences are cleaved, the ER proteins are released and fLuc activity is restored.

A number of drawbacks to this design exist, including that two proteolytic events are required to completely restore luciferase activity, the protease cleavage sites may be inaccessible due to the large flanking ER proteins, and that the usage of ER proteins themselves, which are endogenously expressed in mammalian cells, could provoke overly complex intracellular localization/dynamics, potentially leading to alternative proteolytic pathways and ambiguous bioluminescent signals. Furthermore, it should be noted that although the fLuc bioluminescence increases with increasing caspase-3 activity, this may be abrogated by accelerated degradation of functional enzyme under apoptotic conditions, as observed in this thesis.

Another bioluminescent approach for imaging apoptosis via caspase-3 activation *in vivo* made use of a split fLuc reporter strategy (69). In this sensor, fLuc is expressed in two parts, NH_2- and COOH-terminal sections, rendering it functionally inactive. When the two halves are brought into close enough proximity, enzymatic activity is restored, producing a bioluminescent signal in the presence of proper substrate. In the apoptotic probe design, small, yet strongly interacting, peptides and the DEVD sequence were incorporated to create a caspase-3 activatable sensor(70). Specifically, strongly interacting peptides, peptide A and peptide B (71, 72), were fused to the N- and C-terminal halves of fLuc, respectively, creating ANLuc and BCLuc (Figure 1.6). These fusions are positioned sequentially with and intervening DEVD sequence. Under apoptotic conditions, active caspase-3 cleaves at the DEVD site, which allows peptide A and peptide B to interact, effectively bringing the fLuc halves into favorable proximity, and the bioluminescence activity of fLuc is restored.

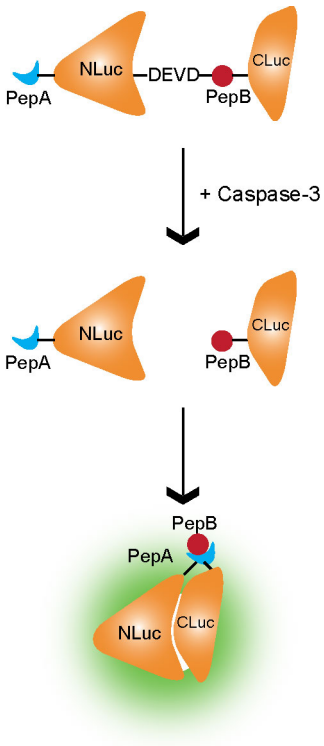

Figure 1.6. Schematic of split fLuc reporter for caspase-3. Under normal conditions, the NH_2- and COOH-terminal sections of fLuc (NLuc and CLuc, respectively) are attached to small, strongly interacting peptides (PePA and PepB) with and intervening DEVD sequence. Under apoptotic conditions, caspase-3 is activated and cleaves the DEVD sequence. The fLuc fragments are separated and PepA and PepB interact to bring the fragments into close enough proximity to reconstitute the activity of the fLuc enzyme.

Although this probe exhibits improvements over previous split reporter technologies, where drawbacks can include high-background and non-ideal signal-to-noise ratios (73), the requirement of two explicit events (i.e., DEVD cleavage and peptideA-peptideB interaction) to generate a functionally indicator of cell death, and the potential for an accelerated rate of enzyme degradation in cells undergoing PCD may present unforeseen difficulties in the utilization of this sensor.

Another activatable bioluminescent sensor for apoptosis that has found success *in vivo* makes use of the DEVD sequence conjugated to aminoluciferin(74, 75). This conjugation renders the luciferin unable to act as a proper substrate for fLuc until the peptide sequence is cleaved off upon caspase-3 activation. This method allowed for the detection of caspase-3 in murine tumor models, however some potential limitations must be addressed. First, it has been reported that the DEVD-luciferin is toxic to the animals(74, 75), forcing all imaging experiments to be ceased 2 hours after DEVD-luciferin injection, thus limiting the temporal dynamic range of this sensor significantly. Additionally, extraneous background signal due to nonspecific degradation in serum, extracellular space, lysosomes and non-apoptotic cells may decrease the sensitivity of this approach. Also, the peptide conjugation may affect the biodistribution and pharmacokinetics of the caged aminoluciferin and this reagent can be quite cost-inefficient.

Phosphatidylserine Targeting Agents

Phosphatidylserine (PS) is a phospholipid that is typically found in the inner-leaflet of cell membranes. In apoptotic cells, PS is often flipped to the outer leaflet of the cell membrane(76). This biological phenomenon has brought about the use of PS as a molecular marker for apoptotic cells, most commonly with Annexin V, a naturally occurring protein with avid binding affinity for PS(77). It has been found that apoptotic cells can be detected *in vivo* by labeling Annexin V with various contrast agents, including fluorescent dyes(78), iron oxide nanoparticles(79), technetium 99m(80) and PET agents(81). The cost-effectiveness of the fluorescently labeled Annexin V make

them an attractive choice for the routine imaging of apoptosis; however autofluorescence remains a concern, as does the non-specific localization of the labeled Annexin V agents in untreated tumors due to the enhanced permeability and retention (EPR) effect.

Commercial Sensors for Apoptosis

Many commercial sensors have been developed to investigate apoptosis and its related molecular processes. The terminal deoxynucleotidyl transferase dUTP nick end labeling (TUNEL) assay, first developed in 1992(82), detects DNA strand breaks after terminal deoxynucleotidyl transferase (TdT) incorporates labeled dUTP at break sites; DNA fragmentation is a hallmark of cells undergoing PCD(83). CytoTox Glo is a bioluminescent assay that measures the activity of certain intracellular proteases (dead-cell proteases) that are released from cells with compromised membranes. Additionally, assays that measure the reduction of various tetrazolium salts, such as MTT(84), XTT(85) and WST-1(86), by intracellular dehydrogenases which are active only in living cells are commonly used. However, it is important to note that these reduction assays are actually a measure of cell viability as opposed to cell death. Although all of these assays clearly have utility in measuring PCD in cell culture, most of them are not appropriate for real-time imaging/detection and/or imaging in animal models of disease. These limitations arise from the need for cell lysis, the use of membrane impermeable substrates, and/or the use of green fluorescent dyes, which are generally masked by autofluorescence *in vivo*.

1.2.2c Current Sensors for Caspase-Independent PCD

While caspase-3 activation is considered a gold standard for identification of cells undergoing apoptosis, caspase-independent PCD has recently been attracting attention in regards to cancer drug development. Anticancer drug resistance and tumorigenesis have been linked to the ability of certain cancer types to evade caspase activation(87, 88); thus it can be envisioned that therapeutics developed to induce caspase-independent PCD could have widespread impact. To date, there exist no molecular imaging sensors to specifically monitor caspase-independent PCD *in vivo*. Certainly, some of the aforementioned assays, namely TUNEL, CytoTox-Glo, MTT, and WST-1 have the capability to provide information on caspase-independent cell death, but suffer from the same previously mentioned limitations.

1.2.3 Reactive Oxygen Species, Oxidative Stress and Cell Death

1.2.3a Overview

Reactive oxygen species (ROS) are natural byproducts of intracellular metabolic processes, such as oxidation of xanthine by xanthine oxidase(89), uncoupling of the mitochondrial transport chain(90, 91) and oxidation of NADPH by NADPH oxidase(92, 93), and have been shown to play a role in cell signaling and function(94-96). For example, it has been shown that the growth factors tumor necrosis factor alpha (TNF alpha) and basic fibroblast growth factor (bFGF) induce increases in ROS production in chondrocytes(97). The ROS production seen here can stimulate the expression of early response genes (e.g., c-fos and c-jun), which play roles in cell proliferation and differentiation. Types of ROS include the hydroxyl radical ($^{\bullet}OH$), the superoxide radical ($O_2^{\bullet-}$), hydrogen peroxide (H_2O_2) and the peroxynitrite anion ($ONOO^-$). In a balanced cellular state, the level of ROS is typically controlled by various antioxidants that are either expressed in cells (e.g. glutathione(98), superoxide dismutase(99) and catalase(100)) or supplied through diet (e.g. vitamin E(101) and β-carotene(102)). When unnecessary excesses of ROS are present, cells enter a state of 'oxidative stress,' wherein various cellular components can be damaged, including DNA(103), RNA(104), proteins(101-104) and lipids(105). Pathological conditions that have been linked to oxidative stress include atherosclerosis(106), cancer(107), cystic fibrosis(108), type-2 diabetes(109) and Alzheimer's disease(110).

1.2.3b Protein modification, damage and degradation by ROS

While ROS-mediated damage of DNA, RNA and lipids are significant topics for discussion, the body of work included in this thesis focuses on the effects of oxidative stress on proteins. A summary of common ROS and mechanisms of protein oxidation is provided in Figure 1.7 and these mechanisms are described in more detail in subsequent sections.

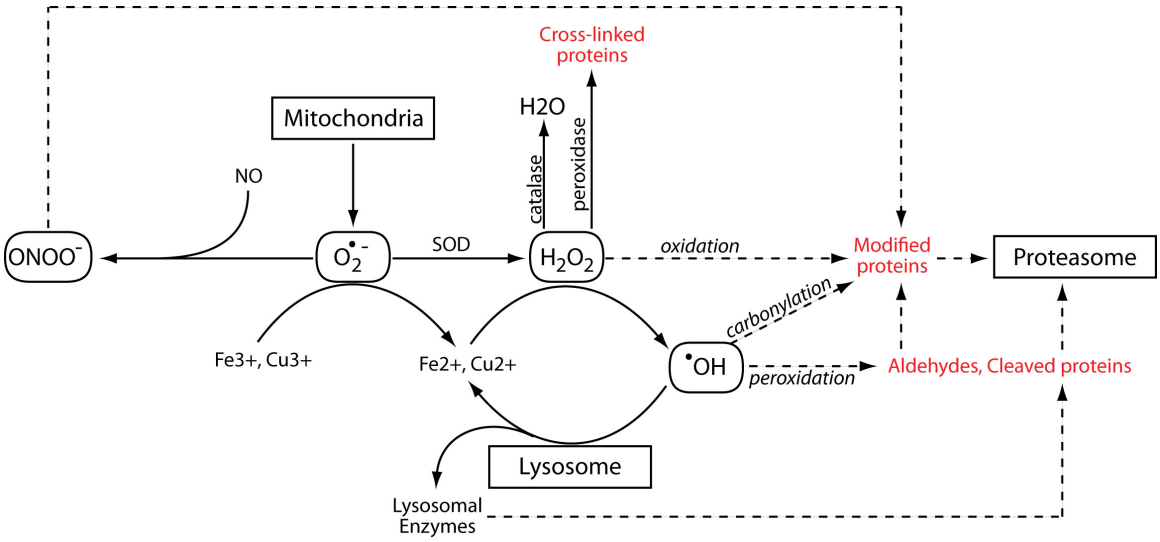

Figure 1.7. Schematic representing potential pathways for intracellular protein modification and/or degradation.

Superoxide

Superoxide ($O_2^{\bullet-}$) is the primary free radical formed within the cell by the reduction of molecular oxygen and it can act as either an oxidant or reductant. The mitochondria produce a large fraction of this radical (see (111) for review) due to their consumption of oxygen to produce energy for the cell. However, $O_2^{\bullet-}$ is not particularly reactive in biological systems and does not itself cause much oxidative damage(112),

rather it serves as a precursor to other oxidizing agents. The principal reaction of $O_2^{\bullet-}$ is to react with itself to produce H_2O_2 and oxygen (O_2), a reaction known as dismutation. Superoxide dismutation can be spontaneous or can be catalyzed by superoxide dismutase (SOD, (99)). Additionally, $O_2^{\bullet-}$ is important in the production of the highly reactive hydroxyl radical ($^{\bullet}OH$). In this process, $O_2^{\bullet-}$ reduces metal ions (e.g. $Fe^{3+} \rightarrow Fe^{2+}$) by donating one electron, and these metal ions then act as catalysts to convert H_2O_2 into $^{\bullet}OH$.

Hydrogen Peroxide

Hydrogen peroxide (H_2O_2) is a natural byproduct of oxygen metabolism and is necessary for the function of many enzymes in the intracellular environment (e.g. protein tyrosine phosphatases and the lipid phosphatase PTEN)(113). An important attribute of H_2O_2 is that it is small enough to pass through cell membranes and thus cannot be excluded from cells. H_2O_2 is a powerful oxidizing agent that can directly and indirectly modify many amino acids (see (114) for review), often creating hydroxyl- or carbonyl-derivatives. While the effect of protein oxidation can vary, it has been shown in some cases that oxidation can destabilize a protein's native structure and result in the impairment of protein function and activity loss(115, 116). Loss of secondary structure has also been shown to enhance the rate of protein degradation by the 20S proteasome(117). In contrast, the presence of oxidized amino acids alone does not seem to be a signal for degradation even though *in vitro* studies have suggested that proteins oxidized by H_2O_2 may be more susceptible to proteolytic attack(118). It should also be noted that in the presence of peroxidase (e.g. myeloperoxidase, lactoperoxidase and

cyclooxygenase) H_2O_2 can also produce tyrosyl radicals, which can subsequently dimerize to form dityrosine, which can further lead to protein cross-linking and aggregation(119-121).

Hydroxyl Radical

The hydroxyl radical ($^{\bullet}OH$) is generally considered to be the most powerful oxidizing species in biological systems, and similarly to H_2O_2, can also pass through membranes and thus cannot be kept out of cells. The oxidative attack of protein backbones is initiated by the $^{\bullet}OH$-dependent abstraction of the α-hydrogen atom of an amino acid residue to form a carbon-centered radical(122). Here, the $^{\bullet}OH$ may be created by the radiolysis of water or the metal-catalyzed cleavage of H_2O_2. In biological systems, the majority of $^{\bullet}OH$ radicals are produced when iron or copper react with H_2O_2, commonly referred to as the Fenton reaction.

Once a carbon-centered radical is formed, it can give rise to protein cross-links, peptide-bond cleavage (via diamide or α-amidation pathways), or direct oxidation of amino acids(122). The direct oxidation of lysine, arginine, proline and threonine residues may result in the formation of carbonyl derivatives (e.g. semialdehydes)(121, 122). Alternatively, carbonyl groups may be introduced into proteins by reactions with aldehydes produced during lipid peroxidation(123) or with other reactive carbonyls generated by the reduction or oxidation of carbohydrates(109). Lipid peroxidation products can diffuse across membranes, thus allowing amino acids and proteins relatively far from the initial site of peroxidation product formation to be modified(124). Interestingly, protein carbonylation as a result of lipid-derived aldehydes is more

prevalent than carbonylation from direct amino acid oxidation(125). The degradation of carbonylated proteins typically occurs via the 20S proteasome; however, the 26S proteasome has also been shown to play a role in the degradation of oxidatively modified proteins(126, 127).

Besides the direct effect of $^{\bullet}OH$ on proteins, they may also damage and destabilize lysosomal membranes, causing the subsequent release of moderate amounts of lysosomal hydrolytic enzymes into the cytosol(128, 129). The release of some of these enzymes, namely cathepsins, has been implicated in PCD(130, 131). Recently, it has been suggested that an intralysosomal pool of redox-active iron is also released upon lysosomal permeabilization, which can lead to the further production of $^{\bullet}OH$ if reacted with intracellular H_2O_2(132).

Peroxynitrite

Peroxynitrite (ONOO-) is formed as a result of the reaction between $O_2^{\bullet-}$ and nitric oxide (NO)(133). ONOO- can be cytotoxic through various mechanisms including initiating lipid peroxidation(134), ssDNA cleavage(135) and glutathione depletion(136). Methionine and cysteine residues are especially vulnerable to oxidation by ONOO-, however tyrosine and tryptophan residues are also selective targets for nitration(122). Tyrosine nitration is particularly damaging to cells because it can interfere with protein phosphorylation, thus compromising intracellular signal transduction networks(122, 137). As with previously mentioned ROS, mild ONOO- modification leads to the selective recognition and degradation of proteins by the proteasome(138).

1.2.3c Common Probes for Imaging ROS/Oxidative Stress

Leuco dyes and fluorescein derivatives

There currently exist a number of activatable fluorescent probes for detecting ROS. Many of these sensors fall under the category of non-fluorescent leuco dyes, i.e. 'dihydro' derivatives of fluorescein, rhodamine and other dyes that are oxidized back to the parent dye by some ROS. Even though these probes have been used to detect oxidative activity in cells and tissue, their oxidation sometimes does not easily discriminate between the various types of ROS. It has been reported that dihydrodichlorofluorescein (H_2DCF) and dihydrorhodamine 123 (DHR) only react with intracellular H_2O_2 in reactions mediated by peroxidase, cytochrome c or Fe^{2+}, rather than with H_2O_2 alone (139-141). Additionally, it has been reported that DHR can also be rapidly oxidized by ONOO-(142). It has been shown that dihydroethidium (DHE) and, more recently, the mitochondrial-targeted derivative of DHE, MitoSOX Red, can provide a more specific signal for superoxide(143, 144); however, the need for these dyes to be excited with a wavelength of 494-510 nm likely prevents their usage in animal models.

While not as commonly utilized as H_2DCF, aminophenyl fluorescein (APF) and hydroxyphenyl fluorescein (HPF) tend to show much more specific reactivity and greater resistance to light-induced oxidation than leuco dyes(145). Until reaction with $^{\bullet}$OH or ONOO-, these fluorescein derivatives are essentially non-fluorescent. Also, since APF also reacts with the hypochlorite anion (-OCl), it is possible to use APF and HPF concomitantly to selectively detect –OCl(145), an ROS not only well-known in neutrophil killing of bacteria, but also in microvascular damage caused by platelet-activating factor(146). As with the leuco dyes, the excitation wavelengths of these

fluorescein derivatives (494 nm) likely limit their usage to *in vitro* assays. Table 1.3 summarizes the leuco dyes and fluorescein derivatives for ROS detection.

Table 1.3. Summary of leuco dyes and fluorescein derivatives for ROS detection.

Reporter	ROS Detected	$\lambda_{Ex}/\lambda_{Em}$ (nm)
H_2DCF	H_2O_2	494/518
DHR	H_2O_2	505/534
DHE	$O_2^{\bullet-}$	510/595
MitoSox Red	$O_2^{\bullet-}$	510/580
APF	$^{\bullet}$OH, ONOO-, -OCl	494/518
HPF	$^{\bullet}$OH, ONOO-	494/518

Luminol and lucigenin

Luminol and lucigenin are chemiluminescent compounds that have been used to report the presence of ROS(147-149). However, a problematic characteristic of these sensors is the requirement of two steps for light emission(150, 151). First, either luminol must be oxidized by $^{\bullet}$OH(152), ONOO-(153), or peroxidase/H_2O_2(154) or lucigenin must be reduced by xanthine oxidase(150), the mitochondrial electron transport chain(155) or NADPH oxidase present in phagocytes(156). Then, the resulting radicals must react with $O_2^{\bullet-}$ to generate a light-emitting product. The intermediate radicals present complicating issues as they can themselves reduce oxygen to $O_2^{\bullet-}$. Therefore, luminol and lucigenin can be both sources and detectors of $O_2^{\bullet-}$, which can obviously lead to ambiguous results. Despite these complications, luminol was recently reported to be a successful method to image myeloperoxidase activity in animal models(157).

Electron Spin Resonance

Electron spin resonance (ESR) spectroscopy is an imaging technique for species that have one or more unpaired electrons, analogous to the spins of atomic nuclei in nuclear magnetic resonance. Theoretically ESR can be used to image ROS in living subjects, however ROS generally do not accumulate enough to be detected(158). To overcome this issue, ROS 'traps' have been developed to intercept reactive/unstable radicals and react with them to form stable radicals that can thus be detected by ESR(159, 160). While initially promising, ROS traps suffer from numerous drawbacks including loss of the ESR signal by enzymatic and/or molecular reductions, potential toxicity from the high concentration of traps needed to generate an ESR signal and perturbations of the traps on normal physiological function(158).

Luciferase-based sensors

The commercial assay GSH-Glo (Promega) is the only luciferase-based assay designed to investigate oxidative stress; it detects intracellular glutathione (GSH) levels, which generally tend to decrease in the presence of reactive species. This assay involves the cleavage of an inactive luciferin derivative by GSH to render the native form of luciferin. The luciferase provided in the assay can then catalyze the luciferin and produce a bioluminescent signal. However there are currently no established luciferase-based sensors designed to directly detect ROS. If achieved, luciferase-based sensors could offer many advantageous attributes including cost-effectiveness, high sensitivity, simplicity and ability to garner temporal information in cells and animal models. Given that current ROS imaging techniques are quite limited in their ability to provide information *in vivo*,

it is expected that a luciferase-based sensor would provide unique insight into the role of ROS in disease progression and in response to therapy under natural biological conditions. Furthermore, the ability to image ROS in animal models would most certainly be expected to facilitate the development and evaluation of new therapeutics, assist with the development of strategies to improve the efficacy of current therapeutics, or limit the unwanted side effects of current therapeutic agents.

1.2.4 The Role of ROS/Oxidative Stress in PCD

It is well established that certain chemotherapeutic agents, such as rituximab(161), bortezomib(162) and adaphostin(163), among others(164-166), generate ROS in their induction of malignant cell death. However, there is growing evidence that ROS may be involved in the regulation of both apoptotic and non-apoptotic (caspase-independent) cell death pathways(167, 168). Recent studies have suggested that various cell death triggers can lead to the direct production of ROS or enhanced mitochondrial outer membrane permeability (MOMP(169, 170)). The direct production of ROS can induce lysosomal membrane permeabilization and the subsequent release of lysosomal enzymes can either induce MOMP or cause lysosomal degradation-mediated autophagic cell death(171, 172). If MOMP is induced, cytochrome c and other pro-apoptotic factors are released into the cytosol; additionally, NADH dehydrogenase and reduced enzyme Q10 divert electrons from the electron transport system to oxygen, and $O_2^{\bullet-}$ are formed(169, 170). Illustration of these processes can be seen in Figure 1.1. These findings suggest that there is substantial interplay between apoptotic and non-apoptotic cell death signaling, and that ROS play significant roles within each mechanism(168). It

is envisioned that ROS/oxidative stress can be used as robust, versatile markers for the various morphologically distinct pathways of cell death.

1.3 References

1. Weissleder R, Mahmood U. Molecular imaging. Radiology 2001;219:316-33.

2. Prescher JA, Contag CH. Guided by the light: visualizing biomolecular processes in living animals with bioluminescence. Curr Opin Chem Biol;14:80-9.

3. Wetterwald A, van der Pluijm G, Que I, et al. Optical imaging of cancer metastasis to bone marrow: a mouse model of minimal residual disease. Am J Pathol 2002;160:1143-53.

4. Ofek P, Fischer W, Calderon M, Haag R, Satchi-Fainaro R. In vivo delivery of small interfering RNA to tumors and their vasculature by novel dendritic nanocarriers. FASEB J.

5. Tang Y, Shah K, Messerli SM, Snyder E, Breakefield X, Weissleder R. In vivo tracking of neural progenitor cell migration to glioblastomas. Hum Gene Ther 2003;14:1247-54.

6. Rocchetta HL, Boylan CJ, Foley JW, et al. Validation of a noninvasive, real-time imaging technology using bioluminescent Escherichia coli in the neutropenic mouse thigh model of infection. Antimicrob Agents Chemother 2001;45:129-37.

7. Luo J, Lin AH, Masliah E, Wyss-Coray T. Bioluminescence imaging of Smad signaling in living mice shows correlation with excitotoxic neurodegeneration. Proc Natl Acad Sci U S A 2006;103:18326-31.

8. Redshaw N, Dickson SJ, Ambrose V, Horswell J. A preliminary investigation into the use of biosensors to screen stomach contents for selected poisons and drugs. Forensic Sci Int 2007;172:106-11.

9. Wilson T, Hastings JW. Bioluminescence. Annu Rev Cell Dev Biol 1998;14:197-230.

10. Zhao H, Doyle TC, Coquoz O, Kalish F, Rice BW, Contag CH. Emission spectra of bioluminescent reporters and interaction with mammalian tissue determine the sensitivity of detection in vivo. J Biomed Opt 2005;10:41210.

11. Miloud T, Henrich C, Hammerling GJ. Quantitative comparison of click beetle and firefly luciferases for in vivo bioluminescence imaging. J Biomed Opt 2007;12:054018.

12. Tannous BA, Kim DE, Fernandez JL, Weissleder R, Breakefield XO. Codon-optimized Gaussia luciferase cDNA for mammalian gene expression in culture and in vivo. Mol Ther 2005;11:435-43.

13. Liu X, Kramer JA, Hu Y, Schmidt JM, Jiang J, Wilson AG. Development of a high-throughput human HepG(2) dual luciferase assay for detection of metabolically activated hepatotoxicants and genotoxicants. Int J Toxicol 2009;28:162-76.

14. Bhaumik S, Gambhir SS. Optical imaging of Renilla luciferase reporter gene expression in living mice. Proc Natl Acad Sci U S A 2002;99:377-82.

15. Lehmann S, Stiehl DP, Honer M, et al. Longitudinal and multimodal in vivo imaging of tumor hypoxia and its downstream molecular events. Proc Natl Acad Sci U S A 2009;106:14004-9.

16. Liu AC, Welsh DK, Ko CH, et al. Intercellular coupling confers robustness against mutations in the SCN circadian clock network. Cell 2007;129:605-16.

17. O'Connell-Rodwell CE, Mackanos MA, Simanovskii D, et al. In vivo analysis of heat-shock-protein-70 induction following pulsed laser irradiation in a transgenic reporter mouse. J Biomed Opt 2008;13:030501.

18. Hightower LE. Heat shock, stress proteins, chaperones, and proteotoxicity. Cell 1991;66:191-7.

19. Naik S, Piwnica-Worms D. Real-time imaging of beta-catenin dynamics in cells and living mice. Proc Natl Acad Sci U S A 2007;104:17465-70.

20. Chen X, Larson CS, West J, Zhang X, Kaufman DB. In vivo detection of extrapancreatic insulin gene expression in diabetic mice by bioluminescence imaging. PLoS One;5:e9397.

21. Gazdhar A, Bilici M, Pierog J, et al. In vivo electroporation and ubiquitin promoter--a protocol for sustained gene expression in the lung. J Gene Med 2006;8:910-8.

22. Zhao F, Liang SQ, Zhou Y, et al. Evaluation of hepatitis B virus promoters for sustained transgene expression in mice by bioluminescence imaging. Virus Res;149:162-6.

23. Semenza GL, Nejfelt MK, Chi SM, Antonarakis SE. Hypoxia-inducible nuclear factors bind to an enhancer element located 3' to the human erythropoietin gene. Proc Natl Acad Sci U S A 1991;88:5680-4.

24. Wang GL, Jiang BH, Rue EA, Semenza GL. Hypoxia-inducible factor 1 is a basic-helix-loop-helix-PAS heterodimer regulated by cellular O2 tension. Proc Natl Acad Sci U S A 1995;92:5510-4.

25. Contag CH, Spilman SD, Contag PR, et al. Visualizing gene expression in living mammals using a bioluminescent reporter. Photochem Photobiol 1997;66:523-31.

26. Edinger M, Sweeney TJ, Tucker AA, Olomu AB, Negrin RS, Contag CH. Noninvasive assessment of tumor cell proliferation in animal models. Neoplasia 1999;1:303-10.

27. McMillin DW, Delmore J, Weisberg E, et al. Tumor cell-specific bioluminescence platform to identify stroma-induced changes to anticancer drug activity. Nat Med;16:483-9.

28. O'Leary DA, Sharif O, Anderson P, et al. Identification of small molecule and genetic modulators of AON-induced dystrophin exon skipping by high-throughput screening. PLoS One 2009;4:e8348.

29. Zhang Y, Byun Y, Ren YR, Liu JO, Laterra J, Pomper MG. Identification of inhibitors of ABCG2 by a bioluminescence imaging-based high-throughput assay. Cancer Res 2009;69:5867-75.

30. Grigorieva I, Thomas X, Epstein J. The bone marrow stromal environment is a major factor in myeloma cell resistance to dexamethasone. Exp Hematol 1998;26:597-603.

31. Karnoub AE, Dash AB, Vo AP, et al. Mesenchymal stem cells within tumour stroma promote breast cancer metastasis. Nature 2007;449:557-63.

32. Zeamari S, Rumping G, Floot B, Lyons S, Stewart FA. In vivo bioluminescence imaging of locally disseminated colon carcinoma in rats. Br J Cancer 2004;90:1259-64.

33. Pichler A, Prior JL, Piwnica-Worms D. Imaging reversal of multidrug resistance in living mice with bioluminescence: MDR1 P-glycoprotein transports coelenterazine. Proc Natl Acad Sci U S A 2004;101:1702-7.

34. Saunders JW, Jr. Death in embryonic systems. Science 1966;154:604-12.

35. Monti D, Troiano L, Tropea F, et al. Apoptosis--programmed cell death: a role in the aging process? Am J Clin Nutr 1992;55:1208S-14S.

36. Kerr JF, Wyllie AH, Currie AR. Apoptosis: a basic biological phenomenon with wide-ranging implications in tissue kinetics. Br J Cancer 1972;26:239-57.

37. Krammer PH, Behrmann I, Daniel P, Dhein J, Debatin KM. Regulation of apoptosis in the immune system. Curr Opin Immunol 1994;6:279-89.

38. Nunez G, Benedict MA, Hu Y, Inohara N. Caspases: the proteases of the apoptotic pathway. Oncogene 1998;17:3237-45.

39. Garcia-Calvo M, Peterson EP, Leiting B, Ruel R, Nicholson DW, Thornberry NA. Inhibition of human caspases by peptide-based and macromolecular inhibitors. J Biol Chem 1998;273:32608-13.

40. Nicholson DW, Ali A, Thornberry NA, et al. Identification and inhibition of the ICE/CED-3 protease necessary for mammalian apoptosis. Nature 1995;376:37-43.

41. Chautan M, Chazal G, Cecconi F, Gruss P, Golstein P. Interdigital cell death can occur through a necrotic and caspase-independent pathway. Curr Biol 1999;9:967-70.

42. Roach HI, Clarke NM. Physiological cell death of chondrocytes in vivo is not confined to apoptosis. New observations on the mammalian growth plate. J Bone Joint Surg Br 2000;82:601-13.

43. Susin SA, Lorenzo HK, Zamzami N, et al. Molecular characterization of mitochondrial apoptosis-inducing factor. Nature 1999;397:441-6.

44. Strasser A, O'Connor L, Dixit VM. Apoptosis signaling. Annu Rev Biochem 2000;69:217-45.

45. Shintani T, Klionsky DJ. Autophagy in health and disease: a double-edged sword. Science 2004;306:990-5.

46. Maiuri MC, Zalckvar E, Kimchi A, Kroemer G. Self-eating and self-killing: crosstalk between autophagy and apoptosis. Nat Rev Mol Cell Biol 2007;8:741-52.

47. Kroemer G, Martin SJ. Caspase-independent cell death. Nat Med 2005;11:725-30.

48. Thompson CB. Apoptosis in the pathogenesis and treatment of disease. Science 1995;267:1456-62.

49. Lowe SW, Bodis S, McClatchey A, et al. p53 status and the efficacy of cancer therapy in vivo. Science 1994;266:807-10.

50. Lu X, Lane DP. Differential induction of transcriptionally active p53 following UV or ionizing radiation: defects in chromosome instability syndromes? Cell 1993;75:765-78.

51. Ellis PA, Saccani-Jotti G, Clarke R, et al. Induction of apoptosis by tamoxifen and ICI 182780 in primary breast cancer. Int J Cancer 1997;72:608-13.

52. Montironi R, Pomante R, Diamanti L, Magi-Galluzzi C. Apoptosis in prostatic adenocarcinoma following complete androgen ablation. Urol Int 1998;60 Suppl 1:25-9; discussion 30.

53. Emlen W, Niebur J, Kadera R. Accelerated in vitro apoptosis of lymphocytes from patients with systemic lupus erythematosus. J Immunol 1994;152:3685-92.

54. Ray CA, Black RA, Kronheim SR, et al. Viral inhibition of inflammation: cowpox virus encodes an inhibitor of the interleukin-1 beta converting enzyme. Cell 1992;69:597-604.

55. Boyd JM, Malstrom S, Subramanian T, et al. Adenovirus E1B 19 kDa and Bcl-2 proteins interact with a common set of cellular proteins. Cell 1994;79:341-51.

56. Rao L, Debbas M, Sabbatini P, Hockenbery D, Korsmeyer S, White E. The adenovirus E1A proteins induce apoptosis, which is inhibited by the E1B 19-kDa and Bcl-2 proteins. Proc Natl Acad Sci U S A 1992;89:7742-6.

57. Bullok K, Piwnica-Worms D. Synthesis and characterization of a small, membrane-permeant, caspase-activatable far-red fluorescent peptide for imaging apoptosis. J Med Chem 2005;48:5404-7.

58. Hug H, Los M, Hirt W, Debatin KM. Rhodamine 110-linked amino acids and peptides as substrates to measure caspase activity upon apoptosis induction in intact cells. Biochemistry 1999;38:13906-11.

59. Leytus SP, Melhado LL, Mangel WF. Rhodamine-based compounds as fluorogenic substrates for serine proteinases. Biochem J 1983;209:299-307.

60. Liu J, Bhalgat M, Zhang C, Diwu Z, Hoyland B, Klaubert DH. Fluorescent molecular probes V: a sensitive caspase-3 substrate for fluorometric assays. Bioorg Med Chem Lett 1999;9:3231-6.

61. Packard BZ, Toptygin DD, Komoriya A, Brand L. Profluorescent protease substrates: intramolecular dimers described by the exciton model. Proc Natl Acad Sci U S A 1996;93:11640-5.

62. Tung CH. Fluorescent peptide probes for in vivo diagnostic imaging. Biopolymers 2004;76:391-403.

63. Zhang HZ, Kasibhatla S, Guastella J, Tseng B, Drewe J, Cai SX. N-Ac-DEVD-N'-(Polyfluorobenzoyl)-R110: novel cell-permeable fluorogenic caspase substrates for the detection of caspase activity and apoptosis. Bioconjug Chem 2003;14:458-63.

64. Ai HW, Hazelwood KL, Davidson MW, Campbell RE. Fluorescent protein FRET pairs for ratiometric imaging of dual biosensors. Nat Methods 2008;5:401-3.

65. Takemoto K, Nagai T, Miyawaki A, Miura M. Spatio-temporal activation of caspase revealed by indicator that is insensitive to environmental effects. J Cell Biol 2003;160:235-43.

66. Tyas L, Brophy VA, Pope A, Rivett AJ, Tavare JM. Rapid caspase-3 activation during apoptosis revealed using fluorescence-resonance energy transfer. EMBO Rep 2000;1:266-70.

67. Shu X, Royant A, Lin MZ, et al. Mammalian expression of infrared fluorescent proteins engineered from a bacterial phytochrome. Science 2009;324:804-7.

68. Laxman B, Hall DE, Bhojani MS, et al. Noninvasive real-time imaging of apoptosis. Proc Natl Acad Sci U S A 2002;99:16551-5.

69. Luker KE, Smith MC, Luker GD, Gammon ST, Piwnica-Worms H, Piwnica-Worms D. Kinetics of regulated protein-protein interactions revealed with firefly luciferase complementation imaging in cells and living animals. Proc Natl Acad Sci U S A 2004;101:12288-93.

70. Coppola JM, Ross BD, Rehemtulla A. Noninvasive imaging of apoptosis and its application in cancer therapeutics. Clin Cancer Res 2008;14:2492-501.

71. Thormeyer D, Ammerpohl O, Larsson O, et al. Characterization of lacZ complementation deletions using membrane receptor dimerization. Biotechniques 2003;34:346-50, 52-5.

72. Zhang Z, Zhu W, Kodadek T. Selection and application of peptide-binding peptides. Nat Biotechnol 2000;18:71-4.

73. Villalobos V, Naik S, Piwnica-Worms D. Current state of imaging protein-protein interactions in vivo with genetically encoded reporters. Annu Rev Biomed Eng 2007;9:321-49.

74. Kizaka-Kondoh S, Itasaka S, Zeng L, et al. Selective killing of hypoxia-inducible factor-1-active cells improves survival in a mouse model of invasive and metastatic pancreatic cancer. Clin Cancer Res 2009;15:3433-41.

75. Shah K, Tung CH, Breakefield XO, Weissleder R. In vivo imaging of S-TRAIL-mediated tumor regression and apoptosis. Mol Ther 2005;11:926-31.

76. Fadok VA, Voelker DR, Campbell PA, Cohen JJ, Bratton DL, Henson PM. Exposure of phosphatidylserine on the surface of apoptotic lymphocytes triggers specific recognition and removal by macrophages. J Immunol 1992;148:2207-16.

77. Andree HA, Reutelingsperger CP, Hauptmann R, Hemker HC, Hermens WT, Willems GM. Binding of vascular anticoagulant alpha (VAC alpha) to planar phospholipid bilayers. J Biol Chem 1990;265:4923-8.

78. Ntziachristos V, Schellenberger EA, Ripoll J, et al. Visualization of antitumor treatment by means of fluorescence molecular tomography with an annexin V-Cy5.5 conjugate. Proc Natl Acad Sci U S A 2004;101:12294-9.

79. Schellenberger EA, Bogdanov A, Jr., Hogemann D, Tait J, Weissleder R, Josephson L. Annexin V-CLIO: a nanoparticle for detecting apoptosis by MRI. Mol Imaging 2002;1:102-7.

80. Kartachova MS, Valdes Olmos RA, Haas RL, Hoebers FJ, van Herk M, Verheij M. 99mTc-HYNIC-rh-annexin-V scintigraphy: visual and quantitative evaluation of early treatment-induced apoptosis to predict treatment outcome. Nucl Med Commun 2008;29:39-44.

81. Collingridge DR, Glaser M, Osman S, et al. In vitro selectivity, in vivo biodistribution and tumour uptake of annexin V radiolabelled with a positron emitting radioisotope. Br J Cancer 2003;89:1327-33.

82. Gavrieli Y, Sherman Y, Ben-Sasson SA. Identification of programmed cell death in situ via specific labeling of nuclear DNA fragmentation. J Cell Biol 1992;119:493-501.

83. Williams JR, Little JB, Shipley WU. Association of mammalian cell death with a specific endonucleolytic degradation of DNA. Nature 1974;252:754-5.

84. Mosmann T. Rapid colorimetric assay for cellular growth and survival: application to proliferation and cytotoxicity assays. J Immunol Methods 1983;65:55-63.

85. Scudiero DA, Shoemaker RH, Paull KD, et al. Evaluation of a soluble tetrazolium/formazan assay for cell growth and drug sensitivity in culture using human and other tumor cell lines. Cancer Res 1988;48:4827-33.

86. Hamasaki K, Kogure K, Ohwada K. A biological method for the quantitative measurement of tetrodotoxin (TTX): tissue culture bioassay in combination with a water-soluble tetrazolium salt. Toxicon 1996;34:490-5.

87. Los M, Herr I, Friesen C, Fulda S, Schulze-Osthoff K, Debatin KM. Cross-resistance of CD95- and drug-induced apoptosis as a consequence of deficient activation of caspases (ICE/Ced-3 proteases). Blood 1997;90:3118-29.

88. Martinez-Lorenzo MJ, Gamen S, Etxeberria J, et al. Resistance to apoptosis correlates with a highly proliferative phenotype and loss of Fas and CPP32 (caspase-3) expression in human leukemia cells. Int J Cancer 1998;75:473-81.

89. Fridovich I. Quantitative aspects of the production of superoxide anion radical by milk xanthine oxidase. J Biol Chem 1970;245:4053-7.

90. Boveris A, Cadenas E, Stoppani AO. Role of ubiquinone in the mitochondrial generation of hydrogen peroxide. Biochem J 1976;156:435-44.

91. Takeshige K, Minakami S. NADH- and NADPH-dependent formation of superoxide anions by bovine heart submitochondrial particles and NADH-ubiquinone reductase preparation. Biochem J 1979;180:129-35.

92. Curnutte JT, Kipnes RS, Babior BM. Defect in pyridine nucleotide dependent superoxide production by a particulate fraction from the cranulocytes of patients with chronic granulomatous disease. N Engl J Med 1975;293:628-32.

93. Iyer GY, Questel JH. NADPH and NADH oxidation by guinea pig polymorphonuclear leucocytes. Can J Biochem Physiol 1963;41:427-34.

94. Aslan M, Ozben T. Oxidants in receptor tyrosine kinase signal transduction pathways. Antioxid Redox Signal 2003;5:781-8.

95. Chang Q, Pan J, Wang X, Zhang Z, Chen F, Shi X. Reduced reactive oxygen species-generating capacity contributes to the enhanced cell growth of arsenic-transformed epithelial cells. Cancer Res;70:5127-35.

96. Mandal D, Fu P, Levine AD. REDOX regulation of IL-13 signaling in intestinal epithelial cells: Usage of alternate pathways mediates distinct gene expression patterns. Cell Signal.

97. Lo YY, Cruz TF. Involvement of reactive oxygen species in cytokine and growth factor induction of c-fos expression in chondrocytes. J Biol Chem 1995;270:11727-30.

98. Hopkins FG. Glutathione: Its Influence in the Oxidation of Fats and Proteins. Biochem J 1925;19:787-819.

99. McCord JM, Fridovich I. Superoxide dismutase. An enzymic function for erythrocuprein (hemocuprein). J Biol Chem 1969;244:6049-55.

100. Evans CA. On the Catalytic Decomposition of Hydrogen Peroxide by the Catalase of Blood. Biochem J 1907;2:133-55.

101. Tappel A, Zalkin H. Inhibition of lipid peroxidation in microsomes by vitamin E. Nature 1960;185:35.

102. Burton GW, Ingold KU. beta-Carotene: an unusual type of lipid antioxidant. Science 1984;224:569-73.

103. Burdon RH, Gill V, Boyd PA, Rahim RA. Hydrogen peroxide and sequence-specific DNA damage in human cells. FEBS Lett 1996;383:150-4.

104. Martinet W, de Meyer GR, Herman AG, Kockx MM. Reactive oxygen species induce RNA damage in human atherosclerosis. Eur J Clin Invest 2004;34:323-7.

105. Halliwell B, Chirico S. Lipid peroxidation: its mechanism, measurement, and significance. Am J Clin Nutr 1993;57:715S-24S; discussion 24S-25S.

106. Cai H, Harrison DG. Endothelial dysfunction in cardiovascular diseases: the role of oxidant stress. Circ Res 2000;87:840-4.

107. Hagen TM, Huang S, Curnutte J, et al. Extensive oxidative DNA damage in hepatocytes of transgenic mice with chronic active hepatitis destined to develop hepatocellular carcinoma. Proc Natl Acad Sci U S A 1994;91:12808-12.

108. Brown RK, Kelly FJ. Evidence for increased oxidative damage in patients with cystic fibrosis. Pediatr Res 1994;36:487-93.

109. Baynes JW. Role of oxidative stress in development of complications in diabetes. Diabetes 1991;40:405-12.

110. Nunomura A, Perry G, Aliev G, et al. Oxidative damage is the earliest event in Alzheimer disease. J Neuropathol Exp Neurol 2001;60:759-67.

111. Lenaz G. The mitochondrial production of reactive oxygen species: mechanisms and implications in human pathology. IUBMB Life 2001;52:159-64.

112. Winterbourn CC, Kettle AJ. Radical-radical reactions of superoxide: a potential route to toxicity. Biochem Biophys Res Commun 2003;305:729-36.

113. Rhee SG, Kang SW, Jeong W, Chang TS, Yang KS, Woo HA. Intracellular messenger function of hydrogen peroxide and its regulation by peroxiredoxins. Curr Opin Cell Biol 2005;17:183-9.

114. Grune T, Reinheckel T, Davies KJ. Degradation of oxidized proteins in mammalian cells. FASEB J 1997;11:526-34.

115. Gao J, Yin DH, Yao Y, et al. Loss of conformational stability in calmodulin upon methionine oxidation. Biophys J 1998;74:1115-34.

116. Volkin DB, Mach H, Middaugh CR. Degradative covalent reactions important to protein stability. Mol Biotechnol 1997;8:105-22.

117. Ferrington DA, Sun H, Murray KK, et al. Selective degradation of oxidized calmodulin by the 20 S proteasome. J Biol Chem 2001;276:937-43.

118. Fligiel SE, Lee EC, McCoy JP, Johnson KJ, Varani J. Protein degradation following treatment with hydrogen peroxide. Am J Pathol 1984;115:418-25.

119. Heinecke JW, Li W, Francis GA, Goldstein JA. Tyrosyl radical generated by myeloperoxidase catalyzes the oxidative cross-linking of proteins. J Clin Invest 1993;91:2866-72.

120. McCormick ML, Gaut JP, Lin TS, Britigan BE, Buettner GR, Heinecke JW. Electron paramagnetic resonance detection of free tyrosyl radical generated by myeloperoxidase, lactoperoxidase, and horseradish peroxidase. J Biol Chem 1998;273:32030-7.

121. Nagano S, Huang X, Moir RD, Payton SM, Tanzi RE, Bush AI. Peroxidase activity of cyclooxygenase-2 (COX-2) cross-links beta-amyloid (Abeta) and generates

Abeta-COX-2 hetero-oligomers that are increased in Alzheimer's disease. J Biol Chem 2004;279:14673-8.

122. Berlett BS, Stadtman ER. Protein oxidation in aging, disease, and oxidative stress. J Biol Chem 1997;272:20313-6.

123. Uchida K, Stadtman ER. Covalent attachment of 4-hydroxynonenal to glyceraldehyde-3-phosphate dehydrogenase. A possible involvement of intra- and intermolecular cross-linking reaction. J Biol Chem 1993;268:6388-93.

124. Benedetti A, Casini AF, Ferrali M, Comporti M. Effects of diffusible products of peroxidation of rat liver microsomal lipids. Biochem J 1979;180:303-12.

125. Grimsrud PA, Xie H, Griffin TJ, Bernlohr DA. Oxidative stress and covalent modification of protein with bioactive aldehydes. J Biol Chem 2008;283:21837-41.

126. Carbone DL, Doorn JA, Petersen DR. 4-Hydroxynonenal regulates 26S proteasomal degradation of alcohol dehydrogenase. Free Radic Biol Med 2004;37:1430-9.

127. Friguet B. Oxidized protein degradation and repair in ageing and oxidative stress. FEBS Lett 2006;580:2910-6.

128. Link G, Pinson A, Hershko C. Iron loading of cultured cardiac myocytes modifies sarcolemmal structure and increases lysosomal fragility. J Lab Clin Med 1993;121:127-34.

129. Mak IT, Weglicki WB. Characterization of iron-mediated peroxidative injury in isolated hepatic lysosomes. J Clin Invest 1985;75:58-63.

130. Deiss LP, Galinka H, Berissi H, Cohen O, Kimchi A. Cathepsin D protease mediates programmed cell death induced by interferon-gamma, Fas/APO-1 and TNF-alpha. EMBO J 1996;15:3861-70.

131. Roberg K. Relocalization of cathepsin D and cytochrome c early in apoptosis revealed by immunoelectron microscopy. Lab Invest 2001;81:149-58.

132. Yu Z, Persson HL, Eaton JW, Brunk UT. Intralysosomal iron: a major determinant of oxidant-induced cell death. Free Radic Biol Med 2003;34:1243-52.

133. Beckman JS, Beckman TW, Chen J, Marshall PA, Freeman BA. Apparent hydroxyl radical production by peroxynitrite: implications for endothelial injury from nitric oxide and superoxide. Proc Natl Acad Sci U S A 1990;87:1620-4.

134. Rubbo H, Radi R, Trujillo M, et al. Nitric oxide regulation of superoxide and peroxynitrite-dependent lipid peroxidation. Formation of novel nitrogen-containing oxidized lipid derivatives. J Biol Chem 1994;269:26066-75.

135. Cuzzocrea S, Caputi AP, Zingarelli B. Peroxynitrite-mediated DNA strand breakage activates poly (ADP-ribose) synthetase and causes cellular energy depletion in carrageenan-induced pleurisy. Immunology 1998;93:96-101.

136. Phelps DT, Ferro TJ, Higgins PJ, Shankar R, Parker DM, Johnson A. TNF-alpha induces peroxynitrite-mediated depletion of lung endothelial glutathione via protein kinase C. Am J Physiol 1995;269:L551-9.

137. Hunter T. Protein kinases and phosphatases: the yin and yang of protein phosphorylation and signaling. Cell 1995;80:225-36.

138. Grune T, Blasig IE, Sitte N, Roloff B, Haseloff R, Davies KJ. Peroxynitrite increases the degradation of aconitase and other cellular proteins by proteasome. J Biol Chem 1998;273:10857-62.

139. Henderson LM, Chappell JB. Dihydrorhodamine 123: a fluorescent probe for superoxide generation? Eur J Biochem 1993;217:973-80.

140. LeBel CP, Ischiropoulos H, Bondy SC. Evaluation of the probe 2',7'-dichlorofluorescin as an indicator of reactive oxygen species formation and oxidative stress. Chem Res Toxicol 1992;5:227-31.

141. Rothe G, Valet G. Flow cytometric analysis of respiratory burst activity in phagocytes with hydroethidine and 2',7'-dichlorofluorescin. J Leukoc Biol 1990;47:440-8.

142. Kooy NW, Royall JA, Ischiropoulos H, Beckman JS. Peroxynitrite-mediated oxidation of dihydrorhodamine 123. Free Radic Biol Med 1994;16:149-56.

143. Budd SL, Castilho RF, Nicholls DG. Mitochondrial membrane potential and hydroethidine-monitored superoxide generation in cultured cerebellar granule cells. FEBS Lett 1997;415:21-4.

144. Robinson KM, Janes MS, Beckman JS. The selective detection of mitochondrial superoxide by live cell imaging. Nat Protoc 2008;3:941-7.

145. Setsukinai K, Urano Y, Kakinuma K, Majima HJ, Nagano T. Development of novel fluorescence probes that can reliably detect reactive oxygen species and distinguish specific species. J Biol Chem 2003;278:3170-5.

146. Suematsu M, Kurose I, Asako H, Miura S, Tsuchiya M. In vivo visualization of oxyradical-dependent photoemission during endothelium-granulocyte interaction in microvascular beds treated with platelet-activating factor. J Biochem 1989;106:355-60.

147. Allen RC, Loose LD. Phagocytic activation of a luminol-dependent chemiluminescence in rabbit alveolar and peritoneal macrophages. Biochem Biophys Res Commun 1976;69:245-52.

148. Hinze WL, Riehl TE, Singh HN, Baba Y. Micelle-enhanced chemiluminescence and application to the determination of biological reductants using lucigenin. Anal Chem 1984;56:2180-91.

149. Totter JR. Light production in alkaline mixtures of reducing agents and dimethylbiacridylium nitrate. Photochem Photobiol 1975;22:203-11.

150. Greenlee L, Fridovich I, Handler P. Chemiluminescence induced by operation of iron-flavoproteins. Biochemistry 1962;1:779-83.

151. Miller EK, Fridovich I. A demonstration that O2- is a crucial intermediate in the high quantum yield luminescence of luminol. J Free Radic Biol Med 1986;2:107-10.

152. O'Brien PJ, Hulett LG. Hydroxyl radical involvement in the luminol chemiluminescence from the reaction of arachidonic acid with sheep vesicular gland microsomes. Prostaglandins 1980;19:683-91.

153. Radi R, Cosgrove TP, Beckman JS, Freeman BA. Peroxynitrite-induced luminol chemiluminescence. Biochem J 1993;290 (Pt 1):51-7.

154. Prichard PM, Cormier MJ. Studies on the mechanism of the horseradish peroxidase catalyzed luminescent peroxidation of luminol. Biochem Biophys Res Commun 1968;31:131-6.

155. Esterline RL, Trush MA. Lucigenin chemiluminescence and its relationship to mitochondrial respiration in phagocytic cells. Biochem Biophys Res Commun 1989;159:584-91.

156. Minkenberg I, Ferber E. Lucigenin-dependent chemiluminescence as a new assay for NAD(P)H-oxidase activity in particulate fractions of human polymorphonuclear leukocytes. J Immunol Methods 1984;71:61-7.

157. Gross S, Gammon ST, Moss BL, et al. Bioluminescence imaging of myeloperoxidase activity in vivo. Nat Med 2009;15:455-61.

158. Halliwell B, Whiteman M. Measuring reactive species and oxidative damage in vivo and in cell culture: how should you do it and what do the results mean? Br J Pharmacol 2004;142:231-55.

159. Berliner LJ, Khramtsov V, Fujii H, Clanton TL. Unique in vivo applications of spin traps. Free Radic Biol Med 2001;30:489-99.

160. Han JY, Takeshita K, Utsumi H. Noninvasive detection of hydroxyl radical generation in lung by diesel exhaust particles. Free Radic Biol Med 2001;30:516-25.

161. Bellosillo B, Villamor N, Lopez-Guillermo A, et al. Complement-mediated cell death induced by rituximab in B-cell lymphoproliferative disorders is mediated in vitro by a caspase-independent mechanism involving the generation of reactive oxygen species. Blood 2001;98:2771-7.

162. Pei XY, Dai Y, Grant S. Synergistic induction of oxidative injury and apoptosis in human multiple myeloma cells by the proteasome inhibitor bortezomib and histone deacetylase inhibitors. Clin Cancer Res 2004;10:3839-52.

163. Shanafelt TD, Lee YK, Bone ND, et al. Adaphostin-induced apoptosis in CLL B cells is associated with induction of oxidative stress and exhibits synergy with fludarabine. Blood 2005;105:2099-106.

164. Berneis K, Kofler M, Bollag W, Kaiser A, Langemann A. The degradation of deoxyribonucleic acid by new tumour inhibiting compounds: the intermediate formation of hydrogen peroxide. Experientia 1963;19:132-3.

165. Mahmutoglu I, Kappus H. Oxy radical formation during redox cycling of the bleomycin-iron (III) complex by NADPH-cytochrome P-450 reductase. Biochem Pharmacol 1985;34:3091-4.

166. Muller I, Niethammer D, Bruchelt G. Anthracycline-derived chemotherapeutics in apoptosis and free radical cytotoxicity (Review). Int J Mol Med 1998;1:491-4.

167. Carmody RJ, Cotter TG. Signalling apoptosis: a radical approach. Redox Rep 2001;6:77-90.

168. Kim R, Emi M, Tanabe K, Murakami S, Uchida Y, Arihiro K. Regulation and interplay of apoptotic and non-apoptotic cell death. J Pathol 2006;208:319-26.

169. Sugioka K, Nakano M, Totsune-Nakano H, Minakami H, Tero-Kubota S, Ikegami Y. Mechanism of O2- generation in reduction and oxidation cycle of ubiquinones in a model of mitochondrial electron transport systems. Biochim Biophys Acta 1988;936:377-85.

170. Tay VK, Wang AS, Leow KY, Ong MM, Wong KP, Boelsterli UA. Mitochondrial permeability transition as a source of superoxide anion induced by the nitroaromatic drug nimesulide in vitro. Free Radic Biol Med 2005;39:949-59.

171. Erdal H, Berndtsson M, Castro J, Brunk U, Shoshan MC, Linder S. Induction of lysosomal membrane permeabilization by compounds that activate p53-independent apoptosis. Proc Natl Acad Sci U S A 2005;102:192-7.

172. Kanzawa T, Germano IM, Komata T, Ito H, Kondo Y, Kondo S. Role of autophagy in temozolomide-induced cytotoxicity for malignant glioma cells. Cell Death Differ 2004;11:448-57.

Chapter 2: Proposed Strategy and Experimental Methods

2.1 Proposed Strategy

Studies in our lab have shown that HeLa cells transiently expressing Firefly Luciferase (fLuc) or Renilla Luciferase (RLuc) exhibited severely diminished bioluminescence when treated with a PCD-inducing drug. However, when stable mutant variants of luciferase were utilized, bioluminescence measurements were less sensitive to these treatment conditions. Based on these observations, it was hypothesized that the bioluminescent ratio (stable luciferase activity:wild-type luciferase activity) could be used to report on the extent of intracellular stress associated with PCD, inducing agents or other environmental factors. A schematic of this hypothesis is illustrated in Figure 2.1; bioluminescence from the stable luciferase variant remains relatively constant over a range of drug dosages/treatment time while wild-type luciferase bioluminescence declines(Figure 2.1A). The ratio of stable:wild-type luciferase activity thus increases over drug dosage or time course, accordingly (Figure 2.1B). Coexpression of the mutant and wild-type luciferases would ultimately create a Ratiometric Bioluminescent sensor (RBS) for cellular stress and PCD.

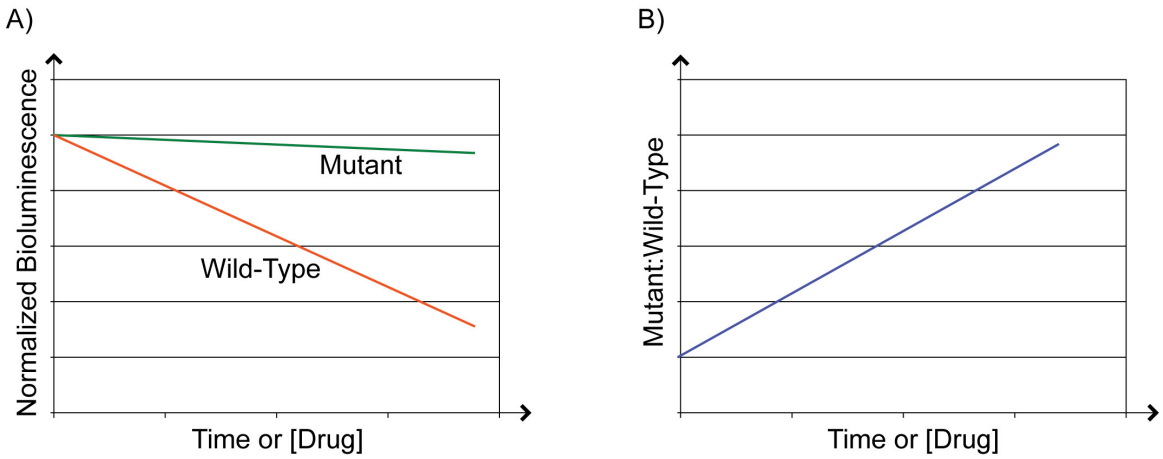

Figure 2.1. Schematic of RBS. (A) Over increasing time or drug dosage it is expected that the mutant luciferase bioluminescence will remain relatively stable while the wild-type luciferase bioluminescence will decrease. (B) Over the same time or drug dosage increase, the ratio (mutant bioluminescence:wild-type bioluminescence) will increase.

When considering which luciferases to incorporate into the RBS, it is necessary that the bioluminescence from each of the proteins can be distinguished. This can be accomplished by selecting stable and wild-type luciferase variants that catalyze different substrates, e.g., luciferin and coelenterazine. Distinct signals can then be obtained from each luciferase by adding one substrate first, measuring the signal, and either washing the substrate out (*in vitro*) or allowing the substrate to clear (*in vivo*) before addition of the second substrate. An alternative for *in vitro* assays involves the use of the Dual-Glo Luciferase assay from Promega. This assay utilizes two proprietary solutions: the first solution contains the substrate for fLuc and the second solution contains a reagent to quench the bioluminescence of fLuc in addition to the substrate for RLuc.

As an alternative to using two different substrates to distinguish between stable and wild-type luciferase variants, luciferase enzymes can also be selected that emit light

at different wavelengths and thus can be differentiated optically. In this scenario, multiple emission filters can be applied during bioluminescence imaging in order to obtain specific signals for each luciferase. For example, the emission wavelength of RLuc is 480 nm and the emission wavelength of fLuc is 612; in this case, both substrates can be administered during the same imaging session, and optically distinct emission filters can be implemented to specifically obtain bioluminescent images from each enzyme. Therefore, it is not necessary to wait for one substrate to clear before the second can be administered and imaged.

2.2 Materials and Methods

2.2.1 Preliminary transient transfection studies

The DNA sequence encoding fLuc was PCR amplified from the pGL3-Basic vector (Promega, Madison, WI) and inserted into the pCDNA3.1+ vector (Invitrogen, Carlsbad, CA) between the BamHI and EcoRI restriction sites, creating fLuc-pCDNA3.1+. The fLuc-pCDNA3.1+ vector was modified with 5 amino acid mutations (F14R, L35Q, V182K, I232K, F465R) using the QuikChange Multi Site Directed Mutagenesis Kit (Stratagene, La Jolla, CA) according to the manufacturer's instructions, ultimately creating fLuc5. The phRL-CMV vector (Promega) encoding Renilla Luciferase was modified to contain eight amino acid mutations within the RLuc sequence (A55T, C124A, S130A, K136R, A143M, M185V, M253L, and S287L) using the QuikChange Multi Site Directed Mutagenesis Kit (Stratagene) according to the manufacturer's instructions, ultimately creating RLuc8. Cells were plated at a density of

24,500 cells/well in a 48-well tissue culture plate (BD Biosciences, Franklin Lakes, NJ) and transiently transfected with either the fLuc-pCDNA3.1+, phRL-CMV (encoding Renilla Luciferase (RLuc)) (Promega), fLuc5 or RLuc8 vectors using Lipofectamine 2000 (Invitrogen) according to the manufacturer's instructions. After 24 hours, culture medium was replaced and the transfected cells were allowed to recover for another 24 hours. Transfected cells were treated with 1 μM Staurosporine (Sigma, St. Louis, MO) or PBS (pH 7.4) for indicated time periods. In certain assays, cells were treated with 20 μg/mL phenylbenzothiazole (PBT, Sigma) in addition to STS. At selected time points, fLuc, RLuc and fLuc5 measurements were taken using a Dual-Glo Luciferase assay system (Promega) according to the manufacturer's instructions and an Infinite 200 plate reader (Tecan, Mannedorf, Switzerland). To measure caspase-3 activity, the Caspase-3/7 Glo assay (Promega) was used according to the manufacturer's instructions and bioluminescence measurements were obtained from an Infinite 200 plate reader (Tecan).

2.2.2 RBS plasmid vector construction

The internal ribosome entry site (IRES) from the pIRES2-DsRed Express Vector (Clontech, Mountain View, CA) was cloned into the pIRES vector (Clontech) using restriction enzymes NheI and KpnI (New England Biolabs, Ipswich, MA), creating the pIRES12 vector. The DNA sequence encoding Firefly Luciferase (fLuc) from the pGL3-Basic vector (Promega) was PCR amplified and inserted into pCDNA3.1+ (Invitrogen) between the BamHI and EcoRI restriction sites. The fLuc sequence was subsequently cloned into pIRES12 using the NheI and XbaI restriction sites of fLuc-pCDNA3.1+ and the XbaI site of pIRES12. RLuc8 was cloned into the pIRES12-fLuc vector at the NheI

and BglII restriction sites. The resulting RLuc8-IRES-fLuc sequence was cloned into the pLENTI6/V-5 TOPO vector (Invitrogen) per the manufacturer's instructions to create the final vector necessary for the Ratiometric Bioluminescent Sensor (RBS). The final RBS plasmid map is shown in Figure 2.2.

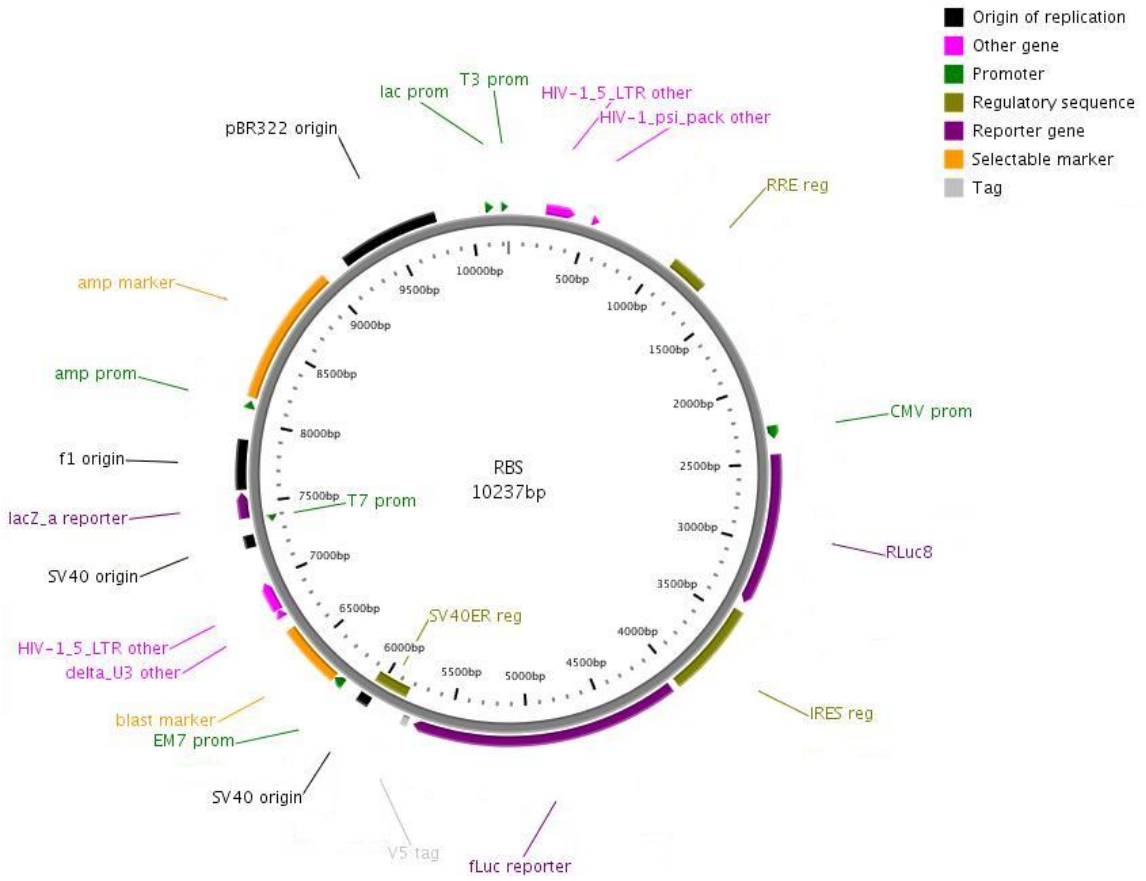

Figure 2.2. Plasmid map of the RBS. Image created using PlasMapper (1).

2.2.3 Reverse RBS plasmid vector construction

The RLuc8 sequence from the phRL-CMV vector (Promega) was PCR amplified and cloned into pCDNA3.1+ (Invitrogen) between the BamHI and EcoRI restriction sites, creating RLuc8-pCDNA2.1+. RLuc8 was subsequently cloned into pIRES12 using the

NheI and XbaI restriction sites of RLuc8-pCDNA3.1+ and the XbaI site of pIRES12, creating pIRES12-RLuc8. The fLuc sequence was PCR amplified and inserted into pCDNA3.1+ between the BamHI and EcoRI restriction sites. The fLuc sequence from the pGL3-Basic vector (Promega) was subsequently cloned into the pIRES12-RLuc8 vector at the NheI and BglII restriction sites. The resulting fluc-pIRES-RLuc8 sequence was cloned into the pLENTI6/V-5 TOPO vector per the manufacturer's instructions to create the final vector necessary for the reverse RBS.

2.2.4 Cell culture

Human cervical carcinoma (HeLa) and human breast adenocarcinoma (MCF7) cells (ATCC, Manassas, VA) were grown in Eagle's Minimum essential medium (Mediatech, Manassas, VA) supplemented with 10% fetal bovine serum (FBS, HyClone, Logan, UT), 1.5 g/L sodium bicarbonate, 100 U/mL penicillin and 100 μg/mL streptomycin (Invitrogen). Human embryonic kidney (293T/17) cells (ATCC) were grown in Dulbecco's Modified Eagle's Medium (DMEM, Mediatech) supplemented with 10% FBS (Hyclone), 1.5 g/L sodium bicarbonate, 100 U/mL penicillin and 100 μg/mL streptomycin (Invitrogen). The genetically modified human embryonic kidney cells (293FT, Invitrogen) for generating lentiviral particles were cultured in Dulbecco's Modified Eagle's Medium (DMEM, Mediatech) supplemented with 10% fetal bovine serum (FBS, HyClone, Logan, UT), 1.5 g/L sodium bicarbonate, 1 mM sodium pyruvate, 0.1 mM MEM non-essential amino acids (NEAA), 6 mM L-glutamine, 100 U/mL penicillin and 100 μg/mL streptomycin (Invitrogen). Cells that were genetically engineered to stably express RBS (described below) also had Blasticidin (Invitrogen)

added at a final concentration of 4 μg/mL. All cells were cultivated in a 37°C humidified incubator with 5% CO_2.

2.2.5 Lentiviral particle production and stable cell line creation

RBS lentiviral particles were produced using the Virapower Lentiviral Directional TOPO Expression Kit (Invitrogen) according to the manufacturer's instructions. Briefly, 293FT cells were transfected with viral packaging plasmids and the RBS lentiviral vector using Lipofectamine 2000 (Invitrogen). Viral supernatant was harvested 48 hours after transfection, concentrated using Peg-it Virus Concentration solution (System Biosciences, Mountain View, CA) and the titer was assessed. Concentrated viral particles were added to HeLa, MCF7 and 293T/17 cells, which were subsequently selected for stable genomic integration using Blasticidin (Invitrogen), resulting in RBS-HeLa, RBS-MCF7 and RBS-293T/17 cells.

2.2.6 Cellular stress and inhibition assays

To induce cellular stress, RBS-cells were treated with various compounds listed in Table I. Stressed and unstressed cells were also incubated with inhibitors that target various intracellular protein degradation/modification pathways. The specific compounds/proteins that were utilized as inhibitors and the respective final working concentrations are also listed in Table 2.1. Inhibitors were added to cells for 1 hour prior to adding inducers of cellular stress and left in the media for the duration of the treatment. Analogous controls were conducted in the absence of stress inducers.

Table 2.1. Summary of reagents.

	Reagent	Induces/Inhibits	Manufacturer	Working Concentration
Stress Inducers	Staurosporine (STS)	PCD, ROS/-	Sigma	0 - 50 μM
	Hydrogen peroxide (H2O2)	ROS/-	Fisher	0 - 10 mM
	Hypoxanthine (HX)	ROS/-	Sigma	50 μM
	Xanthine Oxidase (XO)	ROS/-	Sigma	25 mU/mL
	Doxorubicin (DOX)	PCD/-	Sigma	1 μM
	Camptothecin (CPT)	PCD/-	Sigma	10 μM
	Sodium Selenite (SSe)	PCD/-	MP Biomedicals	0 – 55 μM
	Resveratrol (Res)	PCD/-	Enzo Life Sciences	0 – 1 mM
Inhibitors/Scavengers	MG-132	-/proteasome	Fisher	20 μM
	Epoxomicin	-/proteasome	Enzo Life Sciences	10 μM
	Lactacystin	-/proteasome	Sigma	10 μM
	Calpain Inhibitor III	-/calpains	Calbiochem	100 μM
	Pepstatin A	-/cathepsins	Enzo Life Sciences	100 μM
	Ammonium Chloride	-/autophagy	Alfa Aesar	1 mM
	z-vad-fmk	-/caspases	Sigma	1 μM
	Tiron	-/superoxide	Sigma	10 mM
	TEMPOL	-/superoxide	Sigma	10 mM
	MnTMPyp	-/superoxide	Enzo Life Sciences	100 μM
	Mannitol	-/hydroxyl radical	Sigma	100 mM
	DFO	-/hydroxyl radical	Calbiochem	50 μM
	TEPA	-/hydroxyl radical	Sigma	50 μM
	Catalase	-/hydrogen peroxide	Sigma	40 U/mL
	Allopurinol	-/hydrogen peroxide	MP Biomedicals	100 μM
	Acetylsylic Acid (Aspirin)	-/hydrogen peroxide	Fisher	1 mM
	Uric Acid	-/peroxynitrite	Alfa Aesar	1 mM

2.2.7 Cellular bioluminescence assays

Unless otherwise noted, bioluminescence assays were performed 24 hours after plating 10,000 RBS-HeLa cells/well in a white-walled 96 well tissue culture plate (BD Biosciences). The Dual-Glo Luciferase Assay System (Promega) was utilized according

to the manufacturer's instructions to obtain both fLuc and RLuc8 bioluminescence measurements from an Infinite 200 plate reader (Tecan). In the case of using MnTMPyP as an inhibitor, the cell media was removed, cells were gently washed and the media was replaced before using the Dual-Glo Luciferase Assay System as it was found that the compound interfered with the bioluminescence measurements.

2.2.8 Cellular bioluminescence imaging

RBS-HeLa cells were plated at a density of 10,000 cells/well in a black-walled 96 well tissue culture plate (BD Biosciences). The Dual-Glo Luciferase Assay System (Promega) was utilized according to the manufacturer's instructions in order to obtain bioluminescent images in an Omega 16vs imaging system (UltraLum, Claremont, CA). It should be noted that the exact position of the 96 well plate was kept constant throughout the imaging session in order for accurate ratiometric images to be calculated.

2.2.9 Cellular bioluminescence image analysis

Image analyses were performed using ImageJ (NIH, Bethesda, MD). Image background was determined by measuring 3 regions of interest (ROIs) surrounding the bioluminescent ROI. After background subtraction, the RLuc8 image was divided by the fLuc image using the 'Math' command under the 'Process' menu tab.

2.2.10 Cell death assays

Caspase Activity: PCD was induced (as described above) 24 hours after plating 10,000 cells/well in white-walled 96 well tissue culture plates (BD Biosciences). After indicated treatment times, the Caspase 3/7-Glo Assay (Promega) was performed according to the manufacturer's protocol and bioluminescence measurements were obtained from and Infinite 200 plate reader (Tecan). All values were normalized to controls (i.e. pre-treatment values).

DNA Fragmentation: PCD was induced (as described above) 24 hours after plating 300,000 cells/well in 6 well tissue culture plates (BD Biosciences). After indicated treatment times, TUNEL assays for DNA fragmentation were performed using the TUNEL/ApoBRDU assay kit (Invitrogen) according to the manufacturer's protocol. Percent DNA fragmentation was determined using flow cytometry on a Guava EasyCyte flow cytometer (Guava Technologies, Hayward, CA). Analysis of flow cytometry data was performed using FlowJo software (Treestar, Ashland, OR).

2.2.11 Proteasome inhibition control assay

RBS-HeLa cells were plated at a density of 10,000 cells/well in a white-walled 96-well plate (BD Biosciences). 24 hours later, cells were treated with PBS (pH 7.4), 20 μM MG-132, 10 μM epoxomicin or 10 μM lactacystin for 1 hour. RBS-HeLa cells were then treated with PBS (pH 7.4) or 10 μM Staurosporine (STS) in addition to the inhibitors for 24 hours. Proteasome activity measurements were obtained using the

Proteasome-Glo 3-Substrate Cell-Based Assay system (Promega) according to the manufacturer's instructions.

2.2.12 Protease inhibition control assays

Calpain Inhibitor III: RBS-HeLa cells were plated at a density of 10,000 cells/well in a white-walled 96-well plate (BD Biosciences). 24 hours later, cells were treated with either PBS (pH 7.4) or 100 μM Calpain Inhibitor III for 1 hour. PBS (pH 7.4) or 10 μM STS was subsequently added to the cells, and both compounds remained on the cells for 24 hours. Calpain activity measurements were obtained using the Calpain-Glo Protease Assay (Promega) according to the manufacturer's instructions.

Pepstatin A: RBS-HeLa cells were plated at a density of 10,000 cells/well in a black-walled 96-well plate (BD Biosciences). 24 hours later, cells were treated with either PBS (pH 7.4) or 100 μM pepstatin A for 1 hour, with either PBS (pH 7.4) or 10 μM STS added for another 24 hours. Cathepsin activity was assessed using the CV-Cathepsin B Detection Kit (Enzo Life Sciences) according to the manufacturer's instructions with one exception; after the final wash step, the plate was read on an Infinite 200 plate reader (Tecan) for fluorescence ($550_{ex}/610_{em}$), as opposed to microscopy.

Ammonium Chloride: In lieu of a control assay for ammonium chloride effectively inhibiting lysosome-phagosome fusion, we direct the reader to a seminal paper regarding this phenomena in HeLa cells(2).

z-vad-fmk: RBS-HeLa cells were plated at a density of 10,000 cells/well in a white-walled 96-well plate (BD Biosciences). 24 hours later, cells were treated with either PBS (pH 7.4) or 1 μM z-vad-fmk for 1 hour. PBS (pH 7.4) or 10 μM STS was subsequently added to the cells, and both compounds remained on the cells for 24 hours. Caspase activity measurements were obtained using the Caspase-Glo 3/7 Assay (Promega) according to the manufacturer's instructions.

2.2.13 Superoxide ($O_2^{\bullet-}$) scavenger control assay

RBS-HeLa cells were plated at a density of 120,000 cells per well of a 12 well tissue culture plate (BD Biosciences). 24 hours later, cells were treated with PBS (pH 7.4), 10 mM TEMPOL, 10 mM Tiron or 100 μM MnTMPyP for 1 hour. PBS (pH 7.4) or 10 μM STS was subsequently added to the cells, and both compounds remained on the cells for 24 hours. Intracellular $O_2^{\bullet-}$ levels were then determined by incubating the cells in 5 μM dihydroethidium (DHE, Invitrogen) for 30 minutes at 37°C and subjecting them to flow cytometry using a Guava EasyCyte (Guava Technologies, Hayward, CA). Analysis of flow cytometry data was accomplished using FlowJo software (TreeStar, Ashland, OR).

2.2.14 Hydroxyl Radical ($^{\bullet}OH$) scavenger/inhibitor control assay

RBS-HeLa cells were plated at a density of 120,000 cells per well of a 12 well tissue culture plate (BD Biosciences). 24 hours later, the cells were incubated with 10

μM hydroxyphenylfluorescein (HPF, Sigma) for 30 minutes at 37°C. Cells were then treated with PBS (pH 7.4), 100 mM Mannitol, 50 μM deferoxamine (DFO), 50 μM tetraethylenepentamine (TEPA) or 50 μM DFO plus 50 μM TEPA for 1 hour. PBS (pH 7.4) or 10 μM STS was subsequently added to the cells, and all compounds remained on the cells for 24 hours. Intracellular $^{\bullet}OH$ levels were determined by subjecting the cells to flow cytometry using a Guava EasyCyte (Guava Technologies). Analysis of flow cytometry data was accomplished using FlowJo software (TreeStar).

2.2.15 Hydrogen peroxide (H_2O_2)-related inhibitor control assays

Catalase and Allopurinol: RBS-HeLa cells were plated at a density of 120,000 cells per well of a 12 well tissue culture plate (BD Biosciences). 24 hours later, the cells were incubated with 10 μM CM-H_2DCFDA (Invitrogen) for 30 minutes at 37°C. Cells were then treated with PBS (pH 7.4), 50 U/mL catalase or 100 μM allopurinol for one hour. PBS (pH 7.4) or 10 μM STS was subsequently added to the cells, and all compounds remained on the cells for 24 hours. Intracellular H_2O_2 levels were determined by subjecting the cells to flow cytometry using a Guava EasyCyte (Guava Technologies). Analysis of flow cytometry data was accomplished using FlowJo software (Treestar).

Aspirin: RBS-HeLa cells were plated at a density of 1.2 x 10^6 cells in 100 mM tissue culture dishes (BD Biosciences). 24 hours later, the cells were treated with PBS (pH 7.4) or 1 mM aspirin for one hour, followed by PBS (pH 7.4) or 10 μM STS for 24

hours. Cyclooxygenase (COX) activity was determined by using the Cox Activity Assay Kit (Cayman Chemical Company, Ann Arbor, MI).

2.2.16 Quantitative real-time PCR (qRT-PCR)

Cytoplasmic RNA from RBS-HeLa cells cultured under indicated conditions was isolated using the High Pure RNA Isolation Kit (Roche, Mannheim, Germany) and subsequently reverse-transcribed to single-stranded cDNA using a High-Capacity cDNA Reverse Transcription Kit (Applied Biosystems, Foster City, CA) according to each manufacturer's protocol. Quantitative RT-PCR was performed on an ABI PRISM 7300 Sequence detection system using FAM-labeled Taqman primer sets for RLuc8, fLuc and β-actin (as a control) and the Taqman universal PCR Master Mix (Applied Biosytems) according to the manufacturer's protocol.

2.2.17 Western blot analysis

Following indicated culture conditions, RBS-HeLa cells were washed 3 times with 1x PBS (pH7.4). Proteins were extracted using RIPA extraction buffer (50 mM Tris HCL, pH 7.4, 1% Triton X-100, 0.25% Na-deoxycholate, 150 mM NaCl, 1 mM EDTA and a Complete Mini Protease Inhibitor Cocktail Tablet (Roche)) at 4°C for 30 minutes with constant agitation. Total protein concentrations were measured using a BCA assay (Pierce, Rockford, IL). 30 μg of total protein from each sample were heated to 95°C in Laemmli Sample buffer containing 2% (v/v) 2-mercaptoethanol (Bio-Rad, Hercules, CA). After a 5 minute cooling period, the samples were quickly centrifuged and the

supernatants were immediately run on a 4-15% Tris-HCl gel (Bio-Rad). Proteins separated by electrophoresis were transferred to nitrocellulose membranes in 1X Transfer Buffer (Bio-Rad) at 15V for 30 minutes. Membranes were blocked in Blocking Buffer for Fluorescent Western Blotting (Rockland Immunochemicals, Gilbertsville, PA) for 60 minutes. The membranes were incubated with anti-fLuc (Sigma), anti-rLuc (Millipore, Billerica, MA) or anti-β-actin primary antibodies in blocking buffer overnight. After washing 3 times with TBS-T, the membranes were incubated with either Anti-Mouse IgG Antibody IRDye800 conjugated (fLuc, rLuc) or Anti-Rabbit IgG Antibody IRDye800 conjugated (β-actin) at a 1:10,000 dilution (Rockland Immunochemicals). The fluorescent signal from the membranes was imaged using the Odyssey Infrared Imaging System (Li-Cor Biosciences, Lincoln, NE)

2.2.18 Intracellular hydrogen peroxide detection

Amplex Red: HeLa cells subjected to various treatment conditions, as indicated, were lysed using RIPA buffer and the clarified lysate samples were used in the Amplex Red Hydrogen Peroxide/Peroxidase assay kit (Invitrogen) to determine levels of H_2O_2. Results were normalized to total protein content determined by the BCA assay (Pierce).

CM-H_2DCFDA: Cells were plated at a density of 120,000 cells per well of a 12 well tissue culture plate (BD Biosciences). 24 hours later, the cells were incubated with 10 μM CM-H_2DCFDA (Invitrogen) for 30 minutes at 37°C. The reagent was removed, the cells were washed with PBS (pH 7.4) and PCD was induced as described above. Cells were lifted using a rubber scraper, washed twice with PBS (pH 7.4) and

intracellular H_2O_2 levels were determined by subjecting the cells to flow cytometry using a Guava EasyCyte flow cytometer (Guave Technologies). Analysis of flow cytometry data was accomplished using FlowJo software (TreeStar).

2.2.19 RLuc8 and fLuc protein purification

The DNA sequences encoding RLuc8 and fLuc were PCR amplified and inserted into the pHAT 10 and pHAT 11 vectors (Clontech) between the BamHI and EcoRI restriction sites. 50 mL of bacterial cultures were inoculated in LB medium containing 50 μg/mL ampicillin overnight, shaking at 37°C. Cultures were expanded into 500 mL LB medium containing 50 μg/mL ampicillin for 1.5 hours, shaking at 37°C. Protein expression was induced by adding 500 μM IPTG (Fisher Scientific, Pittsburgh, PA) and shaking for 5 hours at 37°C. After centrifugation at 10,000 x g for 5 minutes, cell pellets were resuspended in 35 mL wash/extraction buffer (50 mM Phosphate, 300 mM NaCl, pH 7.0). Lysozyme (final concentration of 0.75 mg/mL) and PMSF (final concentration of 1 mM) were added and the cells were frozen at -80°C overnight after standing at room temperature for 20 minutes. Lysates were thawed in a 37°C water bath, sonicated and centrifuged at 20,0000 x g for 20 minutes. Clarified cell lysates were applied to a purification column loaded with TALON metal affinity resin (Clontech) and washed several times with wash/extraction buffer. The RLuc8 and fLuc proteins were eluted from the column using an imidazole gradient (10, 60, 150, 300, 450, 600, 700, 1000 mM). Samples from each imidazole concentration were subjected to SDS-PAGE in order to identify the most pure protein samples. Aliquots were heated to 95°C in Laemmli

sample buffer containing 2% (v/v) 2-mercaptoethanol (Bio-Rad). After a 5 minute cooling period the samples were immediately centrifuged and run on a 4-15% Tris-HCl gel (Bio-Rad). Proteins were visualized using the Simply Blue stain (Invitrogen) and the purest samples of each protein (i.e. the samples with the least amount of extraneous bands) were further purified on Amicon Ultra Centrifugal Filtration Devices (Millipore, Billerica, MA) of appropriate molecular weight cutoffs to remove the imidazole.

2.2.20 *In vitro* bioluminescence assays on purified proteins

For the xanthine/xanthine oxidase assay, equivalent concentrations of each protein were resuspended in a sample buffer consisting of phosphate buffered saline (PBS, Invitrogen), 1 mg/mL bovine serum albumin (BSA, Fisher Scientific) and a Complete Mini protease inhibitor cocktail tablet (Roche). Samples were treated with 50 μM hypoxanthine, 25 mU/mL xanthine oxidase (Sigma) or a combination of each and incubated at 37°C for indicated time periods. Luminescence measurements were made on an Infinite 200 plate reader (Tecan) following the addition of Dual-Glo reagents (Promega).

For the H_2O_2 assay, 650 nM of both purified fLuc and RLuc8 proteines were used. Proteins were added to PBS containing a range of H_2O_2 concentrations (0-10 mM) for up to 120 minutes at 37°C. At indicated times, 10 μL aliquots of each sample were subjected to bioluminescence measurements on an Infinite 200 plate reader (Tecan), following the addition of Dual-Glo reagents (Promega).

2.2.21 SDS-PAGE gels on purified proteins treated with H_2O_2

Three protein conditions were used: fLuc alone (650 nM), rLuc alone (650 nM) or fLuc and RLuc together (650 nM total protein). Proteins were added to PBS containing a range of H_2O_2 concentrations (0-10 mM) for up to 120 minutes at 37°C. At indicated times, 10 μL aliquots were removed and heated to 95°C in Laemmli sample buffer containing 2% (v/v) 2-mercaptoethanol (Bio-Rad). After a 5 minute cooling period the samples were immediately centrifuged and run on a 4-15% Tris-HCl gel (Bio-Rad). Proteins were visualized using the Simply Blue stain (Invitrogen) according to the manufacturer's instructions.

2.2.22 Cellular protein carbonylation detection

To assay for protein carbonylation, the OxyBlot Protein Carbonlyation Detection Kit (Millipore) was used according to the manufacturer's instructions. Briefly, RBS-HeLa cells were treated with PBS or STS for 24 hours. Proteins were extracted using RIPA extraction buffer (50 mM Tris HCL, pH 7.4, 1% Triton X-100, 0.25% Na-deoxycholate, 150 mM NaCl, 1 mM EDTA and a Complete Mini Protease Inhibitor Cocktail Tablet) at 4°C for 30 minutes with constant agitation. Total protein concentrations were measured using a BCA assay and 15 μg of total protein was treated with a final concentration of 6% SDS to denature the proteins. The samples were then treated with 2,4-dinitrophenylhydrazine (DNPH) to derivatize the carbonyl groups in the protein side chains to 2,4-dinitrophenylhydrazone (DNP-hydrazone). Also, a second set of samples was treated with Derivatization-Control solution, to serve as a negative

control. The protein samples were run on a 4-15% Tris-HCl gel (Bio-Rad). Proteins separated by electrophoresis were transferred to nitrocellulose membranes in 1X Transfer Buffer (Bio-Rad) at 15V for 30 minutes. The membrane was blocked in blocking/dilution buffer (1%BSA/PBS-T (PBS, pH 7.4, 0.05% Tween-20)) for 1 hour and then incubated with rabbit anti-DNP antibody (1:150 dilution in blocking/dilution buffer) for one hour. After rinsing with PBS-T, the membrane was incubated with HRP-conjugated goat anti-rabbit IgG antibody (1:300 dilution in blocking/dilution buffer) for one hour and again rinsed. The Immun-Star HRP Chemiluminescent kit (Bio-rad) was used and the signal was imaged on an Omega 16vs imaging system (UltraLum).

2.2.23 Purified protein carbonylation detection

To assay for protein carbonylation, the OxyBlot Protein Carbonylation Detection Kit (Millipore) was used according to the manufacturer's instructions. Briefly, 650 nM of pure fLuc and RLuc8 proteins were treated with PBS or 5 mM H_2O_2 for 2 hours, followed by denaturation with SDS (final concentration: 6%). The samples were then treated with 2,4-dinitrophenylhydrazine (DNPH) to derivatize the carbonyl groups in the protein side chains to 2,4-dinitrophenylhydrazone (DNP-hydrazone). The protein samples were run on a 4-15% Tris-HCl gel (Bio-Rad). Proteins separated by electrophoresis were transferred to nitrocellulose membranes in 1X Transfer Buffer (Bio-Rad) at 15V for 30 minutes. The membrane was blocked in blocking/dilution buffer (1%BSA/PBS-T (PBS, pH 7.4, 0.05% Tween-20)) for 1 hour and then incubated with rabbit anti-DNP antibody (1:150 dilution in blocking/dilution buffer) for one hour. After rinsing with PBS-T, the membrane was incubated with Anti-Rabbit IgG Antibody IRDye800 conjugated (β-actin) at a 1:10,000 dilution (Rockland Immunochemicals).

The fluorescent signal from the membranes was imaged using the Odyssey Infrared Imaging System (Li-Cor Biosciences, Lincoln, NE).

2.2.24 Animal imaging

Five week old female nude mice (Charles River Laboratories International LLC, Wilmington, MA) were obtained and given free access to food and water. All experiments conformed to animal care protocols approved by the Institutional Animal Care and Use Committee (IACUC) of the University of Pennsylvania. For tumor induction, 2.5 x 10^6 RBS-HeLa cells were resuspended in PBS (pH 7.4) and subcutaneously implanted in the lower right flank of lightly anesthetized mice (1% isoflurane/oxygen mixture). Once the tumors reached ~ 1 cm in diameter, each group was imaged prior to any inhibitor/drug treatment. Briefly, the animals were i.v. injected with 100 μL of 500 μg/mL sterile coelenterazine (NanoLight, Pinetop, AZ) in a 20/20/60 mixture of USP grade ethanol/propylene glycol/PBS and imaged using an IVIS Lumina II (Caliper Life Sciences, Hopkinton, MA) under anesthesia (2.5% isoflurane/oxygen mixture). The substrate was allowed to clear for 3 hours before the animals received an i.p. injection of 200 μL of sterile 15 mg/mL luciferin (Biosynth, Itasca, IL) in PBS (pH 7.4) and imaged using an IVIS Lumina II under anesthesia (2.5% isoflurane/oxygen mixture). Immediately following the second imaging session animals were divided into 4 groups (PBS/PBS, PBS/STS, Allo/PBS, Allo/STS) and the inhibitor (1 mM Allopurinol) or control (PBS, pH 7.4) was intratumorally injected. After 1 hour, the cell death inducer (500 μM STS) or control (PBS, pH 7.4) was intratumorally injected. All intratumoral

injections were of a volume of 25 μL. 24 hours later, the animals were imaged in the same manner as stated previously.

2.2.25 Animal image analysis

Image analysis was performed using Living Image Software (Caliper Life Sciences). Images were first background subtracted (treating the animal body as the background) and automatic (5% threshold) ROIs were generated around each tumor. Average bioluminescent counts were recorded and used in the ratio calculations. For each group, data was normalized to the day 1 ratio values.

2.3 References

1. Dong X, Stothard P, Forsythe IJ, Wishart DS. PlasMapper: a web server for drawing and auto-annotating plasmid maps. Nucleic Acids Res 2004;32:W660-4.

2. Rote KV, Rechsteiner M. Degradation of microinjected proteins: effects of lysosomotropic agents and inhibitors of autophagy. J Cell Physiol 1983;116:103-10.

Chapter 3: Development of the Ratiometric Bioluminescent Sensor (RBS) and its response to cellular stress in HeLa cells

3.1 Abstract

The use of bioluminescent proteins as optical reporters for PCD and other cellular stress states is advantageous owing to their sensitivity, non-invasiveness, and *in vivo* imaging capability. However, the possibility of reporter degradation during these biological processes must be accounted for. In this chapter, we show that wild-type bioluminescent proteins (luciferases) exhibit a marked decrease in activity in cells undergoing PCD and that certain chemical treatments and mutations can rescue activity. Wild-type fLuc and a stable variant of RLuc (RLuc8) were incorporated into a Ratiometric Bioluminescent Sensor (RBS) and when expressed in HeLa cells, the RBS was capable of detecting PCD in a ratiometric manner.

3.2 Introduction

There are many optical sensors designed to image and/or report on programmed cell death (PCD). Many of these sensors are based on the specific proteolytic cleavage of the amino acid sequence DEVD by caspase-3, the cysteine-aspartic protease that is considered to be absolutely required for apoptotic PCD(1). Some of these caspase-3 dependent sensors are fluorescent in nature and typically involve the separation of a fluorophore and a quencher or overlapping FRET-pairs after DEVD cleavage by caspase-3. The fluorescent molecular reporters(2-4) hold an advantage over fluorogenic peptide

probes(5-11) in their synthesis costs and cellular delivery methods; however both categories of PCD sensors suffer from drawbacks, including autofluorescence and poor light penetration of tissue, making them less than ideal for *in vivo* applications.

To circumvent the issues surrounding fluorescent probes for PCD, several groups have recently utilized bioluminescent proteins as optical reporters for PCD. Bioluminescent proteins are highly sensitive as they emit no light until a specific substrate is present and one of the most prominently used bioluminescent proteins, Firefly luciferase (fLuc), emits a wavelength of light (610 nm) that is much less attenuated in tissues than many fluorescent molecules, making it a promising candidate for *in vivo* studies. Generally, these PCD sensors utilize the cleavage of the caspase-3 recognition sequence, DEVD, as a catalyst for luciferin (substrate) recognition(12, 13), removal of steric hindrance(14), or protein fragment complementation(15).

While the bioluminescent sensors for PCD seem to be superior to fluorescent sensors for *in vivo* imaging purposes, the design of any genetically encoded or peptidic sensor for PCD should take into account the possibility of sensor degradation and modification in cells undergoing PCD. It has been shown that certain proteases (e.g., calpains(16, 17) and cathepsins(18, 19)) can be upregulated during PCD, in addition to the oxidative modifications that can result from increases in various reactive oxygen species (ROS)(20-22). Thus, information garnered from these types of sensors should be highly scrutinized.

In this chapter, we show that wild-type luciferases do indeed suffer from activity loss in cells undergoing PCD. Pretreatment with phenylbenzothiazole (PBT), a compound shown to prevent the intracellular degradation of fLuc(23), abrogated fLuc

activity loss in cells undergoing PCD. Additionally, certain mutant forms of luciferase were analyzed under the same conditions; a fLuc (fLuc5) mutant exhibited slightly more activity than wild-type fLuc while an RLuc mutant (RLuc8) retained significant activity in cells undergoing PCD. Based on these observations, RLuc8 and fLuc were incorporated into one sensor to explore whether the ratio (RLuc8 bioluminescence:fLuc bioluminescence) could be used to report on PCD. It was found that the Ratiometric Bioluminescent Sensor (RBS) was capable of detecting PCD in STS-treated HeLa cells over ranges of time and dosage.

3.3 Results

In order to investigate the sensitivity of bioluminescent proteins to intracellular stresses incurred during PCD, we examined the effects of staurosporine (STS), a PCD-inducing drug(24) that has also been shown to increase intracellular ROS(25), on HeLa cells transiently expressing Firefly and Renilla luciferases (fLuc and RLuc, respectively). The normalized bioluminescence measurements of fLuc and RLuc decreased significantly over time with 1 μM STS treatment as shown in Figure 3.1. By 8 hours, fLuc activity was reduced by ~85% and RLuc activity was reduced by ~95%.

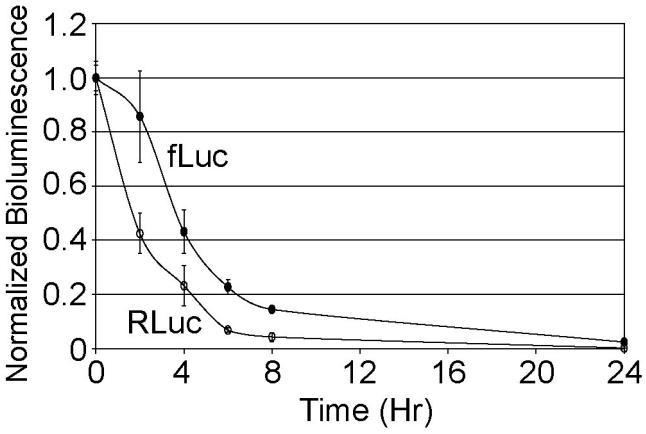

Figure 3.1. Effect of staurosporine on fLuc and RLuc bioluminescence. HeLa cells were transiently transfected with either fLuc or RLuc vectors and treated with 1 μM staurosporine (STS) for a time period of 24 hours. Bioluminescence measurements were taken at various time points and each point was normalized to time 0.

Under the same treatment conditions of 1 μM STS for 24 hours, caspase-3 activity in HeLa cells increased over the course of 12 hours before reaching a plateau and slowly decreasing (Figure 3.2), indicative of PCD. Caspase-3 activity was clearly elevated at time points where fLuc and RLuc bioluminescence was nearly completely diminished. Thus, the use of wild-type luciferases in sensors for PCD must be scrutinized carefully since their signals can be nearly completely abrogated before the appearance of the apoptotic markers (i.e., caspases) they are supposed to detect.

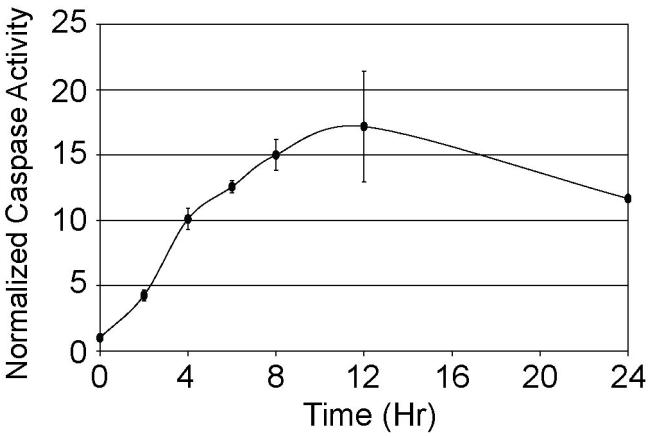

Figure 3.2. Caspase-3 activity during a time course of STS treatment. HeLa cells were treated with 1 μM STS for 24 hours. At selected time points, cells were assayed for caspase-3 activity using Caspase-3/7 Glo and each point was normalized to time 0.

To circumvent the issue of diminished bioluminescence during PCD, we investigated the potential use of a chemical stabilizer to prevent the loss of fLuc activity. Phenylbenzothiazole (PBT) has been shown to prevent the intracellular degradation of fLuc(23) when added to cell cultures. HeLa cells transiently expressing fLuc were treated with either 1 μM STS or 1 μM STS + 20 μg/mL PBT for 24 hours. Figure 3.3 shows that the bioluminescence of the cells treated with PBT in addition to STS was slightly higher and more stable than cells treated with STS alone.

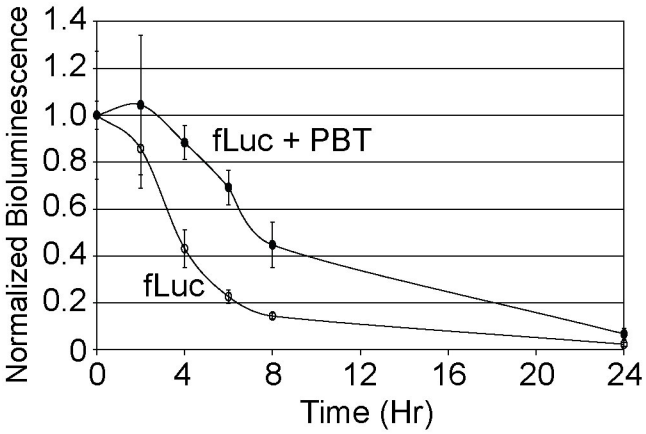

Figure 3.3. Response of fLuc to STS or STS + PBT treatment. HeLa cells transiently expressing fLuc were treated with either 1 μM STS or 1 μM STS + 20 μg/mL PBT for 24 hours. Bioluminescence measurements were taken at various time points and each point was normalized to time 0.

While the *in vitro* utilization of PBT to stabilize fLuc activity exhibited positive results, the use of this chemical may not translate well into *in vivo* models. Thus, we investigated the potential use of bioluminescent proteins that have been mutated to enhance their stability in our PCD sensor. Table 3.1 summarizes some of these proteins and the purported effects of the mutations.

Table 3.1. Luciferase mutations and their reported effects.

Enzyme	Mutations	Effects	Reference
FLuc5	F14R, L35Q, V182K, I232K, F465R	↑ pH tolerance, thermostable up to 45°C	(26)
RLuc8	A55T, C124A, S130A, K136R, A143M, M185V, M253L, and S287L	200x serum inactivation resistance and 4x brighter than WT	(27)

When HeLa cells were transiently transfected with a vector encoding either wild-type fLuc or fLuc5 and treated with 1 μM STS for a time course of 24 hours, the

normalized bioluminescence from the fLuc5 cells was slightly higher and more stable than that of fLuc (Figure 3.4).

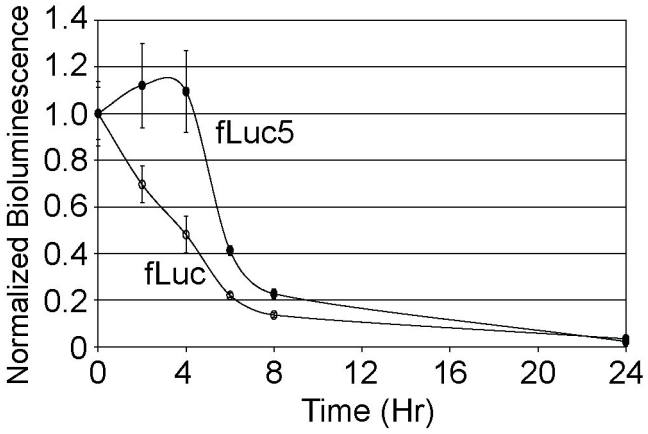

Figure 3.4. Effect of STS on fLuc5 compared to wt fLuc. HeLa cells were transiently transfected with fLuc or fLuc5 and treated with 1 μM STS for a time course of 24 hours. Bioluminescence measurements were taken at various time points and each point was normalized to time 0.

Similarly, when HeLa cells were transiently transfected with a vector encoding either wild-type RLuc or RLuc8 and treated with 1 μM STS for a time course of 24 hours, the normalized bioluminescence from the RLuc8 cells was higher and more stable than that of RLuc (Figure 3.5). RLuc8 clearly exhibits less activity loss than fLuc5, therefore it would ultimately be included in our bioluminescent sensor for PCD.

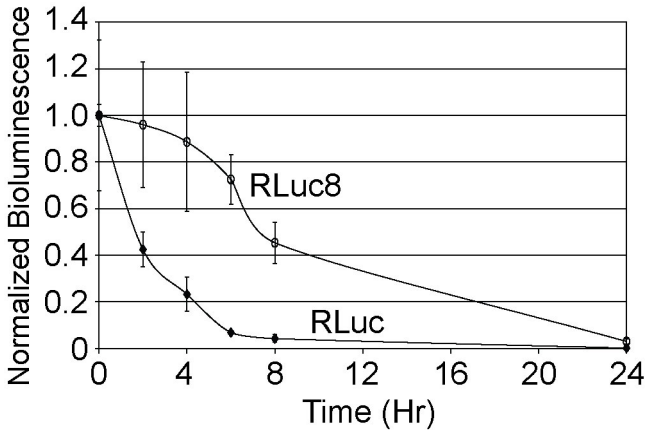

Figure 3.5. Effect of STS on RLuc8 compared to wt RLuc. HeLa cells were transiently transfected with RLuc or RLuc8 and treated with 1 μM STS for a time course of 8 hours. Bioluminescence measurements were taken at various time points and each point was normalized to time 0.

We have shown the fLuc and RLuc bioluminescence decreases significantly under PCD-inducing conditions while the bioluminescence of PBT/fLuc, fluc5, and RLuc8 remains more stable. These observations led us to hypothesize that we could incorporate an unstable luciferase and a stable luciferase into one sensor and that the bioluminescent ratio (stable bioluminescence:unstable luminescence) could be used to report on the extent of intracellular stress associated with PCD. We chose to incorporate fLuc and RLuc8 into this Ratiometric Bioluminescent Sensor, or RBS, for multiple reasons. RLuc8 exhibited the highest level of activity/stability under PCD-inducing conditions. Also, the emission wavelength of fLuc (~600 nm) makes it more suitable for *in vivo* imaging. Further, each of these enzymes utilizes a different substrate, effectively simplifying the distinction between the bioluminescence of fLuc and RLuc8. The fLuc and RLuc8 coding sequences flank an internal ribosomal entry site (IRES) in the plasmid construct, allowing both proteins to be translated from one bicistronic mRNA(28, 29);

this ensures that protein levels (and the thus the ratio) would be unaffected by any changes in promoter activity.

HeLa cells constitutively expressing the RBS (RBS-HeLa cells) were subjected to STS time course and dosage treatments. As seen in Figure 3.6A, upon treatment with 10 μM STS, the fLuc bioluminescence decreases while the RLuc8 bioluminescence remains relatively stable over the time course of 24 hours. This can be presented as an increase in the RLuc8:fLuc ratio (right-hand axis). Representative bioluminescent images obtained from RBS-HeLa cells under the same conditions are shown in Figure 3.6B. The resulting ratiometric images generated from the RLuc8 and fLuc images exemplify similar trends to the ratiometric measurements in Figure 3.6A. When RBS-HeLa cells were treated with a dosage range of STS (0-50 μM) for 6 hours, the RLuc8 bioluminescence remained stable, fLuc bioluminescence decreased and the RLuc8:fLuc ratio increased (Figure 3.6C). Consistent with these findings, bioluminescent images acquired under the same treatment conditions, and the corresponding ratiometric measurements, exhibited similar trends (Figure 3.6D).

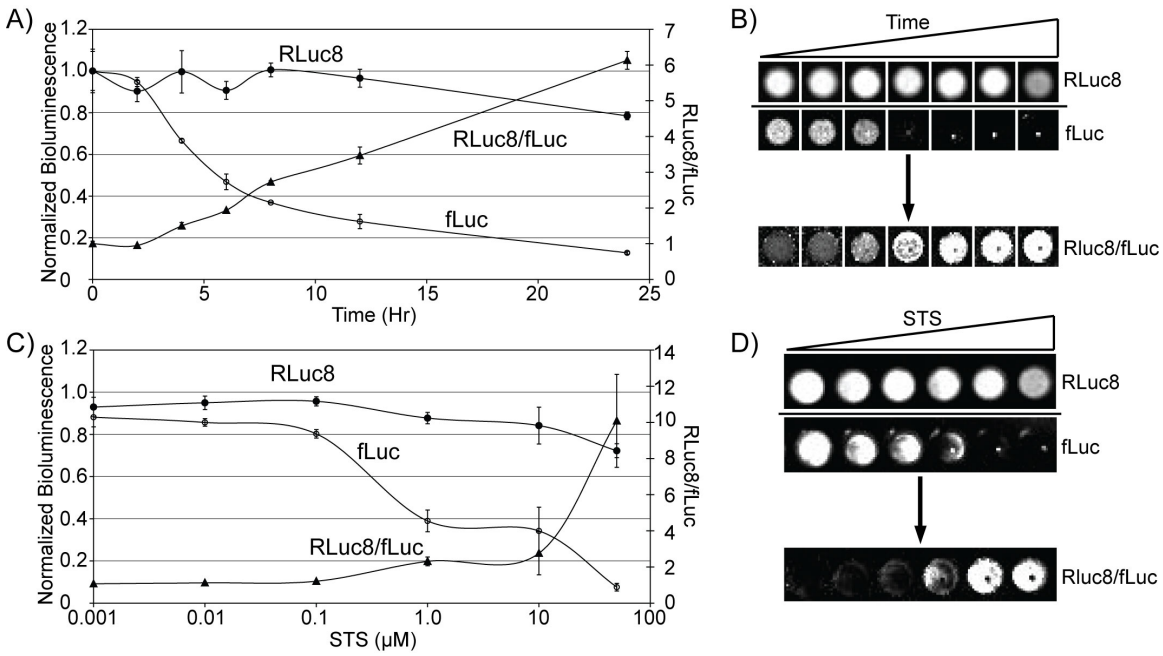

Figure 3.6. Response of RBS-HeLa cells to STS. (A) Bioluminescent measurements of RLuc8 and fLuc were acquired at various times during the course of 10 μM STS treatment. All measurements were normalized to values at time 0. The RLuc8:fLuc ratio was subsequently calculated for each time point (right axis). (B) A representative bioluminescent image of RLuc8 and fLuc activity in STS-treated cells throughout the time course is shown as well as the calculated ratiometric image, RLuc8:fLuc. (C) Bioluminescent measurements of RLuc8 and fLuc activity in cells treated with various doses of STS. The RLuc8:fLuc ratio is also shown (right axis). (D) Representative bioluminescent images of RLuc8 and fLuc activity in cells treated with various doses of STS. The calculated ratiometric image of RLuc8:fLuc is also shown.

To confirm that the RLuc8:fLuc ratio was independent of cell number, RBS-HeLa cells were plated at a range of 0 – 20,000 cells/well and bioluminescence measurements of RLuc8 and fLuc were taken 24 hours later. As shown in figure 3.7A, the RLuc8:fLuc ratio remained constant regardless of the cell seeding density. Additionally, little to no increase in the RLuc8:fLuc ratio was observed in cells that were not treated with STS

over a period of 24 hours (Figure 3.7B). The slight increase in RLuc8 and fLuc bioluminescence that was observed with time likely reflects cell proliferation.

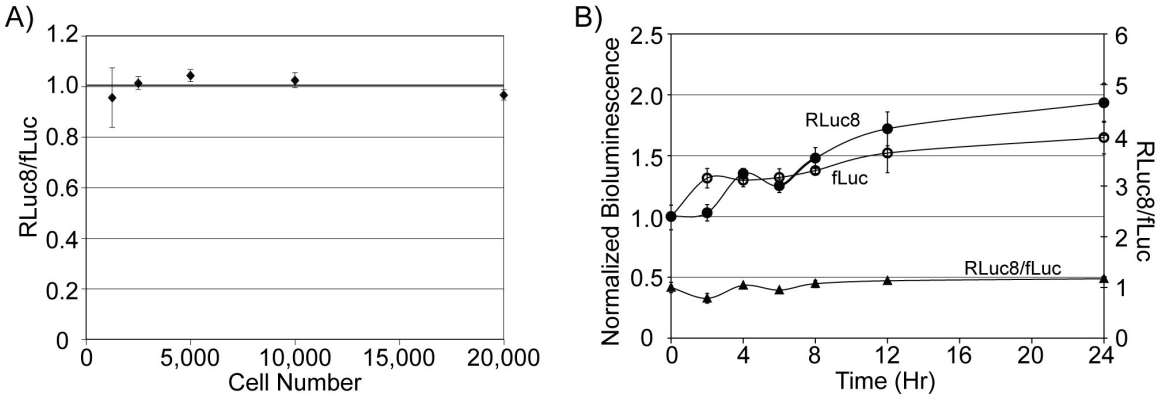

Figure 3.7. Analysis of RLuc8:fLuc ratio as a function of cell number and time. (A) RBS-HeLa cells were plated at various cell densities and the RLuc8:fLuc ratio was measured. (B) For a fixed cell seeding density, the RLuc8 and fLuc bioluminescent signal that was elicited by RBS-HeLa cells (PBS-treated) was detected over the course of 24 hrs (left axis) and the RLuc8:fLuc ratio was calculated at each time point (right axis).

Similar changes in the RLuc8:fLuc ratio were seen regardless of whether the coding sequences for fLuc and RLuc8 were interchanged, relative to the IRES sequence (Figure 3.8). Further, it should be noted that similar bioluminescent measurements were obtained from live and lysed cells. All measurements of fLuc and RLuc8 activity that are shown were acquired using the in vitro assay kit, Dual-Glo (Promega).

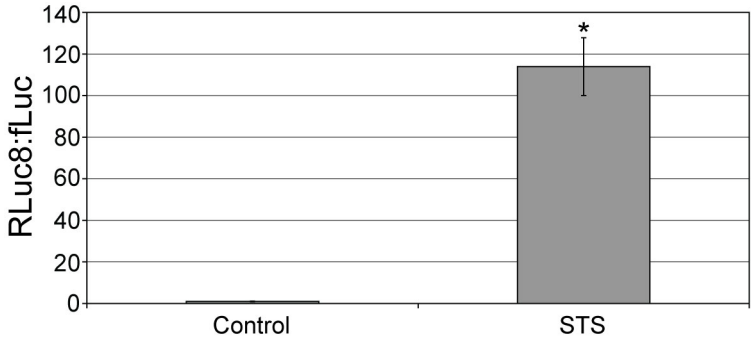

Figure 3.8. Response of reverse RBS-HeLa cells to STS. Reverse RBS-HeLa cells were treated with PBS or 10 μM STS for 24 hours and characterized by measurements of RLuc8:fLuc bioluminescence. Statistical significance: * ($p<0.01$).

To determine the extent of PCD in STS-treated RBS-HeLa cells, TUNEL assays for DNA fragmentation and Caspase-3/7 Glo assays for caspase-3 activation were performed. As shown in Figure 3.9A, the percent of DNA fragmentation over the course of 24 hours with 10 μM STS treatment rises, while untreated control cells exhibit no such increase. Additionally, caspase-3 activation rises initially (up to 8 hours) but then decreases at later time points under the same conditions; untreated control cells show little increase in caspase-3 activation (Figure 3.9B). RBS-HeLa cells treated with a dosage range of STS (0 – 50 μM) for 6 hours experience an increase in percent DNA fragmentation with increasing dose (Figure 3.9C), and an increase in caspase-3 activation (Figure 3.9D).

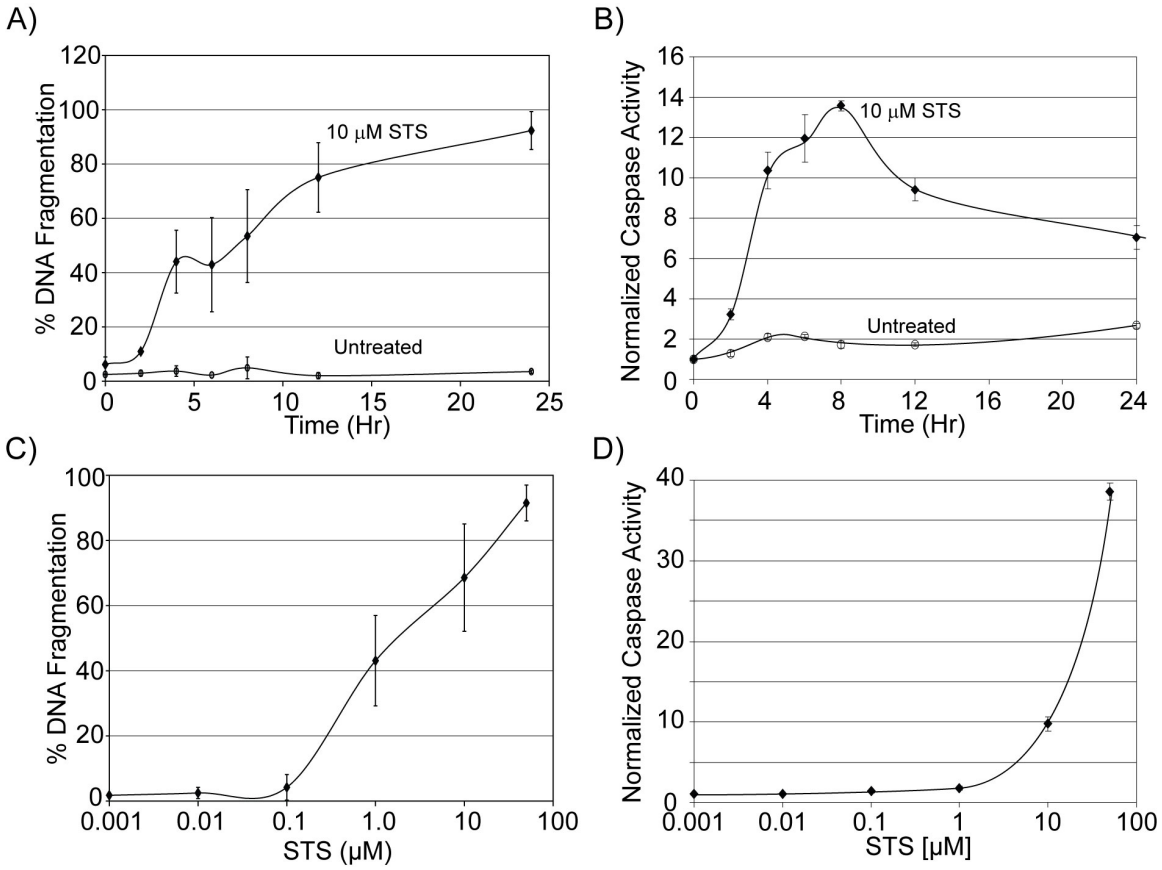

Figure 3.9. Commercial PCD assays on STS-treated RBS-HeLa cells. (A) A TUNEL assay for DNA fragmentation was performed at various times during the course of 10 μM STS or PBS (untreated control) treatment. (B) A Caspase-3/7 Glo assay was performed at various times during the course of 10 μM STS or PBS (untreated control) treatment. (C) A TUNEL assay for DNA fragmentation was performed after 6 hours of 0 – 50 μM STS treatment. (D) A Caspase-3/7 Glo assay was performed after 6 hours of 0 – 50 μM STS treatment.

3.4 Discussion

Preliminary studies on the stabilities of wild-type bioluminescent proteins demonstrated that both RLuc and fLuc exhibit decreased bioluminescence under PCD-inducing conditions. Additionally, caspase-3 activity is markedly elevated under the same conditions, indicative of PCD. The disparity between high caspase-3 activity and nearly completely diminished fLuc and RLuc bioluminescence suggests that the utilization of these proteins in sensors for PCD must be done with caution.

These observations led us to investigate methods of increasing the stabilities of fLuc and RLuc. The application of PBT, a chemical reported to increase the stability of fLuc by preventing its intracellular degradation(23), abrogated the decrease in fLuc bioluminescence in HeLa cells treated with STS. However, the usage of this chemical may not translate well into *in vivo* models. HeLa cells expressing mutant luciferases, fLuc5 and RLuc8, and treated with STS also demonstrated increases in stability, compared to wild-type luciferases.

These results led to the hypothesis that if a stable and unstable luciferase were incorporated into one sensor, the resulting bioluminescence ratio (stable bioluminescence:unstable bioluminescence) could be used to report on the extent of intracellular stress associated with PCD. RLuc8 was chosen as the stable luciferase for the sensor because it remained the most stable out of all of the proteins tested. Wild-type fLuc was chosen as the unstable luciferase for the sensor because its emission wavelength (~600 nm) is better suited for *in vivo* imaging. Additionally, each of these enzymes utilizes a different substrate, effectively simplifying the distinction between the

bioluminescence of fLuc and RLuc8. The sensor incorporating RLuc8 and fLuc was termed the Ratiometric Bioluminescent Sensor, or RBS.

Studies involving STS-treated RBS-HeLa cells indicated that fLuc activity was rapidly lost, while RLuc8 exhibited significantly prolonged functionality. Accordingly, the bioluminescent ratio (RLuc8 activity):(fLuc activity) correlated well with TUNEL and Caspase-3/7 Glo assay results, indicating that the RBS could provide information on cells undergoing PCD.

The RLuc8 and fLuc coding sequences flanked an IRES site in the final plasmid construct of the RBS in order to allow for protein translation from a single, bicistronic mRNA(28, 29). In having both genes under the control of a single (CMV) promoter and expressed as a single mRNA, the RLuc8:fLuc ratio at the transcript level is unaffected by altered promoter activity. However, previous studies have shown that in healthy cells, proteins translated from sequences downstream of the IRES site can be expressed at lower levels compared with upstream sequences(30). Therefore, to ensure that the position of the fLuc and RLuc8 coding sequence with respect to the IRES sequence (i.e., before or after the IRES sequence) was not responsible for the observed correlation between the ratio RLuc8:fLuc and cellular stress, the coding sequences for fLuc and RLuc8 were interchanged. It was found that similar changes in the RLuc8:fLuc ratio were seen regardless of the position of each luciferase relative to the IRES sequence.

Additionally, the RLuc8:fLuc ratios remained unchanged in untreated cells regardless of cell number or incubation time. This highlights the potential transitional use of the RBS, from high-throughput screening where very small samples are used all the way to animal models, where large numbers of cells are usually necessary.

There was an interesting disparity present between caspase-3 activity and percent DNA fragmentation when cells were treated with 10 μM STS over a time course of 24 hours. The caspase-3 activity peaked at 8 hours, while the percent DNA fragmentation continued to increase. Even though caspase-3 activation is considered to be absolutely necessary for apoptosis to occur(1), a hallmark trait for cells undergoing any type of PCD is increased DNA fragmentation(31). Given that the RBS seems to correlate better with the TUNEL assay for DNA fragmentation, it is expected that it will be able to monitor various biochemically and morphologically distinct pathways that lead to PCD.

While the discrepancy between RLuc8 and fLuc bioluminescence in cells undergoing PCD is quite explicit, the mechanism behind this difference remained unknown. There have been various reports indicating that the proteasome plays an essential role in PCD(32-34) and that calpain(16, 17) and cathepsin(18, 19) protease activity is upregulated during PCD. Additionally, increases in ROS that can occur in cells undergoing PCD broach the possibility of potentially damaging oxidative modifications to proteins(20-22). In the subsequent determination of the RBS mechanism, the roles of these proteases and ROS, among others were investigated.

3.5 References

1. Nicholson DW, Ali A, Thornberry NA, et al. Identification and inhibition of the ICE/CED-3 protease necessary for mammalian apoptosis. Nature 1995;376:37-43.

2. Ai HW, Hazelwood KL, Davidson MW, Campbell RE. Fluorescent protein FRET pairs for ratiometric imaging of dual biosensors. Nat Methods 2008;5:401-3.

3. Takemoto K, Nagai T, Miyawaki A, Miura M. Spatio-temporal activation of caspase revealed by indicator that is insensitive to environmental effects. J Cell Biol 2003;160:235-43.

4. Tyas L, Brophy VA, Pope A, Rivett AJ, Tavare JM. Rapid caspase-3 activation during apoptosis revealed using fluorescence-resonance energy transfer. EMBO Rep 2000;1:266-70.

5. Bullok K, Piwnica-Worms D. Synthesis and characterization of a small, membrane-permeant, caspase-activatable far-red fluorescent peptide for imaging apoptosis. J Med Chem 2005;48:5404-7.

6. Hug H, Los M, Hirt W, Debatin KM. Rhodamine 110-linked amino acids and peptides as substrates to measure caspase activity upon apoptosis induction in intact cells. Biochemistry 1999;38:13906-11.

7. Leytus SP, Melhado LL, Mangel WF. Rhodamine-based compounds as fluorogenic substrates for serine proteinases. Biochem J 1983;209:299-307.

8. Liu J, Bhalgat M, Zhang C, Diwu Z, Hoyland B, Klaubert DH. Fluorescent molecular probes V: a sensitive caspase-3 substrate for fluorometric assays. Bioorg Med Chem Lett 1999;9:3231-6.

9. Packard BZ, Toptygin DD, Komoriya A, Brand L. Profluorescent protease substrates: intramolecular dimers described by the exciton model. Proc Natl Acad Sci U S A 1996;93:11640-5.

10. Tung CH. Fluorescent peptide probes for in vivo diagnostic imaging. Biopolymers 2004;76:391-403.

11. Zhang HZ, Kasibhatla S, Guastella J, Tseng B, Drewe J, Cai SX. N-Ac-DEVD-N'-(Polyfluorobenzoyl)-R110: novel cell-permeable fluorogenic caspase substrates for the detection of caspase activity and apoptosis. Bioconjug Chem 2003;14:458-63.

12. Kizaka-Kondoh S, Itasaka S, Zeng L, et al. Selective killing of hypoxia-inducible factor-1-active cells improves survival in a mouse model of invasive and metastatic pancreatic cancer. Clin Cancer Res 2009;15:3433-41.

13. Shah K, Tung CH, Breakefield XO, Weissleder R. In vivo imaging of S-TRAIL-mediated tumor regression and apoptosis. Mol Ther 2005;11:926-31.

14. Laxman B, Hall DE, Bhojani MS, et al. Noninvasive real-time imaging of apoptosis. Proc Natl Acad Sci U S A 2002;99:16551-5.

15. Coppola JM, Ross BD, Rehemtulla A. Noninvasive imaging of apoptosis and its application in cancer therapeutics. Clin Cancer Res 2008;14:2492-501.

16. Aw TY, Nicotera P, Manzo L, Orrenius S. Tributyltin stimulates apoptosis in rat thymocytes. Arch Biochem Biophys 1990;283:46-50.

17. McConkey DJ, Hartzell P, Amador-Perez JF, Orrenius S, Jondal M. Calcium-dependent killing of immature thymocytes by stimulation via the CD3/T cell receptor complex. J Immunol 1989;143:1801-6.

18. Guenette RS, Mooibroek M, Wong K, Wong P, Tenniswood M. Cathepsin B, a cysteine protease implicated in metastatic progression, is also expressed during regression of the rat prostate and mammary glands. Eur J Biochem 1994;226:311-21.

19. Sensibar JA, Liu XX, Patai B, Alger B, Lee C. Characterization of castration-induced cell death in the rat prostate by immunohistochemical localization of cathepsin D. Prostate 1990;16:263-76.

20. Berlett BS, Stadtman ER. Protein oxidation in aging, disease, and oxidative stress. J Biol Chem 1997;272:20313-6.

21. Davies KJ. Protein damage and degradation by oxygen radicals. I. general aspects. J Biol Chem 1987;262:9895-901.

22. Volkin DB, Mach H, Middaugh CR. Degradative covalent reactions important to protein stability. Mol Biotechnol 1997;8:105-22.

23. Thompson JF, Hayes LS, Lloyd DB. Modulation of firefly luciferase stability and impact on studies of gene regulation. Gene 1991;103:171-7.

24. Jarvis WD, Turner AJ, Povirk LF, Traylor RS, Grant S. Induction of apoptotic DNA fragmentation and cell death in HL-60 human promyelocytic leukemia cells by pharmacological inhibitors of protein kinase C. Cancer Res 1994;54:1707-14.

25. Gil J, Almeida S, Oliveira CR, Rego AC. Cytosolic and mitochondrial ROS in staurosporine-induced retinal cell apoptosis. Free Radic Biol Med 2003;35:1500-14.

26. Law GH, Gandelman OA, Tisi LC, Lowe CR, Murray JA. Mutagenesis of solvent-exposed amino acids in Photinus pyralis luciferase improves thermostability and pH-tolerance. Biochem J 2006;397:305-12.

27. Loening AM, Fenn TD, Wu AM, Gambhir SS. Consensus guided mutagenesis of Renilla luciferase yields enhanced stability and light output. Protein Eng Des Sel 2006;19:391-400.

28. Jackson RJ, Howell MT, Kaminski A. The novel mechanism of initiation of picornavirus RNA translation. Trends Biochem Sci 1990;15:477-83.

29. Jang SK, Davies MV, Kaufman RJ, Wimmer E. Initiation of protein synthesis by internal entry of ribosomes into the 5' nontranslated region of encephalomyocarditis virus RNA in vivo. J Virol 1989;63:1651-60.

30. Houdebine LM, Attal J. Internal ribosome entry sites (IRESs): reality and use. Transgenic Res 1999;8:157-77.

31. Williams JR, Little JB, Shipley WU. Association of mammalian cell death with a specific endonucleolytic degradation of DNA. Nature 1974;252:754-5.

32. Chang YC, Lee YS, Tejima T, et al. mdm2 and bax, downstream mediators of the p53 response, are degraded by the ubiquitin-proteasome pathway. Cell Growth Differ 1998;9:79-84.

33. Grimm LM, Goldberg AL, Poirier GG, Schwartz LM, Osborne BA. Proteasomes play an essential role in thymocyte apoptosis. EMBO J 1996;15:3835-44.

34. Nakajima T, Morita K, Ohi N, et al. Degradation of topoisomerase IIalpha during adenovirus E1A-induced apoptosis is mediated by the activation of the ubiquitin proteolysis system. J Biol Chem 1996;271:24842-9.

Chapter 4: The RBS mechanism relies on hydrogen peroxide

4.1 Abstract

The molecular processes involved in PCD are undoubtedly complicated, however it is generally accepted that protein degradation is readily involved in this phenomenon. Given the complex nature of the cytosol, there are naturally many avenues that can eventually lead to protein degradation. Some of the most prominent mechanisms for protein degradation involve the proteasome, caspases, lysosomal proteases and oxidatively damaging reactive oxygen species (ROS). In this chapter, comprehensive inhibition/scavenging studies were performed to determine the cause of the disparity seen between fLuc and RLuc8 in the RBS. It was shown that this disparity stems from H_2O_2-mediated oxidative damage that preferentially affected fLuc over RLuc8.

4.2 Introduction

Intracellular proteases play various, sometimes complicated, roles in the process of programmed cell death (see (1), for review). The 26S proteasome is a proteolytic complex that is present in all mammalian cell types and is responsible for most of the protein degradation that occurs in cells. Proteins that are covalently conjugated to ubiquitin are targeted for rapid proteolysis by the proteasome(2). Ubiquitin production has been shown to increase in γ-irradiated thymocytes (3) and proteasome inhibition can result in abrogation of apoptosis (4, 5).

Calpains are cytosolic proteins that depend on Ca^{2+} for activation(6). They typically degrade cytoskelatal proteins(7-9), but do not cleave a specific target sequence

within proteins(10). Increases in intracellular Ca^{2+} during apoptosis have previously been reported (11, 12) and calpains have been shown to be active during apoptosis in many different cell types(13-15). Additionally, calpain inhibitors have reportedly resulted in the inhibition of apoptosis in response to certain apoptotic stimuli(16, 17).

Cathepsins are cysteine, zinc and aspartyl proteases that are present primarily in lysosomes and endosomes, but have been shown to be secreted into the cytosol under certain conditions(18, 19). Additionally, damage to lysosomal membranes via hydroxyl radicals ($^{\bullet}OH$) can result in the release of cathepsins into the cytosol(20, 21). Cathepsin B and D mRNA and protein levels have been shown to be upregulated in cells undergoing apoptosis(22, 23) and inhibition studies have shown that when these proteases are inhibited, apoptosis may also be inhibited(24, 25). Following synthesis, cathepsins need to be proteolytically processed(26, 27); further, they may be activated in a cascade-like manner(25), similar to caspases, as it has been reported that cathepsin B is directly cleaved by cathepsin D to become activated(28, 29).

Perhaps the most thoroughly characterized proteases involved in programmed cell death are the caspase family of proteases (see (30) for review). Caspases are defined by the specific amino acids sequences they cleave(31) and caspase-3 is required in order for a cell to fully complete the apoptotic process(32).

In addition to proteases, ROS can contribute to the degradation or damage of proteins in dying cells. The superoxide radical ($O_2^{\bullet-}$) does not cause much damage on its own(33), but it can react with other radicals ($^{\bullet}OH$)(34) or intracellular iron, leading to the production of $^{\bullet}OH$ which is highly reactive. The hydroxyl radical ($^{\bullet}OH$) is generally considered to be the most powerful oxidizing species in biological systems; the oxidative

attack of protein backbones is initiated by the •OH-dependent abstraction of the α-hydrogen atom of an amino acid residue to form a carbon-centered radical(35). Once a carbon-centered radical is formed, it can give rise to protein cross-links, peptide-bond cleavage (via diamide or α-amidation pathways), or direct oxidation of amino acids(35) The direct oxidation of lysine, arginine, proline and threonine residues may result in the formation of carbonyl derivatives (e.g. semialdehydes)(36, 37). Hydrogen peroxide (H_2O_2) is a powerful oxidizing agent that can directly and indirectly modify many amino acids (see (38) for review), often creating hydroxyl- or carbonyl-derivatives. While the effect of protein oxidation can vary, it has been shown in some cases that oxidation can destabilize a protein's native structure and result in the impairment of protein function and activity loss(39, 40).

In this chapter, after eliminating mRNA as a source of RLuc8 and fLuc activity discrepancy, we employed a series of inhibition studies on the aforementioned proteases and ROS on RBS-HeLa cells treated with STS. We have found that the disparity in fLuc and RLuc8 activity is likely directly related to intracellular H_2O_2 levels.

4.3 Results

Quantitative RT-PCR revealed that the relative expression of fLuc and RLuc8 mRNA within RBS-HeLa cells did not significantly change regardless of whether being treated with STS or PBS (Figure 4.1A). In contrast, Western blot analysis revealed that fLuc protein levels decreased over the time course of STS treatment, while RLuc8 protein levels remained relatively stable (Figure 4.1B). Notably, some fLuc staining was observed at higher than expected molecular weights at later time points, particularly at 24

hours. Based on these findings, we began to investigate various cellular pathways involved in protein degradation and/or modification.

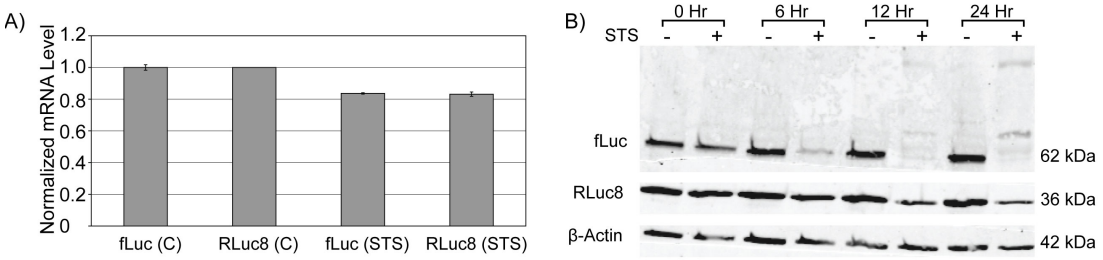

Figure 4.1. Assessment of mRNA and protein levels in STS-treated RBS-HeLa cells. (A) Normalized RLuc8 and fLuc mRNA levels in RBS-HeLa cells treated with PBS (control, C) or 10 μM STS (STS) for 24 hours. mRNA levels were determined by qRT-PCR. (B) Western blot of RBS-HeLa cells treated with PBS (-) or 10 μM STS (+) over a time course of 24 hours. β-actin is shown as a loading control.

To investigate pathways related to protein degradation and modification, a comprehensive series of inhibition studies were performed. It was expected that certain inhibitors would rescue fLuc activity, resulting in a decrease in the RLuc8:fLuc ratio in STS-treated RBS-HeLa cells. Since the proteasome is a prominent source of intracellular protein degradation, it was naturally one of the first molecular entities we investigated for the inhibition studies. Three proteasome inhibitors were tested, and all three inhibit the chymotryptic, peptidylglutamic peptidase and tryptic proteasome activity of the proteasome. MG-132 acts as a 'suicide substrate'(41), epoxomicin covalently binds to and modifies specific proteasomal subunits(42) and lactacystin covalently binds to and irreversibly modifies all β-subunits of the proteasome(43). When the proteasome inhibitors were employed (Figure 4.2A), the RLuc8:fLuc ratio increased, i.e. fLuc

activity was even further reduced relative to RLuc8. The efficacy of the proteasome inhibitors was confirmed by performing analogous studies with Proteasome-GLO (Figure 4.2B).

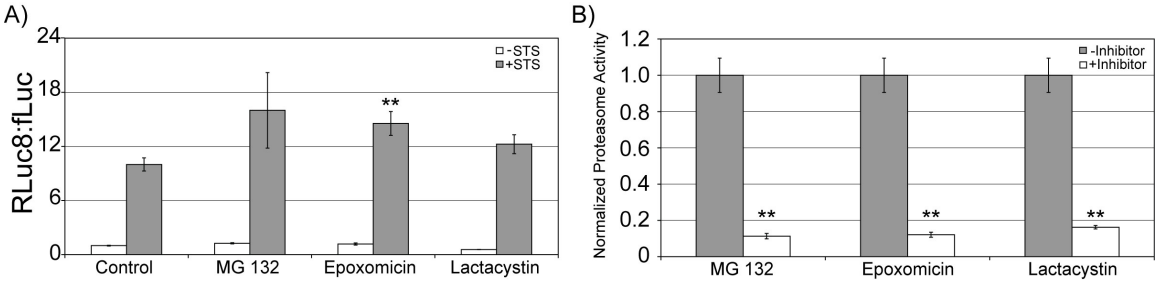

Figure 4.2. RBS response to proteasome inhibition. (A) RBS-HeLa cells were pretreated with PBS (control), 20 μM MG-132, 10 μM Epoxomicin or 10 μM Lactacsytin for 1 hour before the addition of 10 μM STS or PBS for 24 hours. RLuc8 and fLuc bioluminescence measurements were taken and the RLuc8:fLuc ratio is reported. (B) RBS-HeLa cells were pretreated with PBS or the inhibitors mentioned in (A) for 1 hour prior to the addition of 10 μM STS for 24 hours. Proteasome activity was assayed using Proteasome-Glo and the inhibited bioluminescence values were normalized to uninhibited controls. Statistical significance: **$p<0.01$.

Next, inhibitors for various proteases associated with apoptosis and lysosomal degradation were evaluated, namely calpain Inhibitor III (inhibits calpains), Pepstatin A (inhibits aspartyl proteases), ammonium chloride (inhibits phagosome-lysosome fusion), and z-vad-fmk (pan caspase inhibitor). As shown in figure 4.3A, none of these inhibitors significantly affected the RLuc8:fLuc ratio of STS-treated cells. The efficacy of the various protease inhibitors was confirmed by appropriate commercial assays (Figure 4.3B). As noted in Chapter 2, in lieu of a control assay for ammonium chloride

effectively inhibiting lysosome-phagosome fusion, we direct the reader to a seminal paper regarding this phenomenon in HeLa cells(44).

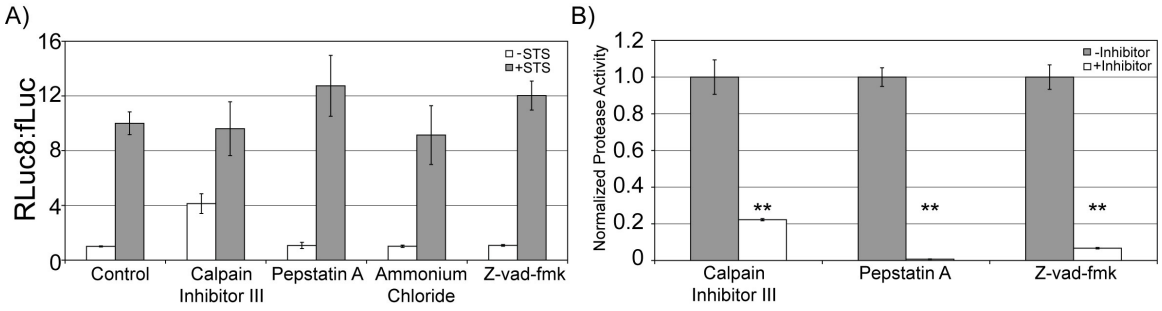

Figure 4.3. RBS response to various protease inhibitors. (A) RBS-HeLa cells were pretreated with PBS (control), 100 μM Calpain Inhibitor III, 100 μM Pepstatin A, 1 mM ammonium chloride or 1 μM z-vad-fmk for 1 hour before the addition of 10 μM STS or PBS for 24 hours. RLuc8 and fLuc bioluminescence measurements were taken and the RLuc8:fLuc ratio is reported. (B) RBS-HeLa cells were pretreated with PBS or the inhibitors mentioned in (A) for 1 hour prior to the addition of 10 μM STS for 24 hours. Protease activity was assayed using appropriate commercial assays and the inhibited values were normalized to uninhibited controls. Statistical significance: **$p<0.01$.

Once the proteasome and various proteases were shown to have insignificant effects on the mechanism responsible for the increase in the RLuc8:fLuc ratio in STS-treated cells, focus was shifted to three oxygen byproducts associated with oxidative stress: superoxide ($O_2^{\bullet-}$), hydroxyl radical ($^{\bullet}OH$) and hydrogen peroxide (H_2O_2). Three $O_2^{\bullet-}$ scavengers were tested - Tiron, TEMPOL (both cell-permeable $O_2^{\bullet-}$ scavengers) and MnTMPyP (a cell-permeable superoxide dismutase (SOD) mimetic) - for their ability to reduce the RLuc8:fLuc ratio by rescuing fLuc activity. Figure 4.4A indicates that none

of these scavengers had any significant effect on the RLuc8:fLuc ratio. The efficacy of the $O_2^{\bullet-}$ scavengers was confirmed by performing a dihydroethidium assay (Figure 4.4B).

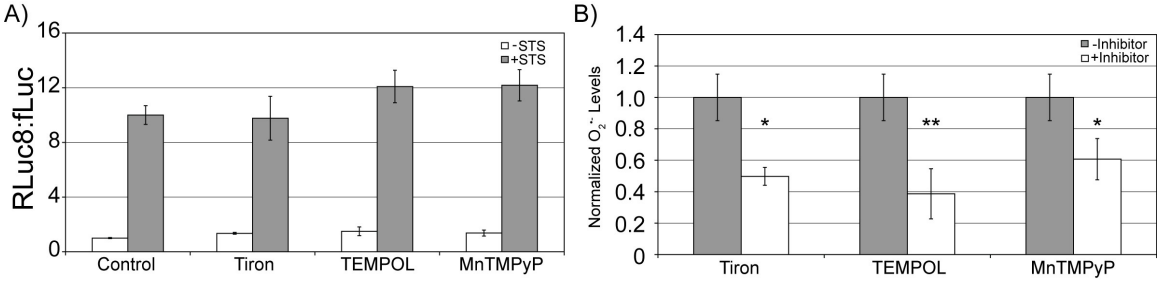

Figure 4.4. RBS response to O2·- scavengers. (A) RBS-HeLa cells were pretreated with PBS (control), 10 mM Tiron, 10 mM TEMPOL or 100 μM MnTMPyP for 1 hour before the addition of 10 μM STS or PBS for 24 hours. RLuc8 and fLuc bioluminescence measurements were taken and the RLuc8:fLuc ratio is reported. (B) RBS-HeLa cells were pretreated with PBS or the inhibitors mentioned in (A) for 1 hour prior to the addition of 10 μM STS for 24 hours. $O_2^{\bullet-}$ scavenging capability was tested using a dihydroethidium assay and inhibited values were normalized to uninhibited controls. Statistical significance: *$p<0.05$, **$p<0.01$.

Next, three $^{\bullet}OH$ scavengers/inhibitors, namely mannitol (specific $^{\bullet}OH$ scavenger), deferoxamine (DFO, iron chelator) and tetraethylenepentamine (TEPA, copper chelator) were examined. The two metal chelators, alone and in combination, were used to effectively reduce the amounts of metals available for the Fenton reaction ($Fe^{2+} + H_2O_2 \rightarrow Fe^{3+} + {}^{\bullet}OH + OH^-$). Interestingly, none of the $^{\bullet}OH$ scavengers/inhibitors significantly affected the RLuc8:fLuc ratio observed in STS-treated cells (Figure 4.5A). The effective reduction of intracellular $^{\bullet}OH$ following the addition of each

scavenger/inhibitor was confirmed by a decrease in hydroxyphenyl fluorescein fluorescence (Figure 4.5B).

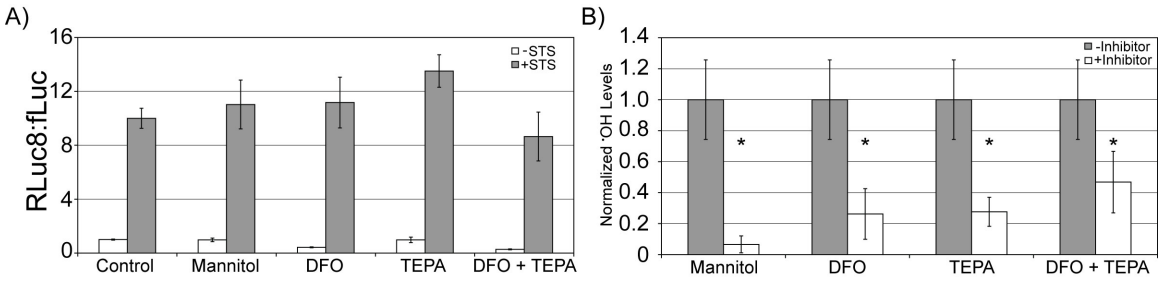

Figure 4.5. RBS response to ·OH scavengers. (A) RBS-HeLa cells were pretreated with PBS (control), 100 mM Mannitol, 50 μM DFO, 50 μM TEPA or 50 μM DFO + 50 μM TEPA for 1 hour before the addition of 10 μM STS or PBS for 24 hours. RLuc8 and fLuc bioluminescence measurements were taken and the RLuc8:fLuc ratio is reported. (B) RBS-HeLa cells were pretreated with PBS or the inhibitors mentioned in (A) for 1 hour prior to the addition of 10 μM STS for 24 hours. $^{\bullet}$OH scavenging capability was tested using a hydroxyphenyl fluorescein assay and inhibited values were normalized to uninhibited controls. Statistical significance: *$p<0.05$.

The next group of inhibitors/scavengers that was examined was associated with reducing intracellular H_2O_2 levels: catalase (scavenger), allopurinol (xanthine oxidase (XO) inhibitor), and acetylsalicylic acid (aspirin, cyclooxygenase (COX) inhibitor). Catalase converts H_2O_2 to water, allopurinol inhibits XO, an enzyme that catalyzes the oxidation of hypoxanthine and xanthine, creating H_2O_2 as a byproduct, and aspirin inhibits COX enzymes, which possess peroxidase activity. The addition of all three of these reagents resulted in significant reduction ($p<0.01$) in the RLuc8:fLuc ratio, as seen in Figure 4.6A. A reduction in intracellular H_2O_2 following the addition of each inhibitor/scavenger was confirmed by a decrease in CM-H_2DCFDA fluorescence (Figure

4.6B). Given these results, catalase, allopurinol and aspirin were subjected to additional dosing studies and a Western blot to further characterize their behavior.

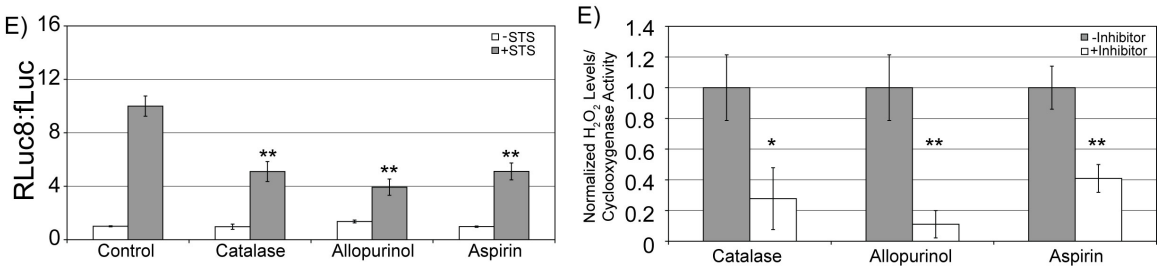

Figure 4.6. RBS response to H_2O_2 related scavengers. (A) RBS-HeLa cells were pretreated with PBS (control), 50 U/mL catalase, 100 μM allopurinol or 1 mM aspirin for 1 hour before the addition of 10 μM STS or PBS for 24 hours. RLuc8 and fLuc bioluminescence measurements were taken and the RLuc8:fLuc ratio is reported. (B) RBS-HeLa cells were pretreated with PBS or the inhibitors mentioned in (A) for 1 hour prior to the addition of 10 μM STS for 24 hours. H_2O_2 scavenging capability was tested using appropriate commercial assays and inhibited values were normalized to uninhibited controls. Statistical significance: *$p<0.05$, **$p<0.01$.

The final ROS-related inhibitor tested was uric acid, a peroxynitrite (ONOO-) scavenger. When RBS-HeLa cells were pretreated with 1 mM uric acid for one hour prior to 10 μM STS for 24 hours, a slight but insignificant increase in the RLuc8:fLuc ratio was exhibited compared to cells without this pretreatment (Figure 4.7). As there are currently no commercial assays available that specifically detect ONOO- only, we referred to previously published reports indicating that this concentration of uric acid effectively reduced intracellular ONOO-(45-47).

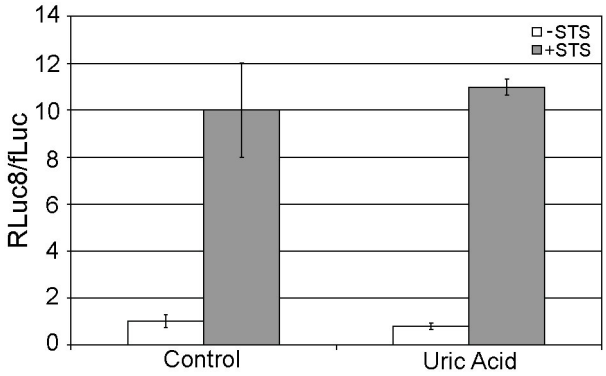

Figure 4.7. RBS response to an ONOO- scavenger, uric acid. (A) RBS-HeLa cells were pretreated with PBS (Control) or 1 mM uric acid for 1 hour before the addition of 10 μM STS or PBS for 24 hours. RLuc8 and fLuc bioluminescence measurements were taken and the RLuc8:fLuc ratio is reported after normalization to PBS/PBS treated controls.

Catalase, allopurinol and aspirin were explored further since they had the greatest effect on the RLuc8:fLuc ratio of RBS-HeLa cells treated with STS. RBS-HeLa cells were pretreated with increasing doses of catalase (Figure 4.8A), allopurinol (Figure 4.8B) or aspirin (Figure 4.8C) for 1 hour prior to the addition of 10 μM STS. After a 24 hour incubation period with the various H_2O_2 inhibitors/scavengers and STS, the bioluminescent ratio was measured. It was found that each inhibitor/scavenger effectively reduced the RLuc8:fLuc ratio in a dose-dependent manner. A Western blot was also performed (using the same pretreatment conditions from Figure 4.6A) to directly determine the effect of the various H_2O_2 inhibitors/scavengers on bioluminescent protein levels. Consistent with the observed recovery in fLuc activity, STS treated RBS-HeLa cells that were pretreated with catalase, allopurinol, and aspirin exhibited higher levels of fLuc protein (Figure 4.8D, column 3-5) compared to cells treated with STS in the absence of inhibitor (i.e. PBS, column 2).

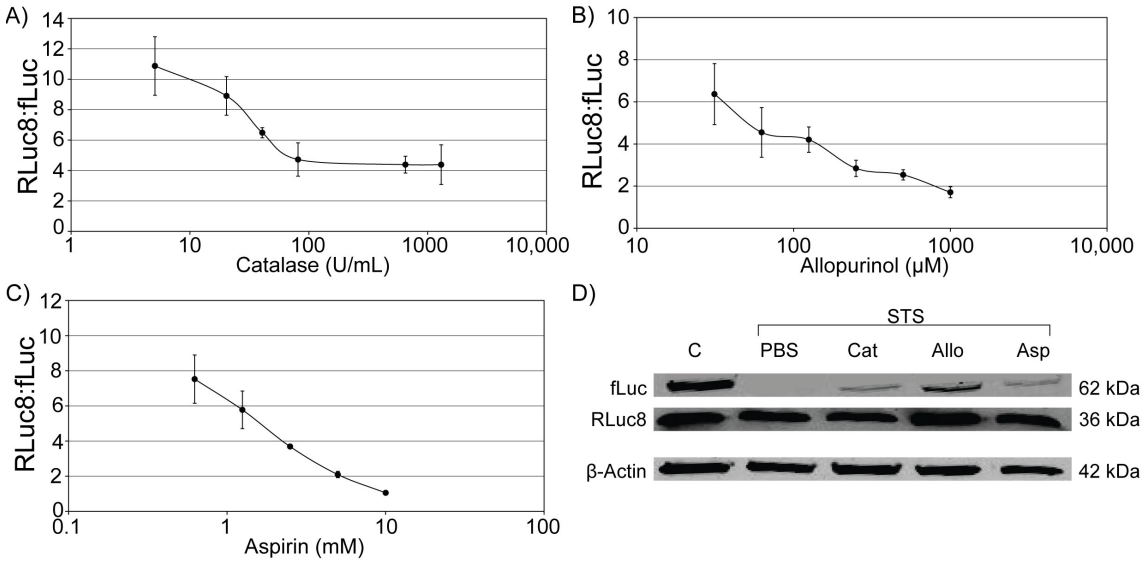

Figure 4.8. Dose response and Western blot analysis of STS-treated cells to H_2O_2-related scavengers. RBS-HeLa cells were pretreated with a dosage range of (A) catalase, (B) allopurinol, or (C) aspirin for 1 hour prior to 24 hours of 10 μM STS. The RLuc8:fLuc ratio was calculated and reported. (D) Western blot on RBS-HeLa cells pretreated for 1 hour with PBS, 50 U/mL catalase, 100 μM allopurinol or 1 mM aspirin (columns 2-5) before 10 μM STS for 24 hours. β-actin is shown as a loading control.

Having shown that inhibitors/scavengers of H_2O_2 affected the signal elicited by the RBS, additional studies were performed that dealt with H_2O_2 more directly. First, RBS-HeLa cells that were treated with 10 μM STS for up to 24 hours were analyzed for H_2O_2 production using the Amplex Red assay. Figure 4.9A shows that the intracellular H_2O_2 concentration increased nearly three-fold under these conditions, compared with PBS-treated controls. The H_2O_2 levels in RBS-HeLa cells also increased with STS dose (6 hour incubation, Figure 4.9B). These trends mirror the increase in the RLuc8:fLuc ratio that was observed with the RBS (Figure 4.1). To further evaluate the effect of H_2O_2

on the RBS, we investigated the response of RBS-HeLa cells to 1 mM H_2O_2 in serum, for incubation times ranging from 0 to 24 hours. Interestingly, it was found that the bioluminescent ratio increased dramatically, reaching levels that were drastically higher than what was observed previously with STS treatment (Figure 4.9C). Treating RBS-HeLa cells with a range of exogenous H_2O_2 concentrations for 6 hours also resulted in a more striking increase of RLuc8:fLuc when compared with the STS dosage study (Figure 4.9D). Additionally, it was found that exposing purified RLuc8 and fLuc proteins to the HX-XO reaction led to a significant increase ($p<0.01$) in the RLuc8:fLuc ratio over all controls. These findings suggest that the RBS may be specifically responsive to intracellularly produced H_2O_2 alone, and not other upstream or downstream reactions involving other oxygen radicals or enzymes.

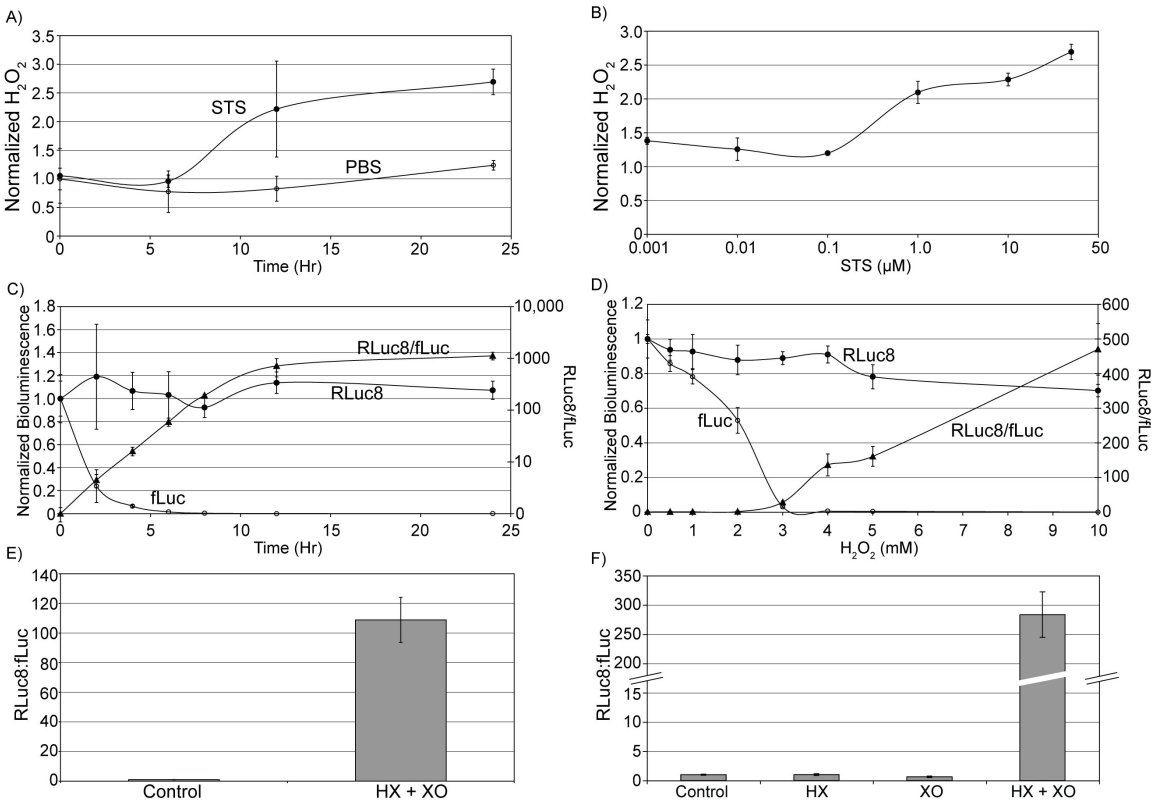

Figure 4.9. Analysis of intracellular H_2O_2, exogenous application of H_2O_2, and the hypoxanthine-xanthine oxidase reaction. RBS-HeLa cells treated with (A) 10 μM STS over a course of 24 hours or (B) a dosage range of STS for 6 hours were assayed for H_2O_2 concentrations using the Amplex Red Hydrogen Peroxide/Peroxidase assay. RBS-HeLa cells were treated with (C) 5 mM H_2O_2 in serum over a course of 24 hours or (D) a dosage of H_2O_2 for 6 hours and the normalized RLuc and fLuc bioluminescence measurements (left axis) and the RLuc8:fLuc ratio (right axis) were determined. (E) RBS-HeLa cells were subjected to PBS (Control) or the HX-XO reaction (50 μM HX, 25 mU/mL XO) for 24 hours. The RLuc8:fLuc ratio was calculated and reported. (F) Purified RLuc8 and fLuc proteins were treated *in vitro* with PBS (Control), 50 μM HX, 25 mU/mL XO or 50 μM HX + 25 mU/mL XO for 4 hours. The RLuc8:fLuc ratio was calculated and reported.

To investigate whether reductions in the level of H_2O_2, specifically through the use of allopurinol pretreatment, protected STS-treated RBS-HeLa cells from cell death, a TUNEL assay was performed. As can be seen in Figure 4.10A, allopurinol had no effect on DNA fragmentation levels, indicating that it had no effect on cell death. Bioluminescence measurements from HeLa cells pretreated with allopurinol before STS indicated a significant ($p<0.01$) decrease in the RLuc8:fLuc ratio compared to cells pretreated with PBS (Figure 4.10B). A CM-H_2DCFDA assay was performed to assess intracellular H_2O_2 levels under the same conditions, and as shown in Figure 4.10C, these levels were significantly reduced ($p<0.01$) by allopurinol pretreatment compared to PBS pretreatment. These results provide further support that changed in the RLuc8:fLuc ratio that are observed in apoptotic cells are likely mediated by H_2O_2.

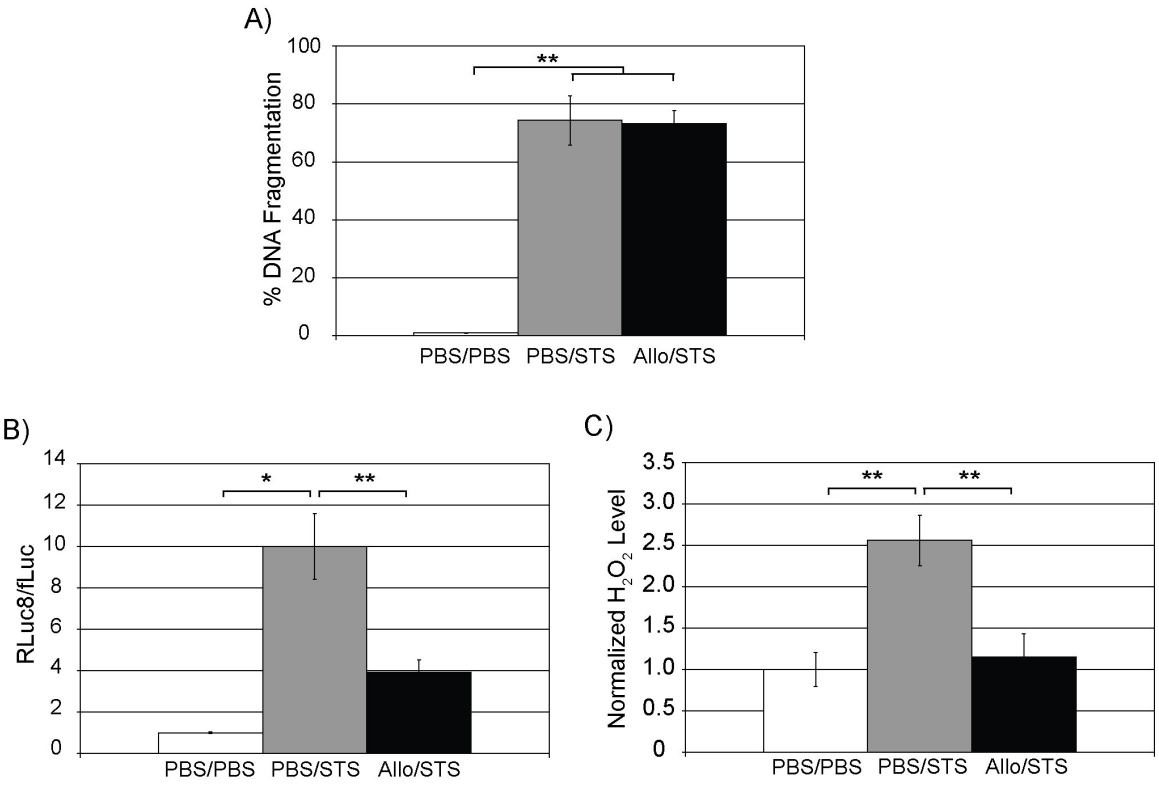

Figure 4.10. Summary of RBS-HeLa responses to allopurinol pretreatment. RBS-HeLa cells were pretreated with either PBS or 100 μM allopurinol for 1 hour prior to PBS or 10 μM STS for 24 hours. (A) DNA fragmentation levels from a TUNEL assay. (B) RLuc8:fLuc bioluminescence ratios from fLuc and RLuc8 bioluminescence measurements. (C) Intracellular H_2O_2 levels as measured by CM-H_2DCFDA. For (B) and (C), measurements were normalized to PBS/PBS controls. Statistical significance: *($p<0.05$), **($p<0.01$).

In order to obtain a more definitive understanding of the role of H_2O_2 in the mechanism of the RBS, we exposed purified RLuc8 and fLuc to increasing concentrations of H_2O_2 (0, 1, 5 and 10 mM) for 2 hours. Each well contained 650 nM

fLuc or 650 nM RLuc8. Aliquots from each reaction were removed every 30 minutes and subjected to SDS-PAGE. When fLuc was treated with H_2O_2, protein levels decreased with increasing time and dose, compared to untreated controls as can be seen in Figure 4.11 (first lane of each panel). Smearing of the fLuc band is seen from 30-90 minutes for 5 and 10 mM H_2O_2, indicative of possible degradation. In the case of RLuc8 treated with H_2O_2, little change was observed over either time or dose (Figure 4.11, second lane of each panel).

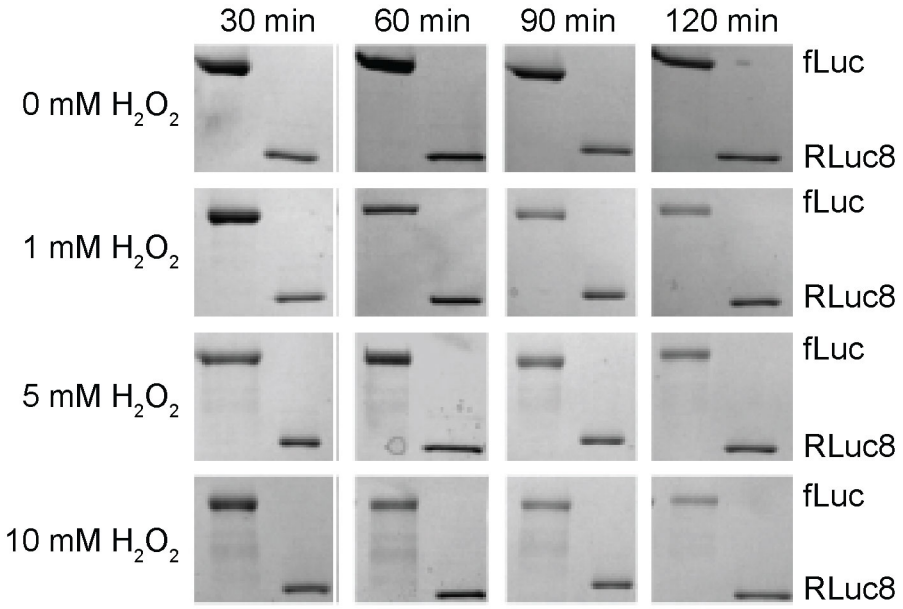

Figure 4.11. Response of purified fLuc and RLuc8 proteins to H_2O_2 visualized with SDS-PAGE. Proteins (650 nM fLuc or 650 nM RLuc8) were treated with 0-10 mM H_2O_2 for up to 120 minutes. Every 30 minutes, aliquots were removed and subjected to SDS-PAGE. For every panel, Lane 1: fLuc, Lane 2: RLuc8.

During the same study, aliquots from each reaction were removed and analyzed for bioluminescence. A dose and time dependent decrease in fLuc bioluminescence was demonstrated when fLuc was treated with H_2O_2 (Figure 4.12A), while RLuc8

bioluminescence remained quite stable under the same conditions (Figure 4.12B). The resulting RLuc8:fLuc ratio is presented in Figure 4.12C, and this ratio increases over both time and dose.

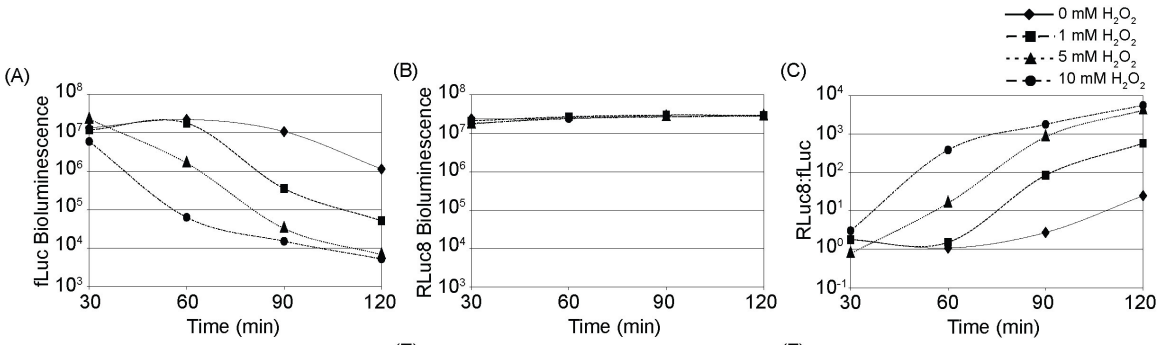

Figure 4.12. Bioluminescence response of purified fLuc and RLuc8 proteins to H_2O_2. Proteins (650 nM fLuc or 650 nM RLuc8) were treated with 0-10 mM H_2O_2 for up to 120 minutes. Every 30 minutes, aliquots were removed and subjected to bioluminescence measurements using Dual-Glo. (A) Bioluminescence measurements of fLuc treated with 0-10 mM H_2O_2 for up to 120 minutes. (B) Bioluminescence measurements of RLuc8 treated with 0-10 mM H_2O_2. (C) Bioluminescence ratios (RLuc8:fLuc) of measurements from (A) and (B).

When fLuc was treated with H_2O_2, fLuc bioluminescence appeared to decay at a faster rate than protein levels for all H_2O_2 concentrations tested. For example, bioluminescence values were less than 1% of control values after 120 minutes (Figure 4.12A), but fLuc protein levels were clearly higher when compared to control (Figure 4.11). These observations indicate that H_2O_2 may have oxidatively modified or damaged the fLuc proteins, rendering them inactive, prior to degradation/protein loss.

A possible mechanism causing the modification and subsequent degradation of fLuc is protein carbonylation, as this modification can damage/inactivate enzymes and

serve as a trigger for protein degradation (see (48) for review). Proteins can become carbonylated directly through oxidative attack on amino acid side chains as well as indirectly through reaction with lipid radicals, carbohydrate radicals and nucleic acid radicals(38). Interestingly, a recent study has suggested that protein carbonylation caused by lipid radicals is actually more common than carbonylation caused by direct amino acid side chain oxidative attack(49). Our studies on RBS-HeLa cells treated with STS for 24 hours have shown increased protein carbonylation compared to PBS treated control cells as shown in Figure 4.13A. The carbonylation assay uses DNP antibodies to detect protein carbonyls that have been derivatized to DNP using DNPH. Lanes 1 and 3 represent RBS-HeLa cells treated with PBS or STS and a derivatization control solution, while lanes 2 and 4 represent PBS or STS and DNPH treated cells. A marked increase can be seen in carbonylated proteins between lanes 2 and 4.

To further investigate carbonylation levels specifically in fLuc and RLuc8, purified samples of these proteins were treated with either PBS or 5 mM H_2O_2 for 2 hours and then subjected to the same carbonylation assay. As seen in Figure 4.13B, fLuc proteins treated with H_2O_2 exhibit a striking increase in carbonylation levels compared to PBS-treated controls (lanes 3 and 1, respectively). In contrast, very little difference in carbonylation is seen between PBS- and H_2O_2-treated RLuc8 proteins (lanes 2 and 4, respectively). Further, the relatively higher levels of carbonylation seen in PBS-treated fLuc proteins (lane 1) compared to PBS-treated RLuc8 proteins (lane 2) may explain the decrease in fLuc bioluminescence seen in PBS-treated fLuc in Figure 4.12A at the 120 minute time point.

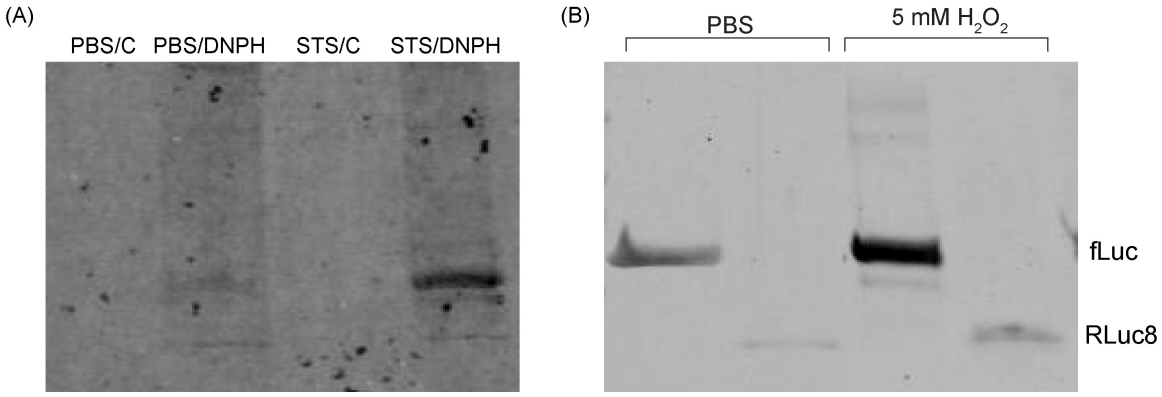

Figure 4.13. Analysis of protein carbonylation in STS-treated RBS-HeLa cells and H_2O_2-treated fLuc and RLuc8 proteins. (A) Proteins from RBS-HeLa cells treated with PBS (columns 1 and 2) or STS (columns 3 and 4) were extracted and treated with Derivatization-Control solution (C, columns 1 and 3) or DNPH (columns 2 and 4). The resulting proteins were subsequently analyzed by Western blot. (B) Purified fLuc and RLuc8 proteins were treated with either PBS (columns 1 and 2) or 5 mM H_2O_2 for 2 hours. After treatment with DNPH, the samples were analyzed by Western blot.

4.4 Discussion

Quantitative RT-PCR and western blot analyses were performed to determine whether changes in RNA or protein levels were responsible for the loss of fLuc activity, but not RLuc8 activity. Previous studies have shown that oxidative stress can trigger the degradation of both mRNA (50) and proteins(38). If RNA was degraded, we would expect to see a drastic difference in the relative level of fLuc and RLuc8 mRNA expression after STS treatment, compared with PBS-treated controls; however, this was not the case. In contrast, western blot analysis revealed that the fLuc protein levels decreased over time, while the RLuc8 protein levels remained relatively stable. Additionally, several higher molecular weight bands were observed after fLuc staining at the later time points, introducing the possibility of protein cross-linking and/or post-translational modification. These results indicated that 'activation' of the RBS can be attributed to the susceptibility of the bioluminescent proteins themselves to cellular stresses.

To explicate the root cause responsible for the loss in fLuc activity in STS-treated cells and the corresponding increase in the RLuc8:fLuc ratio, systematic inhibition/scavenger studies were performed to individually silence key pathways known to cause protein degradation/modification. It was expected that certain inhibitors would rescue fLuc activity, resulting in a decrease in the RLuc8:fLuc ratio in STS-treated RBS-HeLa cells. Since the proteasome is a prominent source of intracellular protein degradation, it was naturally one of the first molecular entities we investigated for the inhibition studies. Surprisingly, employment of the proteasome inhibitors MG-132, epoxomicin and lactacystin did not rescue fLuc activity and actually demonstrated an

increase in the RLuc8:fLuc ratio. These results provided strong evidence that enhanced proteasomal degradation was not responsible for the loss of fLuc activity in STS-treated cells. Since proteasome inhibitors have previously been shown to increase intracellular ROS levels(51-54) these findings hinted at ROS as a potential cause for the loss of fLuc activity.

Next, various proteases associated with the apoptotic and lysosomal pathways were inhibited to examine their effects on the RBS sensor. None of the inhibitors tested (Calpain Inhibitor III, Pepstatin A, ammonium chloride and z-vad-fmk) significantly affected the RLuc8:fLuc ratio, indicating the unlikelihood of the related proteases' involvement in the RBS mechanism. While the increase in the RLuc8:fLuc ratio observed upon use of the Calpain Inhibitor III on untreated (–STS) cells requires further exploration, one possible explanation may involve the decrease of intracellular antioxidant glutathione (GSH) levels and the associated increase in oxidative stress that has been shown to occur with the addition of this inhibitor(55).

After eliminating the proteasome and various proteases as primary candidates responsible for the increase in the RLuc8:fLuc ratio in STS-treated cells, we began examining the effects of scavengers for oxygen byproducts to determine the role of oxidative stress on the RBS. The three $O_2^{\bullet-}$ scavengers that were tested (Tiron, TEMPOL and MnTMPyP) showed no significant change in the RLuc8:fLuc ratio, concluding that $O_2^{\bullet-}$ alone is likely not responsible for the trends observed in STS-treated RBS-HeLa cells. This was somewhat expected given the short half-life of $O_2^{\bullet-}$ and its function as a precursor to other oxidizing agents. The three scavengers/inhibitors of $^{\bullet}OH$ (mannitol, DFO and TEPA) also did not significantly reduce the RLuc8:fLuc ratio in STS treated

RBS-HeLa cells, effectively eliminating the likelihood that $^{\bullet}OH$ as a direct contributor to the loss in fLuc activity. It may be argued that the slight increase in RLuc8:fLuc ratio that was observed following the addition of TEPA to the RBS-HeLa cells could be a result of excess H_2O_2 buildup from the prevention of the Fenton reaction, however further studies are warranted especially since the combination of DFO + TEPA did not yield an additive effect. In contrast to the previous inhibition studies, all three inhibitors/scavengers of H_2O_2 tested (catalase, allopurinol and aspirin), yielded a significant reduction ($p<0.01$) in the RLuc8:fLuc ratio, suggesting that fLuc activity can be recovered in STS-treated RBS-HeLa cells through removal of H_2O_2. It should be noted that catalase cannot cross cell membranes, but our results are consistent with previous studies reporting that extracellularly added catalase is effective at removing intracellular H_2O_2 (56, 57).

The final ROS investigated was ONOO-, by employing uric acid, an intracellular antioxidant that scavenges and becomes nitrosated by ONOO-(58). Pretreatment of RBS-HeLa cells with 1 mM uric acid prior to 10 μM STS for 24 hours had no effect on the RLuc8:fLuc ratio. Interestingly, ONOO- has been reported to deplete intracellular GSH levels(59); therefore it would be expected that the scavenging of ONOO- by uric acid would alleviate this depletion, effectively reducing ROS and the RLuc8:fLuc ratio. However, the RLuc8:fLuc ratio did not decrease with uric acid pretreatment, suggesting that GSH may not be a primary target for ONOO-.

Dosing studies of the three H_2O_2 related inhibitors on STS-treated RBS-HeLa cells revealed a reduction in the RLuc8:fLuc ratio in a dose-dependent manner, confirming that fLuc activity could be recovered by reducing H_2O_2 levels in STS-treated

cells. Additionally, a Western blot performed on STS-treated RBS-HeLa pretreated with each inhibitor/scavenger resulted in the rescue of fLuc protein levels when compared to STS treatment alone. Therefore, H_2O_2 inhibitors/scavengers were able to significantly reduce the degradation and/or modification of fLuc. The increase in H_2O_2 levels of STS-treated RBS-HeLa cells over time further supports the intrinsic involvement of H_2O_2 on the RBS mechanism, as does the striking increase in the RLuc8:fLuc ratio of these cells when treated directly with H_2O_2 in serum.

Since the highest level of fLuc rescue was seen when RBS-HeLa cells were pretreated with allopurinol, an XO inhibitor, an additional cellular assay was performed with HX and XO added to the media of RBS-HeLa cells. Here, the RLuc8:fLuc ratio also increased significantly ($p<0.01$) after 24 hours. While it has been thought that this reaction produces the superoxide anion in addition to H_2O_2, recent studies have shown that H_2O_2 is the dominant oxidant produced in this reaction(60). The magnitude of the increase was above that of STS treatment, but lower than H_2O_2 treatment, which was expected given that this reaction is expected to produce H_2O_2 more directly than STS but is obviously not as harsh as direct H_2O_2 application.

Additionally, it was found that exposing purified RLuc8 and fLuc proteins to the HX-XO reaction led to a significant increase ($p<0.01$) in the RLuc8:fLuc ratio over all controls. These findings suggest that the RBS may be specifically responsive to intracellularly produced H_2O_2 alone, and not other upstream or downstream reactions involving other oxygen radicals or enzymes.

Interestingly, when RBS-HeLa cells were pretreated with allopurinol for 1 hour prior to STS, no change in DNA fragmentation levels were seen. In parallel assays, this

pretreatment significantly reduced both the RLuc8:fLuc ratio and intracellular H_2O_2 level compared to cells pretreated with PBS. The correlation between the RLuc8:fLuc ratio and intracellular H_2O_2 levels supports the notion that the RBS is specifically responsive to H_2O_2 and not other processes associated with cell death. Further, the inability of allopurinol to affect cell death suggests that H_2O_2 production is a consequence of cell death, not a catalyst for cell death.

To investigate the specific effects of H_2O_2 on fLuc and RLuc8, these proteins were treated with 0-10 mM H_2O_2. SDS-PAGE gels and bioluminescence measurements of each reaction were obtained throughout the course of 120 minutes and it was found that fLuc bioluminescence and protein levels decreased when it was treated alone, while both of these metrics remained relatively stable for RLuc8 under the same conditions. Interestingly, fLuc bioluminescence appeared to decay more rapidly than fLuc protein levels at all H_2O_2 concentrations tested. These observations indicate that H_2O_2 may have oxidatively modified or damaged the fLuc proteins, rendering them inactive, prior to degradation/protein loss.

It is hypothesized that H_2O_2 may differentially affect the proteins of the RBS through protein carbonylation prior to degradation, as an increase in this phenomenon was seen in STS treated cells versus PBS treated cells. Additionally, purified fLuc proteins exhibited higher levels of carbonylation versus RLuc8 when treated with H_2O_2. Protein carbonylation is irreversible(61), can cause protein aggregates to form(62, 63) and targets the damaged proteins for degradation(64).

In summary, we have shown that the bioluminescent ratio (RLuc8 activity):(fLuc activity) could be used to report on the extent of intracellular stress. Through various

inhibition assays, it has been determined that the likely candidate causing the discrepancy between fLuc and RLuc8 activity in STS-treated cells is H_2O_2. The specific affect that H_2O_2 has on fLuc compared to RLuc8 has yet to be determined. An initial theory involved specific amino acid modifications on the proteins by H_2O_2. For example, H_2O_2 can modify certain amino acids, including but not limited to methionine (M), cysteine (C), histidine(H), tyrosine (Y) and phenylalanine (F), (see(38), for review), often creating hydroxyl- or carbonyl-derivatives. The proposed active site for fLuc is 244H-H-Glycine-F-247 (65) while the proposed active site for rLuc is a catalytic triad composed of aspartic acid (D) 120, glutamic acid (E) 144, and H285(66). Given that both of these active sites contain amino acids that are commonly oxidatively modified, it is not clear whether the differential sensitivity of fLuc and RLuc8 to H_2O_2 can be attributed to this alone.

We have determined that the RBS has the potential to relay important information regarding hydrogen peroxide in HeLa cells undergoing cell death. Given that caspases did not influence the RBS (Figure 3A), we anticipate that the RBS may be quite useful in studies examining caspase-independent cell death, especially since these pathways generally involve an increase in ROS (67, 68). Caspase-independent cell death has recently been garnering attention in terms of cancer drug development since anticancer drug resistance and tumorigenesis have been linked to the ability of certain cancers to circumvent caspase activation(69, 70). It is envisioned that the *in vitro* findings presented here will correlate well with *in vivo* work, potentially opening doors for advances in therapeutic and antioxidant research.

4.5 References

1. Johnson DE. Noncaspase proteases in apoptosis. Leukemia 2000;14:1695-703.

2. Waxman L, Fagan JM, Goldberg AL. Demonstration of two distinct high molecular weight proteases in rabbit reticulocytes, one of which degrades ubiquitin conjugates. J Biol Chem 1987;262:2451-7.

3. Delic J, Morange M, Magdelenat H. Ubiquitin pathway involvement in human lymphocyte gamma-irradiation-induced apoptosis. Mol Cell Biol 1993;13:4875-83.

4. Grimm LM, Goldberg AL, Poirier GG, Schwartz LM, Osborne BA. Proteasomes play an essential role in thymocyte apoptosis. EMBO J 1996;15:3835-44.

5. Sadoul R, Fernandez PA, Quiquerez AL, et al. Involvement of the proteasome in the programmed cell death of NGF-deprived sympathetic neurons. EMBO J 1996;15:3845-52.

6. Guroff G. A Neutral, Calcium-Activated Proteinase from the Soluble Fraction of Rat Brain. J Biol Chem 1964;239:149-55.

7. Ishizaki Y, Tashiro T, Kurokawa M. A calcium-activated protease which preferentially degrades the 160-kDa component of the neurofilament triplet. Eur J Biochem 1983;131:41-5.

8. Reddy MK, Rabinowitz M, Zak R. Stringent requirement for Ca2+ in the removal of Z-lines and alpha-actinin from isolated myofibrils by Ca2+-activated neutral proteinase. Biochem J 1983;209:635-41.

9. Yoshida H, Murachi T, Tsukahara I. Degradation of actin and vimentin by calpain II, a Ca2+-dependent cysteine proteinase, in bovine lens. FEBS Lett 1984;170:259-62.

10. Wolf BB, Goldstein JC, Stennicke HR, et al. Calpain functions in a caspase-independent manner to promote apoptosis-like events during platelet activation. Blood 1999;94:1683-92.

11. McConkey DJ, Hartzell P, Amador-Perez JF, Orrenius S, Jondal M. Calcium-dependent killing of immature thymocytes by stimulation via the CD3/T cell receptor complex. J Immunol 1989;143:1801-6.

12. Aw TY, Nicotera P, Manzo L, Orrenius S. Tributyltin stimulates apoptosis in rat thymocytes. Arch Biochem Biophys 1990;283:46-50.

13. Squier MK, Miller AC, Malkinson AM, Cohen JJ. Calpain activation in apoptosis. J Cell Physiol 1994;159:229-37.

14. Knepper-Nicolai B, Savill J, Brown SB. Constitutive apoptosis in human neutrophils requires synergy between calpains and the proteasome downstream of caspases. J Biol Chem 1998;273:30530-6.

15. Waterhouse NJ, Finucane DM, Green DR, et al. Calpain activation is upstream of caspases in radiation-induced apoptosis. Cell Death Differ 1998;5:1051-61.

16. Vanags DM, Porn-Ares MI, Coppola S, Burgess DH, Orrenius S. Protease involvement in fodrin cleavage and phosphatidylserine exposure in apoptosis. J Biol Chem 1996;271:31075-85.

17. Spinedi A, Oliverio S, Di Sano F, Piacentini M. Calpain involvement in calphostin C-induced apoptosis. Biochem Pharmacol 1998;56:1489-92.

18. Westley B, Rochefort H. A secreted glycoprotein induced by estrogen in human breast cancer cell lines. Cell 1980;20:353-62.

19. Mort JS, Recklies AD. Interrelationship of active and latent secreted human cathepsin B precursors. Biochem J 1986;233:57-63.

20. Mak IT, Weglicki WB. Characterization of iron-mediated peroxidative injury in isolated hepatic lysosomes. J Clin Invest 1985;75:58-63.

21. Link G, Pinson A, Hershko C. Iron loading of cultured cardiac myocytes modifies sarcolemmal structure and increases lysosomal fragility. J Lab Clin Med 1993;121:127-34.

22. Sensibar JA, Liu XX, Patai B, Alger B, Lee C. Characterization of castration-induced cell death in the rat prostate by immunohistochemical localization of cathepsin D. Prostate 1990;16:263-76.

23. Guenette RS, Mooibroek M, Wong K, Wong P, Tenniswood M. Cathepsin B, a cysteine protease implicated in metastatic progression, is also expressed during regression of the rat prostate and mammary glands. Eur J Biochem 1994;226:311-21.

24. Roberts LR, Kurosawa H, Bronk SF, et al. Cathepsin B contributes to bile salt-induced apoptosis of rat hepatocytes. Gastroenterology 1997;113:1714-26.

25. Roberts LR, Adjei PN, Gores GJ. Cathepsins as effector proteases in hepatocyte apoptosis. Cell Biochem Biophys 1999;30:71-88.

26. Erickson AH. Biosynthesis of lysosomal endopeptidases. J Cell Biochem 1989;40:31-41.

27. Fujita H, Tanaka Y, Noguchi Y, Kono A, Himeno M, Kato K. Isolation and sequencing of a cDNA clone encoding rat liver lysosomal cathepsin D and the structure of three forms of mature enzymes. Biochem Biophys Res Commun 1991;179:190-6.

28. Nishimura Y, Kawabata T, Kato K. Identification of latent procathepsins B and L in microsomal lumen: characterization of enzymatic activation and proteolytic processing in vitro. Arch Biochem Biophys 1988;261:64-71.

29. Rowan AD, Mason P, Mach L, Mort JS. Rat procathepsin B. Proteolytic processing to the mature form in vitro. J Biol Chem 1992;267:15993-9.

30. Nunez G, Benedict MA, Hu Y, Inohara N. Caspases: the proteases of the apoptotic pathway. Oncogene 1998;17:3237-45.

31. Garcia-Calvo M, Peterson EP, Leiting B, Ruel R, Nicholson DW, Thornberry NA. Inhibition of human caspases by peptide-based and macromolecular inhibitors. J Biol Chem 1998;273:32608-13.

32. Nicholson DW, Ali A, Thornberry NA, et al. Identification and inhibition of the ICE/CED-3 protease necessary for mammalian apoptosis. Nature 1995;376:37-43.

33. Winterbourn CC, Kettle AJ. Radical-radical reactions of superoxide: a potential route to toxicity. Biochem Biophys Res Commun 2003;305:729-36.

34. Davies KJ. Protein damage and degradation by oxygen radicals. I. general aspects. J Biol Chem 1987;262:9895-901.

35. Berlett BS, Stadtman ER. Protein oxidation in aging, disease, and oxidative stress. J Biol Chem 1997;272:20313-6.

36. Shringarpure R, Davies KJ. Protein turnover by the proteasome in aging and disease. Free Radic Biol Med 2002;32:1084-9.

37. Stadtman ER. Oxidation of free amino acids and amino acid residues in proteins by radiolysis and by metal-catalyzed reactions. Annu Rev Biochem 1993;62:797-821.

38. Grune T, Reinheckel T, Davies KJ. Degradation of oxidized proteins in mammalian cells. FASEB J 1997;11:526-34.

39. Gao J, Yin DH, Yao Y, et al. Loss of conformational stability in calmodulin upon methionine oxidation. Biophys J 1998;74:1115-34.

40. Volkin DB, Mach H, Middaugh CR. Degradative covalent reactions important to protein stability. Mol Biotechnol 1997;8:105-22.

41. Rock KL, Gramm C, Rothstein L, et al. Inhibitors of the proteasome block the degradation of most cell proteins and the generation of peptides presented on MHC class I molecules. Cell 1994;78:761-71.

42. Meng L, Mohan R, Kwok BH, Elofsson M, Sin N, Crews CM. Epoxomicin, a potent and selective proteasome inhibitor, exhibits in vivo antiinflammatory activity. Proc Natl Acad Sci U S A 1999;96:10403-8.

43. Craiu A, Gaczynska M, Akopian T, et al. Lactacystin and clasto-lactacystin beta-lactone modify multiple proteasome beta-subunits and inhibit intracellular protein degradation and major histocompatibility complex class I antigen presentation. J Biol Chem 1997;272:13437-45.

44. Rote KV, Rechsteiner M. Degradation of microinjected proteins: effects of lysosomotropic agents and inhibitors of autophagy. J Cell Physiol 1983;116:103-10.

45. Foresti R, Sarathchandra P, Clark JE, Green CJ, Motterlini R. Peroxynitrite induces haem oxygenase-1 in vascular endothelial cells: a link to apoptosis. Biochem J 1999;339 (Pt 3):729-36.

46. Kooy NW, Royall JA. Agonist-induced peroxynitrite production from endothelial cells. Arch Biochem Biophys 1994;310:352-9.

47. Regoli F, Winston GW. Quantification of total oxidant scavenging capacity of antioxidants for peroxynitrite, peroxyl radicals, and hydroxyl radicals. Toxicol Appl Pharmacol 1999;156:96-105.

48. Nystrom T. Role of oxidative carbonylation in protein quality control and senescence. EMBO J 2005;24:1311-7.

49. Yuan Q, Zhu X, Sayre LM. Chemical nature of stochastic generation of protein-based carbonyls: metal-catalyzed oxidation versus modification by products of lipid oxidation. Chem Res Toxicol 2007;20:129-39.

50. Martinet W, de Meyer GR, Herman AG, Kockx MM. Reactive oxygen species induce RNA damage in human atherosclerosis. Eur J Clin Invest 2004;34:323-7.

51. Alexandrova A, Petrov L, Georgieva A, Kirkova M, Kukan M. Effects of proteasome inhibitor, MG132, on proteasome activity and oxidative status of rat liver. Cell Biochem Funct 2008;26:392-8.

52. Gil J, Almeida S, Oliveira CR, Rego AC. Cytosolic and mitochondrial ROS in staurosporine-induced retinal cell apoptosis. Free Radic Biol Med 2003;35:1500-14.

53. Kikuchi S, Shinpo K, Tsuji S, et al. Effect of proteasome inhibitor on cultured mesencephalic dopaminergic neurons. Brain Res 2003;964:228-36.

54. Wu HM, Chi KH, Lin WW. Proteasome inhibitors stimulate activator protein-1 pathway via reactive oxygen species production. FEBS Lett 2002;526:101-5.

55. Han YH, Kim SH, Kim SZ, Park WH. Intracellular GSH levels rather than ROS levels are tightly related to AMA-induced HeLa cell death. Chem Biol Interact 2008;171:67-78.

56. Herve-Grepinet V, Veillard F, Godat E, Heuze-Vourc'h N, Lecaille F, Lalmanach G. Extracellular catalase activity protects cysteine cathepsins from inactivation by hydrogen peroxide. FEBS Lett 2008;582:1307-12.

57. Preston TJ, Muller WJ, Singh G. Scavenging of extracellular H2O2 by catalase inhibits the proliferation of HER-2/Neu-transformed rat-1 fibroblasts through the induction of a stress response. J Biol Chem 2001;276:9558-64.

58. Skinner KA, White CR, Patel R, et al. Nitrosation of uric acid by peroxynitrite. Formation of a vasoactive nitric oxide donor. J Biol Chem 1998;273:24491-7.

59. Phelps DT, Ferro TJ, Higgins PJ, Shankar R, Parker DM, Johnson A. TNF-alpha induces peroxynitrite-mediated depletion of lung endothelial glutathione via protein kinase C. Am J Physiol 1995;269:L551-9.

60. Fatokun AA, Stone TW, Smith RA. Hydrogen peroxide mediates damage by xanthine and xanthine oxidase in cerebellar granule neuronal cultures. Neurosci Lett 2007;416:34-8.

61. Dalle-Donne I, Giustarini D, Colombo R, Rossi R, Milzani A. Protein carbonylation in human diseases. Trends Mol Med 2003;9:169-76.

62. Bota DA, Davies KJ. Lon protease preferentially degrades oxidized mitochondrial aconitase by an ATP-stimulated mechanism. Nat Cell Biol 2002;4:674-80.

63. Grune T, Jung T, Merker K, Davies KJ. Decreased proteolysis caused by protein aggregates, inclusion bodies, plaques, lipofuscin, ceroid, and 'aggresomes' during oxidative stress, aging, and disease. Int J Biochem Cell Biol 2004;36:2519-30.

64. Grune T, Merker K, Sandig G, Davies KJ. Selective degradation of oxidatively modified protein substrates by the proteasome. Biochem Biophys Res Commun 2003;305:709-18.

65. Branchini BR, Magyar RA, Marcantonio KM, et al. Identification of a firefly luciferase active site peptide using a benzophenone-based photooxidation reagent. J Biol Chem 1997;272:19359-64.

66. Loening AM, Fenn TD, Wu AM, Gambhir SS. Consensus guided mutagenesis of Renilla luciferase yields enhanced stability and light output. Protein Eng Des Sel 2006;19:391-400.

67. Martinvalet D, Dykxhoorn DM, Ferrini R, Lieberman J. Granzyme A cleaves a mitochondrial complex I protein to initiate caspase-independent cell death. Cell 2008;133:681-92.

68. Rudolf E, Rudolf K, Cervinka M. Selenium activates p53 and p38 pathways and induces caspase-independent cell death in cervical cancer cells. Cell Biol Toxicol 2008;24:123-41.

69. Los M, Herr I, Friesen C, Fulda S, Schulze-Osthoff K, Debatin KM. Cross-resistance of CD95- and drug-induced apoptosis as a consequence of deficient activation of caspases (ICE/Ced-3 proteases). Blood 1997;90:3118-29.

70. Martinez-Lorenzo MJ, Gamen S, Etxeberria J, et al. Resistance to apoptosis correlates with a highly proliferative phenotype and loss of Fas and CPP32 (caspase-3) expression in human leukemia cells. Int J Cancer 1998;75:473-81.

Chapter 5: The RBS can detect caspase-dependent PCD in multiple cell lines using multiple inducers

5.1 Abstract

Many imaging sensors currently utilized to investigate PCD rely on the cleavage of the amino acid sequence DEVD by caspase-3. However, caspase-3 activity is transiently activated and thus does not always directly correlate with the extent of cell death. Further, since caspase-7 can also cleave DEVD, PCD sensors based on caspase-3 activity may lead to ambiguous findings and inaccurate conclusions. In this chapter, we show RBS measurements consistently correlate with the extent of cell death, even in cases where caspase-3 probes fail. The RBS was used to detect PCD in MCF7 and 293T/17 cells treated with STS and in HeLa cells treated with DOX and Cpt to demonstrate the robustness of this approach.

5.2 Introduction

According to the American Cancer Society, cancer remains one of the most devastating diseases in the United States with over 500,000 deaths and 1.5 million new cases in 2009. Although great strides have been made in the pursuit of cancer therapeutics, the vast array of cancer phenotypes makes it an elusive target for definitive cures. As a result, there remains much to be discovered in terms of improving treatment.

Many therapies that have been developed to treat cancer involve inducing apoptosis, a type of programmed cell death (PCD), that is mechanistically characterized by a proteolytic cascade involving caspases (See (1) for comprehensive review).

Accordingly, a variety of sensors have been developed to image and monitor apoptosis, or more specifically caspase activity, to further assist in the discovery, development, and evaluation of apoptosis-inducing agents. Most of these sensors are based on fluorescence resonance energy transfer (FRET) or ground-state quenching, whereby removal of an acceptor fluorophore or quenching moiety, respectively, following cleavage of a caspase-specific recognition sequence results in detectable change in fluorescence(2-11).

Bioluminescence is an appealing alternative to fluorescence due to its sensitivity, cost-effectiveness, simplicity, virtually non-existent background signals, high-throughput screening potential and ability to acquire temporal information in cells and in live animal models. Recently, several bioluminescent sensors for apoptosis have also been developed. In general, these sensors have utilized the cleavage of the caspase-3 recognition sequence, DEVD, as a catalyst for luciferin (substrate) recognition(12, 13), removal of steric hindrance(14), or protein fragment complementation(15). However, many drugs that induce PCD act through a caspase-independent mechanism (see (16) for review), which would render caspase-specific sensors futile. Another confounding factor in regarding sensors for caspase-3 is that caspase-7 recognizes and cleaves the same amino acid sequence (DEVD) as caspase-3. Thus, sensors designed specifically for caspase-3 activity as a biomarker for apoptosis may not accurately report on intracellular mechanisms associated with cell death or the extent of cell death when used alone.

We have previously determined that the RBS is activated in HeLa cells undergoing apoptosis and that the response correlates with intracellular H_2O_2 levels. In this chapter, we show that the RBS also functions in MCF7 and 293T/17 cell lines treated with STS and in HeLa cells treated with doxorubicin (DOX) and camptothecin (Cpt), two

drugs known to induce apoptosis in HeLa cells(17, 18). The capability of the RBS to detect PCD induced in multiple cell types and with different drugs demonstrates its versatility and robustness.

5.3 Results

When RBS-MCF7 cells were treated with the apoptosis inducing drug staurosporine (STS) for 6 hours, the fLuc bioluminescence decreased by up to 90% in a dose-dependent manner. In contrast, the RLuc8 bioluminescence was much less sensitive to the treatment, only decreasing by 20% at the maximum dosage (Figure 5.1A). The resulting bioluminescent ratio RLuc8:fLuc increased accordingly with dosage. It was previously shown in Chapter 4, with purified bioluminescent proteins and in living cells, that changes in the ratio RLuc8:fLuc correlate with the level of H_2O_2. Consistent with this assessment, the intracellular H_2O_2 levels in MCF7 cells also increased with STS dose, as determined by a CM-H_2DCFDA assay (Figure 5.1B). To confirm that the STS treatment was causing apoptosis, two cell death assays were performed in parallel. As can be seen in Figures 5.1C and 5.1D, both caspase 3/7 activity and DNA fragmentation, well-known hallmarks of apoptosis(19, 20), increased under the same treatment conditions.

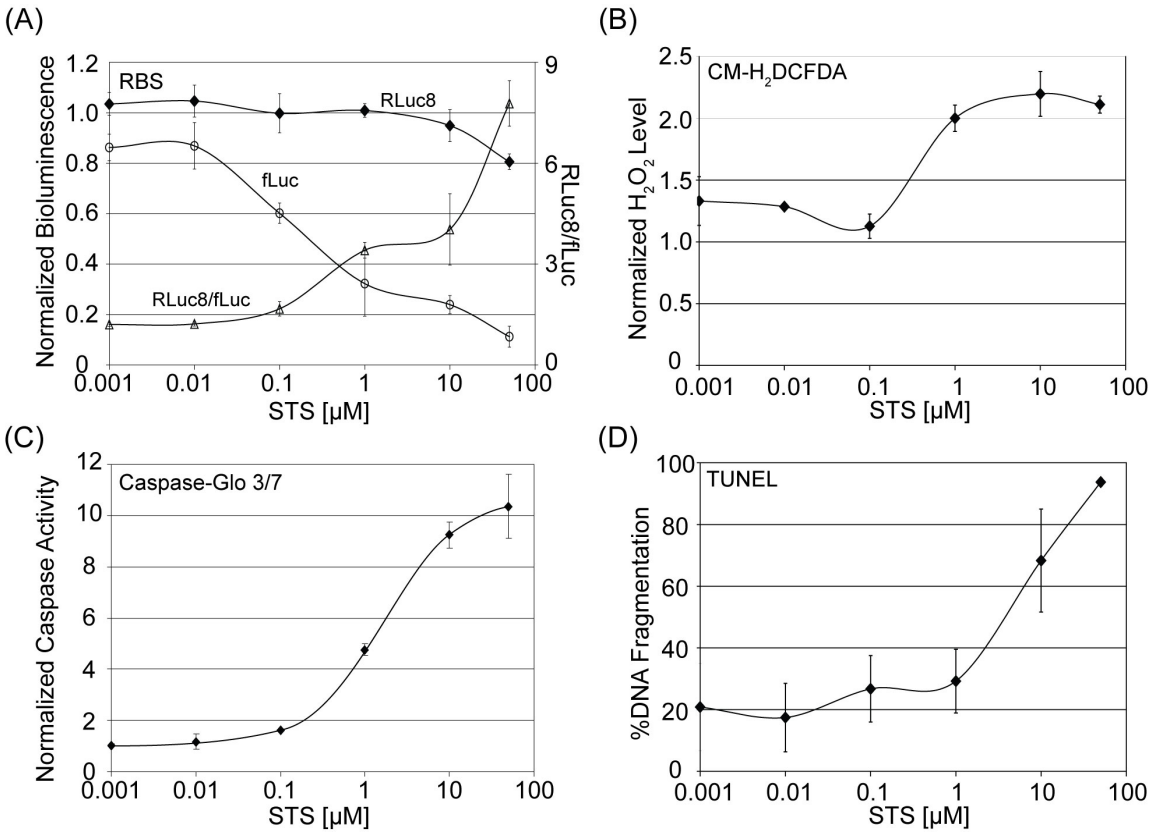

Figure 5.1. Response of RBS-MCF7 cells to increasing STS dosage. RBS-MCF7 cells were treated with a dosage range of STS (0-50 μM) for 6 hours. (A) Bioluminescent measurements of RLuc8 and fLuc were acquired for each STS concentration after 6 hours (left axis). The RLuc8:fLuc ratio was subsequently calculated for each STS concentration (right axis). (B) Intracellular H_2O_2 levels were assessed using CM-H_2DCFDA at each STS concentration. (C) A Caspase 3/7 Glo assay was performed to measure caspase activity at each STS concentration. (D) A TUNEL assay for DNA fragmentation was performed at each STS concentration.

As described in Chapter 4, fLuc bioluminescence in STS-treated RBS-HeLa cells can be rescued by pretreatment with allopurinol, resulting in a corresponding reduction in the ratio RLuc8:fLuc. Allopurinol is a xanthine oxidase (XO) inhibitor that is known to reduce the intracellular level of H_2O_2(21). To investigate the effects of this pretreatment on RBS-MCF7 cells, 100 μM of allopurinol was added to the cells one hour before treatment with 1 μM STS for 6 hours. As expected, this resulted in a significant decrease in the RLuc8:fLuc ratio ($p < 0.05$) compared to STS treatment alone (Figure 5.2A). Interestingly, pretreatment with allopurinol had no effect on cell death, as shown by unchanged caspase 3/7 activity and DNA fragmentation in Figures 5.2B and 5.2C. However, a significant ($p < 0.05$) decrease in intracellular H_2O_2 was seen when MCF7 cells were pretreated with allopurinol before the addition of STS (Figure 5.2D).

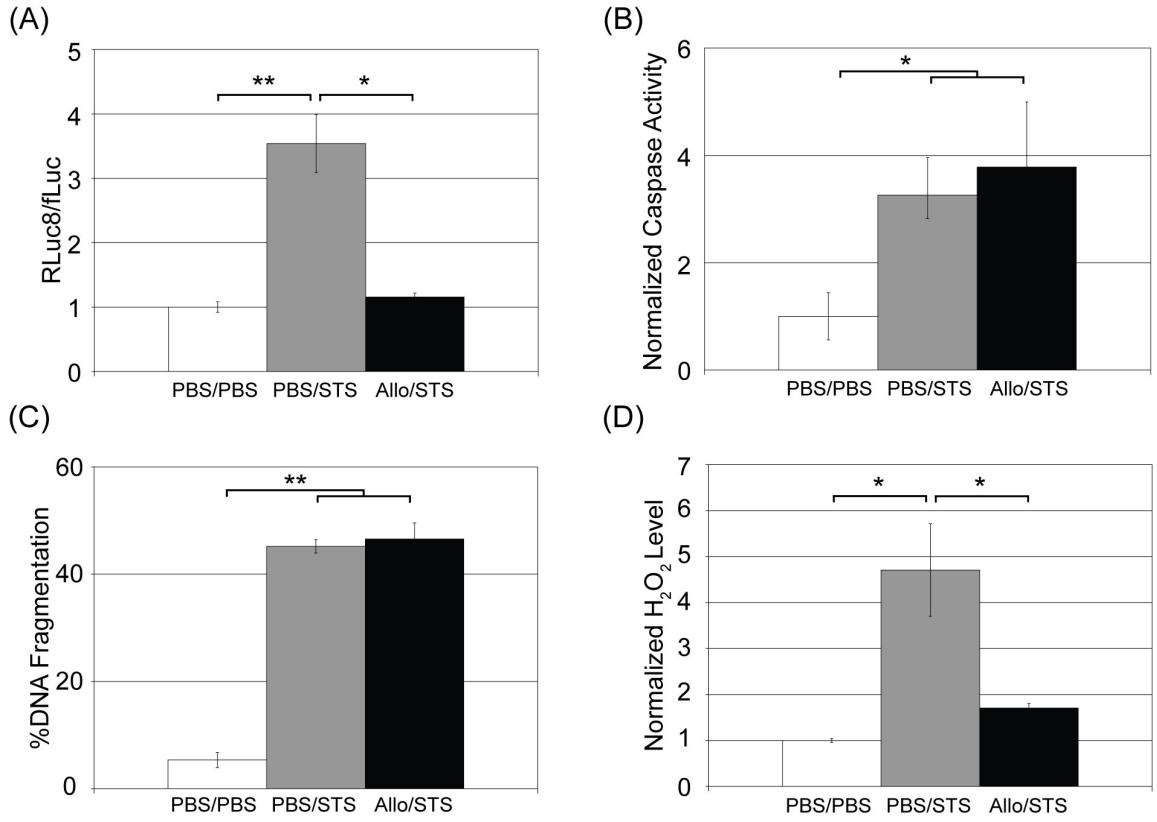

Figure 5.2. Response of STS-treated RBS-MCF7 cells to allopurinol pretreatment. RBS-MCF7 cells were pretreated with 100 μM allopurinol for 1 hour prior to 1 μM STS for 6 hours (A) RLuc8:fLuc ratios were acquired for cells exposed to PBS pretreatment followed by PBS as drug treatment (i.e. PBS/PBS), PBS/STS or Allo/STS. (B) Caspase 3/7 activity was acquired for cells exposed to PBS/PBS, PBS/STS or Allo/STS. (C) TUNEL assays for DNA fragmentation were performed on cells exposed to PBS/PBS, PBS/STS or Allo/STS. (D) Intracellular H_2O_2 measurements were acquired for cells exposed to PBS/PBS, PBS/STS or Allo/STS. In all studies (except TUNEL assays, which provide an absolute measure of cell death), measurements were normalized to control (0 μM STS). Statistical significance: * ($p<0.05$), ** ($p<0.01$).

The STS treatment studies were expanded over a time course of 24 hours using 10 μM STS on RBS-MCF7 cells. As shown in Figure 5.3A, the RLuc8:fLuc ratio increased dramatically over this time course while the PBS treated controls exhibited little change. Consistent with the RBS measurements, the intracellular H_2O_2 levels continually increased from 0 to 24 hours with STS treatment and exhibited little change with only PBS treatment (Figure 5.3B).

Interestingly, caspase activity did not continuously increase with time following the addition of STS, but rather reached a peak at the 6 hour time point and returned to control values by 24 hours (Figure 5.3C). In contrast, the TUNEL assay revealed that cell death remained elevated for the entire 24 hours after STS treatment (Figure 5.3D).

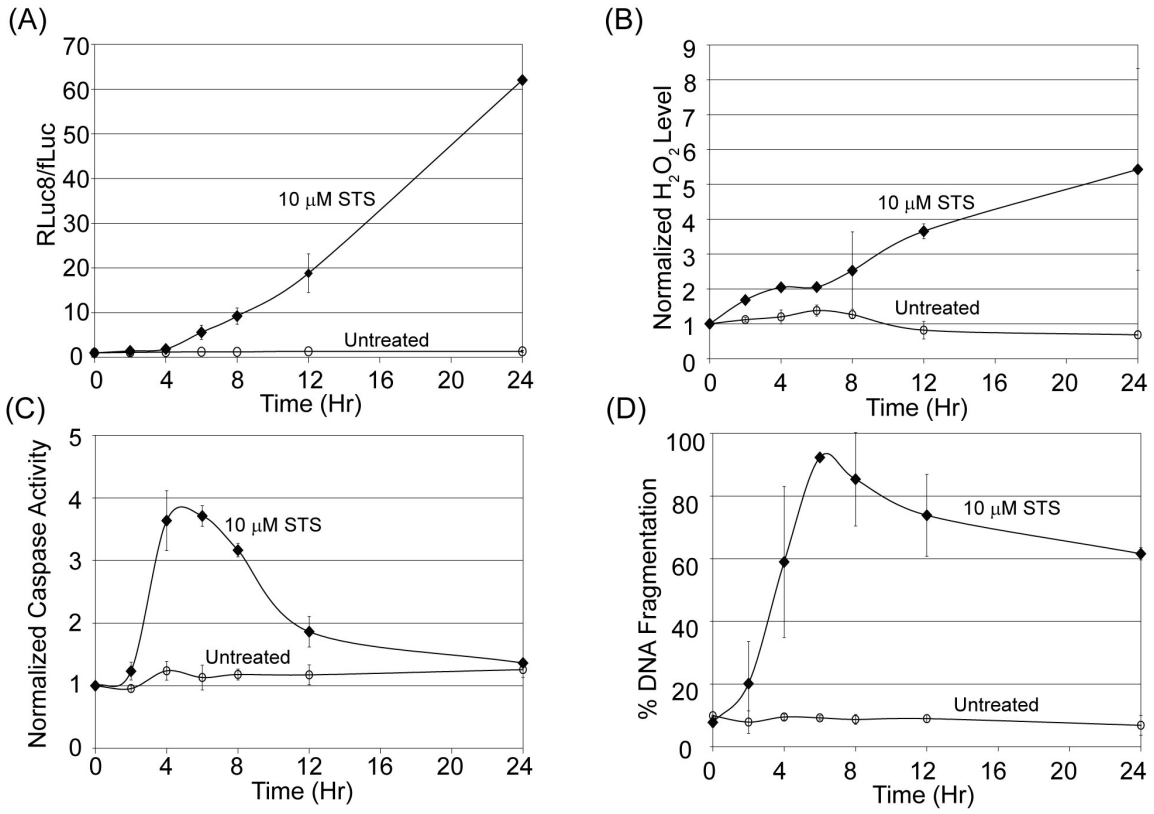

Figure 5.3. Response of RBS-MCF7 to treatment with PBS (untreated control) or 10 μM STS over the course of 24 hours. (A) Bioluminescent measurements of RLuc8 and fLuc were acquired at various times following treatment with STS or PBS (left axis) and the RLuc8:fLuc ratios were subsequently calculated (right axis). (B) Intracellular H_2O_2 levels were measured during the course of treatment. (C) Caspase activity measurements were acquired at various time points. (D) The percent DNA fragmentation was determined at various time points using a TUNEL assay. In all studies (except TUNEL assays, which provide an absolute measure of cell death), measurements were normalized to control (time = 0).

The versatility of the RBS was tested further in 293T/17 cells. When RBS-293T/17 cells were treated with a dosage range of STS (0-50 μM) for 6 hours, fLuc bioluminescence decreased and RLuc8 bioluminescence remained relatively stable with increasing dosage (Figure 5.4A, left axis); thus an increase in the RLuc8:fLuc ratio was

observed (Figure 5.4A, right axis). Under the same treatment conditions, a rise in intracellular H_2O_2 was exhibited (Figure 5.4B). The two control assays for cell death revealed that caspase-3 activity increased (Figure 5.4C) along with DNA fragmentation (Figure 5.4D), indicating that increasing STS dosage led to a corresponding increase in PCD.

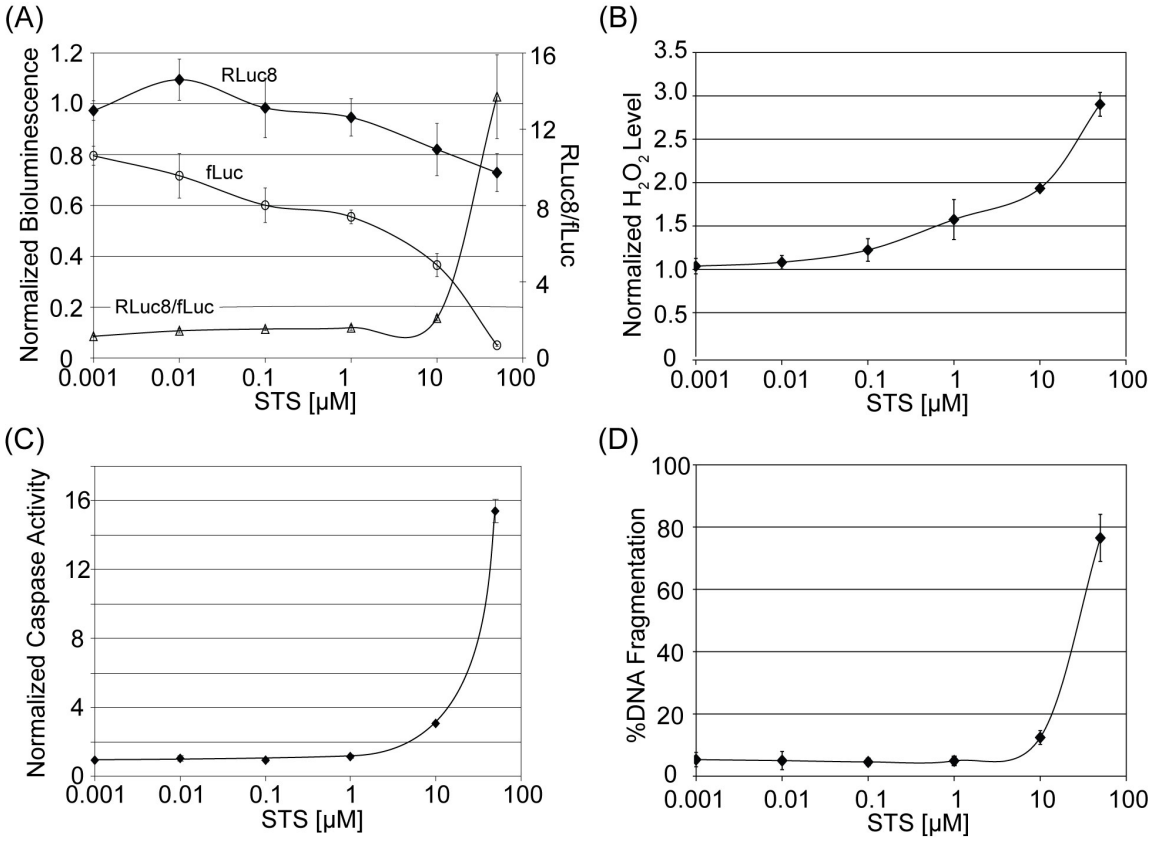

Figure 5.4. Response of 293T/17 cells to increasing STS dosage. RBS-293T/17 cells were treated with a dosage range of STS (0-50 μM) for 6 hours. (A) Bioluminescence measurements of RLuc8 and fLuc were acquired for each STS concentration after 6 hours (left axis). The RLuc8:fLuc ratio was subsequently calculated for each STS concentration (right axis). (B) Intracellular H_2O_2 levels were assessed using CM-H_2DCFDA at each STS concentration. (C) A Caspase 3/7 Glo assay was performed to measure caspase activity at each STS concentration. (D) A TUNEL assay for DNA fragmentation was performed at each STS concentration.

The effects of 10 μM STS over the course of 24 hours were also examined in RBS 293T/17 cells. As expected, the RLuc8:fLuc ratio increased with time, as shown in Figure 5.5A, while the PBS treated control remained unchanged. Similarly, intracellular H_2O_2 (Figure 5.5B) levels increased when treated with 10 μM STS for up to 24 hours compared to PBS treated controls. The two control assays for cell death indicated that caspase-3 activity increased (Figure 5.5C) and DNA fragmentation (Figure 5.5D), also increased with time.

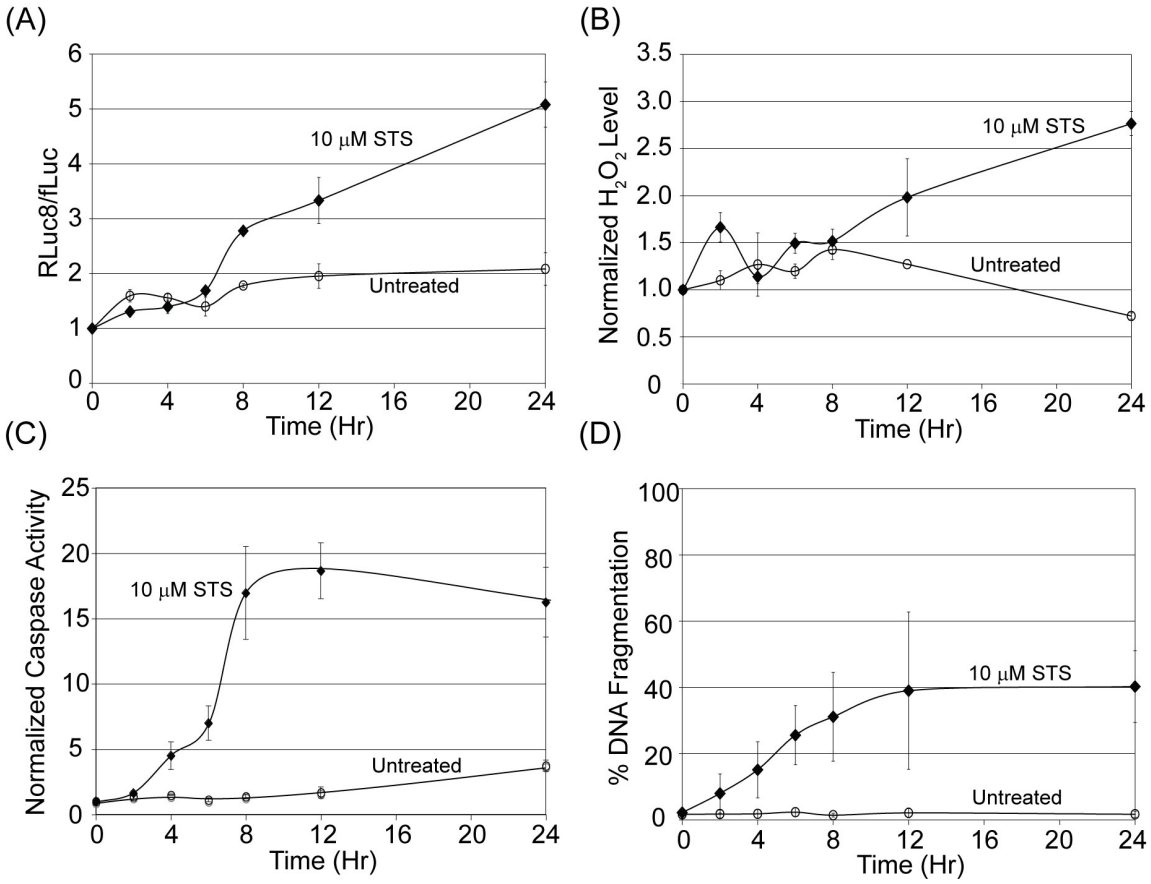

Figure 5.5. Response of RBS-293T/17 to treatment with PBS (untreated control) or 10 μM STS over the course of 24 hours. (A) Bioluminescent measurements of RLuc8 and fLuc were acquired at various times following treatment with STS or PBS (left axis) and the RLuc8:fLuc ratios were subsequently calculated (right axis). (B) Intracellular H_2O_2 levels were measured during the course of treatment. (C) Caspase activity measurements were acquired at various time points. (D) The percent DNA fragmentation was determined at various time points using a TUNEL assay. In all studies (except TUNEL assays, which provide an absolute measure of cell death), measurements were normalized to control (time = 0).

Similar to RBS-MCF7 and RBS-HeLa cells, RLuc8:fLuc ratio and intracellular H_2O_2 levels in STS-treated RBS-293T/17 cells (10 μM STS for 24 hours) could be significantly reduced ($p<0.05$) by the application of 100 μM allopurinol for one hour

prior to STS, as shown in Figure 5.6A and 5.6B, respectively. These results further support the notion that the PCD detection of the RBS is related to H_2O_2 levels.

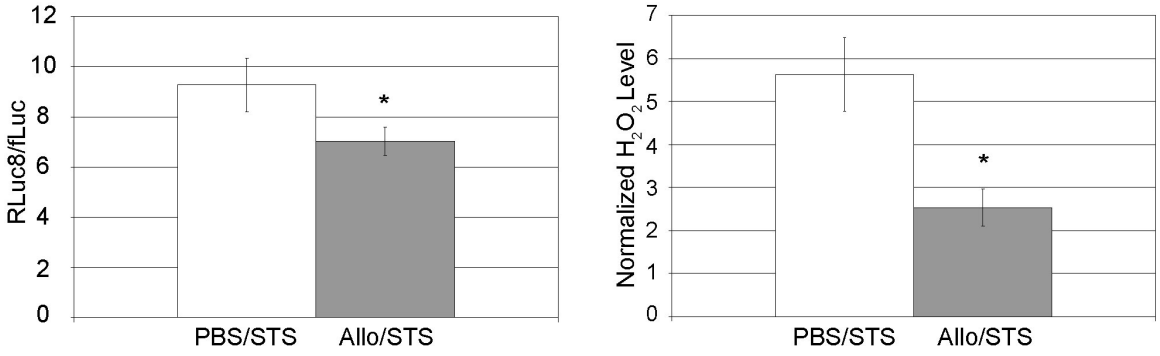

Figure 5.6. Effect of allopurinol on PBS (-STS) and STS treated RBS-293T/17 cells. 100 μM allopurinol or PBS was added to the cells for 1 hour prior to PBS or 10 μM STS application for 24 hours. (A) RLuc8 and fLuc bioluminescence measurements were obtained and the RLuc8:fLuc ratio is calculated and reported. (B) Intracellular H_2O_2 levels were measured using CM-H_2DCFDA. For both assays, values were normalized to PBS/PBS treated controls. Statistical significance: *($p<0.05$).

Further investigation of the capabilities of the RBS involved treating RBS-HeLa cells with doxorubicin (DOX) and camptothecin (Cpt). RBS-HeLa cells treated with 1 μM DOX exhibited an increase in the RLuc8:fLuc ratio over the time course of 48 hours, compared to control (Figure 5.7A). In addition, intracellular H_2O_2 levels also increased in DOX-treated cells compared to controls (Figure 5.7B). The application of 10 μM Cpt for up to 48 hours elicited similar results for the RLuc8:fLuc ratio (Figure 5.7C) and intracellular H_2O_2 levels (Figure 5.7D).

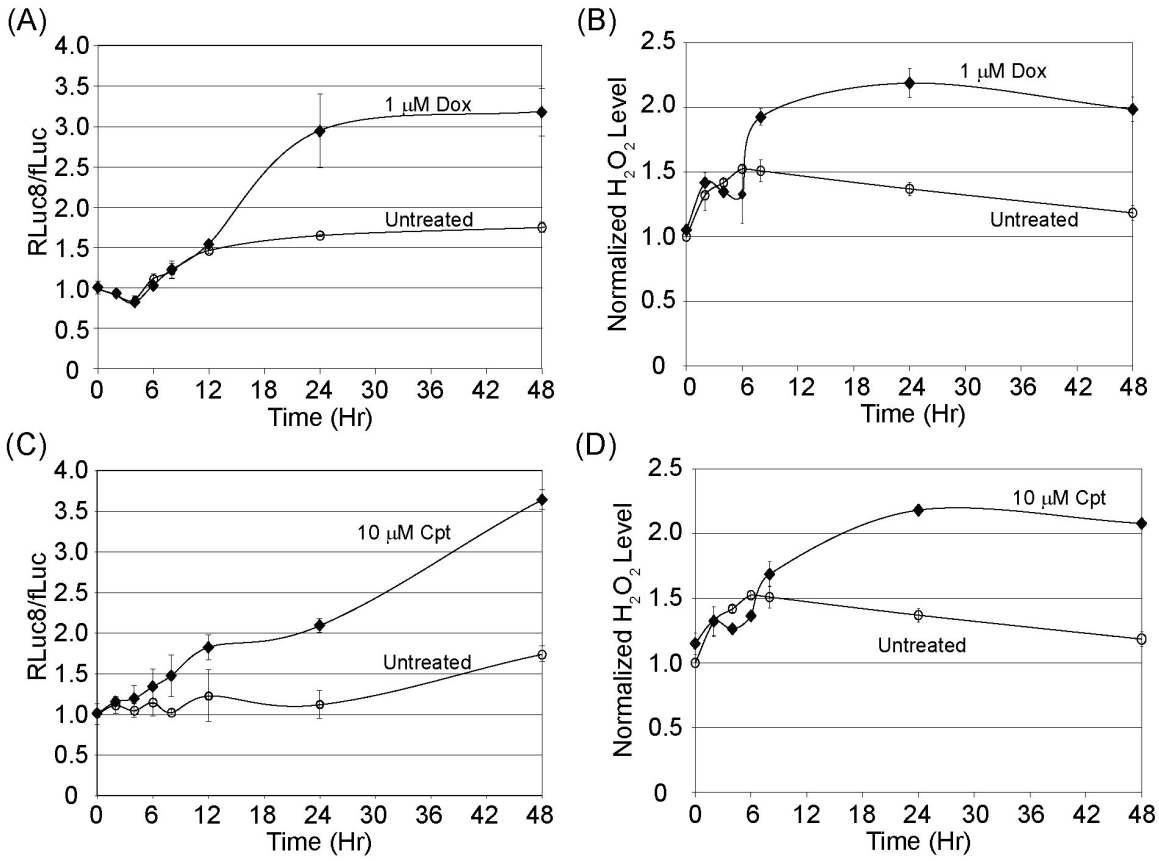

Figure 5.7. Effects of DOX and Cpt on RBS-HeLa cells. RBS-HeLa cells were treated with PBS (i.e. untreated control), 1 μM DOX or 10 μM Cpt over the time course of 48 hours. RLuc8 and fLuc bioluminescence measurements were taken at various time points following treatment with (A) DOX or (C) Cpt or PBS and the RLuc8:fLuc ratio was calculated. Intracellular H_2O_2 levels were measured in cells treated with (B) DOX, (D) Cpt or PBS. All reported values were normalized to time 0.

When RBS-HeLa cells were treated with 1 μM DOX over a time course of 48 hours, caspase-3 activity increased, compared to PBS treated control (Figure 5.8A). Under the same treatment conditions, DNA fragmentation percentage increased predominantly from 24 to 48 hours (Figure 5.8B). The application of 10 μM Cpt on

RBS-HeLa cells for 48 hours yielded a similar increase in caspase-3 activity (Figure 5.8C). The percent of DNA fragmentation increased earlier in the Cpt treated cells (Figure 5.8D) compared to DOX-treated cells, but the kinetic profile was similar between 24 and 48 hours.

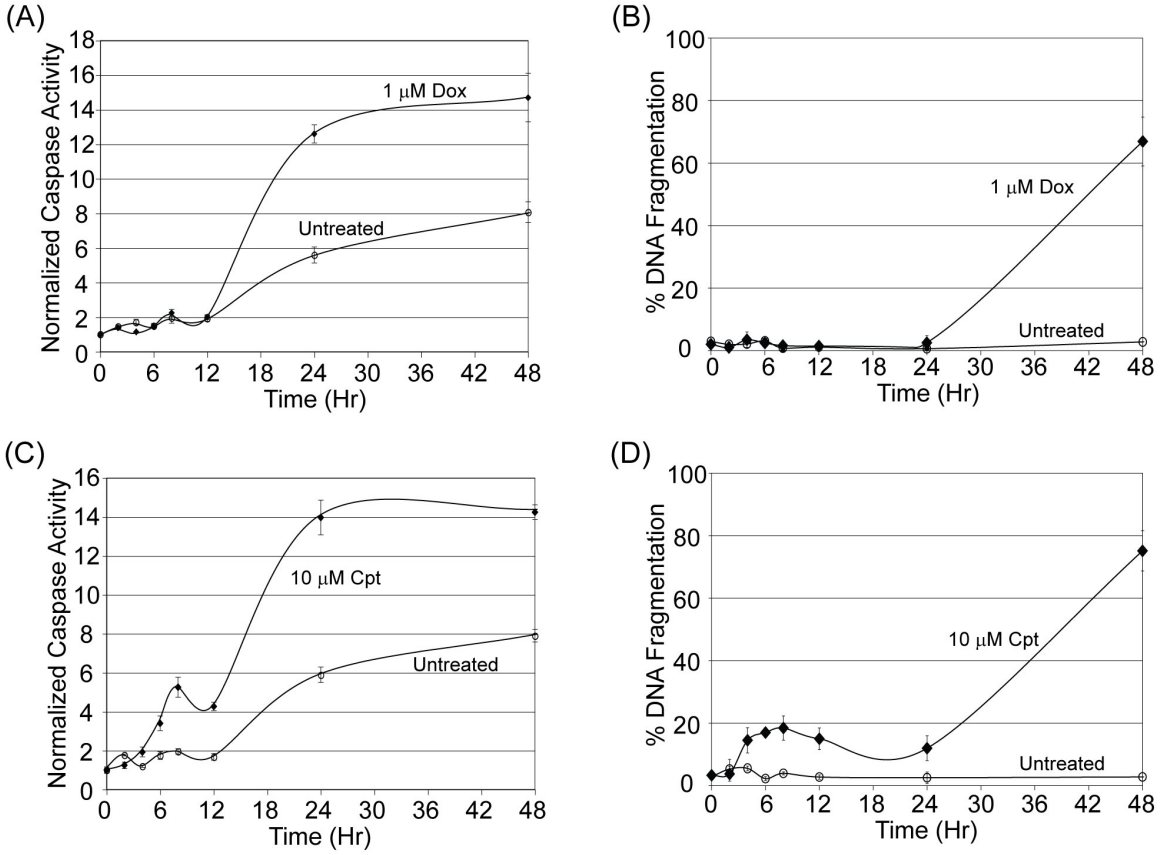

Figure 5.8. Response of commercial cell death assays in RBS-HeLa cells treated with DOX or Cpt. Caspase activity measurements were taken at various time points using Caspase-3/7 Glo after (A) 1 μM DOX , (C) 10 μM Cpt or PBS treatment on RBS-HeLa cells. Values were normalized to PBS (untreated) control at time 0. TUNEL assays for DNA fragmentation were performed on cells treated with (B) DOX, (D) Cpt, or PBS. In all studies (except TUNEL assays, which provide an absolute measure of cell death), measurements were normalized to control (time = 0).

To investigate the role of H_2O_2 in the mechanism of the RBS in HeLa cells treated with DOX and Cpt, RBS-HeLa cells were pretreated with 100 μM allopurinol for 1 hour prior to drug treatment. Allopurinol pretreatment prior to 1 μM DOX application yielded a significant ($p<0.05$) decrease in the RBS ratio compared to PBS pretreated control (Figure 5.9A). Intracellular H_2O_2 levels also decreased significantly ($p<0.01$) with allopurinol pretreatment before DOX application (Figure 5.9B). Similar significant decreases ($p<0.01$) in the RLuc8:fLuc ratio and intracellular H_2O_2 levels were demonstrated in RBS-HeLa cells treated with allopurinol prior to 10 μM Cpt (Figure 5.9C and 5.9D, respectively).

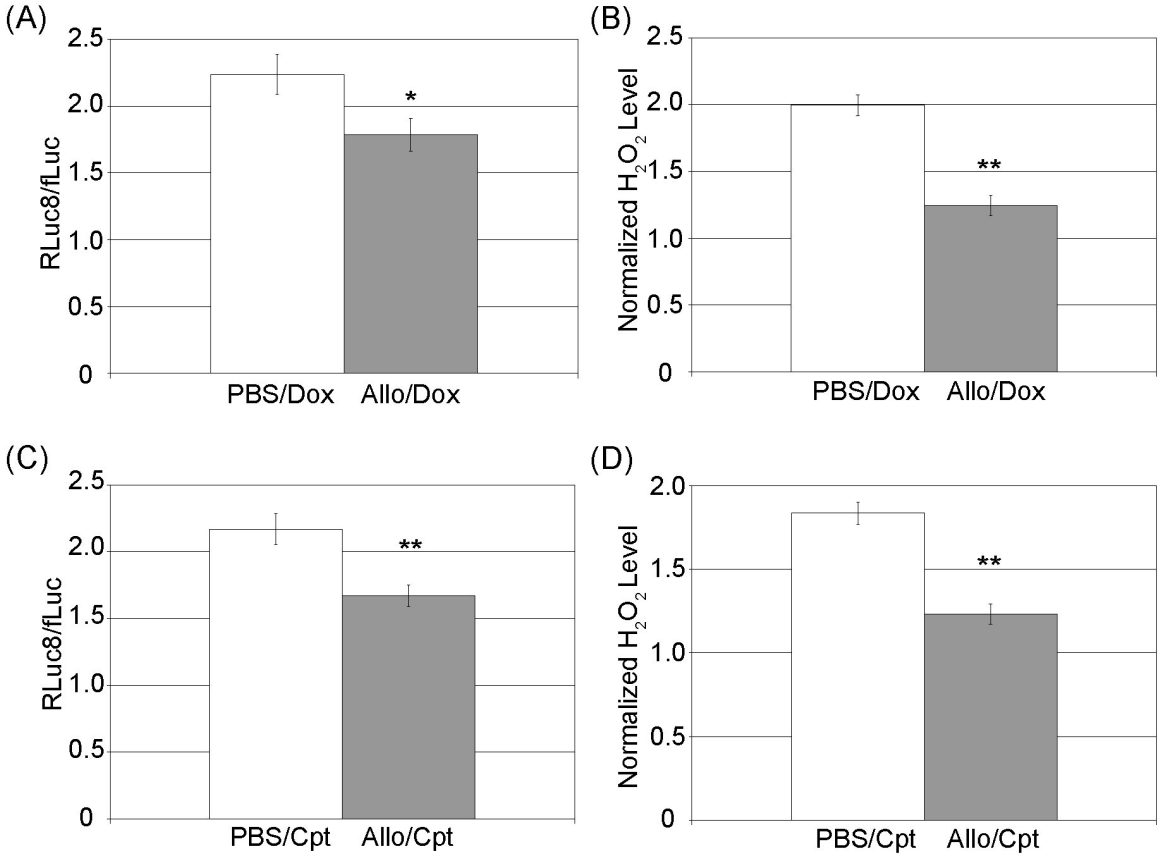

Figure 5.9. Response of DOX and Cpt treated RBS-HeLa cells to allopurinol pretreatment. RBS-HeLa cells were treated with PBS or 100 μM allopurinol for 1 hour prior to 1 μM DOX or 10 μM Cpt for 48 hours. RLuc8 and fLuc bioluminescence measurements were taken at various time points following treatment with (A) DOX or (C) Cpt and the RLuc8:fLuc ratio was calculated. Intracellular H_2O_2 levels were measured in cells treated with (B) DOX, (D) Cpt or PBS. All reported values were normalized PBS/PBS treated controls.

5.4 Discussion

It was shown in chapter 3 that the RBS is responsive to cell death induced by STS in HeLa cells. To begin to investigate the span of cell types in which the RBS could

function, RBS-MCF7 and RBS-293T/17 cells were also subjected to STS dosage and time course studies. The RBS exhibited an increase in the RLuc8:fLuc ratio in both cell lines with an increase in STS dosage (6 hour treatment); additionally, the RLuc8:fLuc ratio increased with time in RBS-MCF7 and RBS-293T/17 cells treated with 10 μM STS for up to 24 hours. Corresponding assays for cell death demonstrated that both cell lines were undergoing PCD under these conditions, which was expected based on previous reports of STS inducing PCD in MCF7 (22) and 293T/17 cells(23). The ability of the RBS to relay information on cell death in MCF7 and 293T/17 cells in addition to HeLa cells indicates its versatility and potential for utilization over a wide range of cellular research endeavors.

Similar to HeLa cells, when MCF7 and 293T/17 cells are treated with STS, cell death was accompanied by an increase in H_2O_2. These findings suggest that H_2O_2 levels are increased in a wide range of cell lines as a consequence of STS-induced PCD, consistent with previous reports(24, 25). As shown in chapter 4, the RLuc8:fLuc ratio can be reduced in STS-treated RBS-HeLa cells by pretreatment with allopurinol, and this reduction is due to the rescue of functional fLuc protein levels. Allopurinol, a xanthine oxidase (XO) inhibitor(21), prevents the oxidation of xanthine or hypoxanthine by XO, thereby reducing production of the dominant oxidant of H_2O_2(26). The treatment of RBS-MCF7 cells with allopurinol for 1 hour prior to STS effectively reduced the RBS ratio and intracellular H_2O_2 levels, while leaving caspase-3 activity and DNA fragmentation unchanged. The correlation between the decrease in intracellular H_2O_2 and the reduction in the RLuc8:fLuc ratio further supports the notion that the RBS is specifically responsive to H_2O_2 during cell death. However, the inability of allopurinol to

affect the extent of cell death suggests that H_2O_2 production is a consequence of cell death, not a catalyst for cell death.

The STS time course studies on RBS-MCF7 cells introduced an interesting disparity between caspase-3 activity and DNA fragmentation, RBS ratio and intracellular H_2O_2 levels; namely, caspase-3 activity returned to near-control levels while the remaining three parameters continued to increase. These results highlight how the use of caspase-3 activity as a biomarker for cell death could potentially lead to ambiguous findings, due to the transient nature of its activation. Here, the RBS may hold an advantage over traditional cell death assays, since it is capable of detecting cell death when caspase activity assays cannot and it possesses real-time detection ability. Additionally, the RBS can be used for *in vivo* assays, an ability that is not characteristic of the TUNEL assay. The correlation between the TUNEL assay and the RBS, even in the absence of caspase activity, suggests that the RBS may be able to provide insight on cells undergoing caspase-independent PCD. This would not be entirely surprising considering that many previous studies have shown that caspase-independent cell death pathways can involve ROS(27-32).

Inducing caspase-dependent cell death (apoptosis) in tumor cells remains a topic of interest regarding cancer therapeutics, and DOX and Cpt are two well-established therapeutics (see (33, 34) for reviews, respectively). The overall increasing trend in RLuc8:fLuc ratio, DNA fragmentation and H_2O_2 levels following DOX- and Cpt-treatment suggests that the RBS will likely detect cell death under a vast array of induction methods. Many other drugs have also been shown to result in an increase in H_2O_2 levels. For example, it has been shown that murine epidermal cells treated with

vanadate undergo apoptosis and exhibit an increase in intracellular H_2O_2 cells(35). Also, apoptosis induced by erbstatin (36), vinblastine and inostamycin (37) in human small cell lung carcinoma cells is accompanied by increased intracellular H_2O_2 levels.

In summary, we have determined that the RBS is capable of detecting PCD in multiple cell lines using multiple inducers. It is envisioned that the RBS will prove to be useful for investigations of any death-inducing conditions that are accompanied by an increase in H_2O_2 levels. Given that the RBS does not rely on caspases for its functionality, it is hypothesized that it may perform well during instances of caspase-independent PCD as well.

5.5 References

1. Nunez G, Benedict MA, Hu Y, Inohara N. Caspases: the proteases of the apoptotic pathway. Oncogene 1998;17:3237-45.

2. Ai HW, Hazelwood KL, Davidson MW, Campbell RE. Fluorescent protein FRET pairs for ratiometric imaging of dual biosensors. Nat Methods 2008;5:401-3.

3. Bullok K, Piwnica-Worms D. Synthesis and characterization of a small, membrane-permeant, caspase-activatable far-red fluorescent peptide for imaging apoptosis. J Med Chem 2005;48:5404-7.

4. Hug H, Los M, Hirt W, Debatin KM. Rhodamine 110-linked amino acids and peptides as substrates to measure caspase activity upon apoptosis induction in intact cells. Biochemistry 1999;38:13906-11.

5. Leytus SP, Melhado LL, Mangel WF. Rhodamine-based compounds as fluorogenic substrates for serine proteinases. Biochem J 1983;209:299-307.

6. Liu J, Bhalgat M, Zhang C, Diwu Z, Hoyland B, Klaubert DH. Fluorescent molecular probes V: a sensitive caspase-3 substrate for fluorometric assays. Bioorg Med Chem Lett 1999;9:3231-6.

7. Packard BZ, Toptygin DD, Komoriya A, Brand L. Profluorescent protease substrates: intramolecular dimers described by the exciton model. Proc Natl Acad Sci U S A 1996;93:11640-5.

8. Takemoto K, Nagai T, Miyawaki A, Miura M. Spatio-temporal activation of caspase revealed by indicator that is insensitive to environmental effects. J Cell Biol 2003;160:235-43.

9. Tung CH. Fluorescent peptide probes for in vivo diagnostic imaging. Biopolymers 2004;76:391-403.

10. Tyas L, Brophy VA, Pope A, Rivett AJ, Tavare JM. Rapid caspase-3 activation during apoptosis revealed using fluorescence-resonance energy transfer. EMBO Rep 2000;1:266-70.

11. Zhang HZ, Kasibhatla S, Guastella J, Tseng B, Drewe J, Cai SX. N-Ac-DEVD-N'-(Polyfluorobenzoyl)-R110: novel cell-permeable fluorogenic caspase substrates for the detection of caspase activity and apoptosis. Bioconjug Chem 2003;14:458-63.

12. Shah K, Tung CH, Breakefield XO, Weissleder R. In vivo imaging of S-TRAIL-mediated tumor regression and apoptosis. Mol Ther 2005;11:926-31.

13. Kizaka-Kondoh S, Itasaka S, Zeng L, et al. Selective killing of hypoxia-inducible factor-1-active cells improves survival in a mouse model of invasive and metastatic pancreatic cancer. Clin Cancer Res 2009;15:3433-41.

14. Laxman B, Hall DE, Bhojani MS, et al. Noninvasive real-time imaging of apoptosis. Proc Natl Acad Sci U S A 2002;99:16551-5.

15. Coppola JM, Ross BD, Rehemtulla A. Noninvasive imaging of apoptosis and its application in cancer therapeutics. Clin Cancer Res 2008;14:2492-501.

16. Broker LE, Kruyt FA, Giaccone G. Cell death independent of caspases: a review. Clin Cancer Res 2005;11:3155-62.

17. Skladanowski A, Konopa J. Adriamycin and daunomycin induce programmed cell death (apoptosis) in tumour cells. Biochem Pharmacol 1993;46:375-82.

18. Whitacre CM, Berger NA. Factors affecting topotecan-induced programmed cell death: adhesion protects cells from apoptosis and impairs cleavage of poly(ADP-ribose)polymerase. Cancer Res 1997;57:2157-63.

19. Nicholson DW, Ali A, Thornberry NA, et al. Identification and inhibition of the ICE/CED-3 protease necessary for mammalian apoptosis. Nature 1995;376:37-43.

20. Williams JR, Little JB, Shipley WU. Association of mammalian cell death with a specific endonucleolytic degradation of DNA. Nature 1974;252:754-5.

21. Elion GB. Enzymatic and metabolic studies with allopurinol. Ann Rheum Dis 1966;25:608-14.

22. Sayeed A, Konduri SD, Liu W, Bansal S, Li F, Das GM. Estrogen receptor alpha inhibits p53-mediated transcriptional repression: implications for the regulation of apoptosis. Cancer Res 2007;67:7746-55.

23. Ray P, De A, Patel M, Gambhir SS. Monitoring caspase-3 activation with a multimodality imaging sensor in living subjects. Clin Cancer Res 2008;14:5801-9.

24. Gil J, Almeida S, Oliveira CR, Rego AC. Cytosolic and mitochondrial ROS in staurosporine-induced retinal cell apoptosis. Free Radic Biol Med 2003;35:1500-14.

25. Prehn JH, Jordan J, Ghadge GD, et al. Ca2+ and reactive oxygen species in staurosporine-induced neuronal apoptosis. J Neurochem 1997;68:1679-85.

26. Fatokun AA, Stone TW, Smith RA. Hydrogen peroxide mediates damage by xanthine and xanthine oxidase in cerebellar granule neuronal cultures. Neurosci Lett 2007;416:34-8.

27. Carmody RJ, Cotter TG. Signalling apoptosis: a radical approach. Redox Rep 2001;6:77-90.

28. Erdal H, Berndtsson M, Castro J, Brunk U, Shoshan MC, Linder S. Induction of lysosomal membrane permeabilization by compounds that activate p53-independent apoptosis. Proc Natl Acad Sci U S A 2005;102:192-7.

29. Kanzawa T, Germano IM, Komata T, Ito H, Kondo Y, Kondo S. Role of autophagy in temozolomide-induced cytotoxicity for malignant glioma cells. Cell Death Differ 2004;11:448-57.

30. Kim R, Emi M, Tanabe K, Murakami S, Uchida Y, Arihiro K. Regulation and interplay of apoptotic and non-apoptotic cell death. J Pathol 2006;208:319-26.

31. Sugioka K, Nakano M, Totsune-Nakano H, Minakami H, Tero-Kubota S, Ikegami Y. Mechanism of O2- generation in reduction and oxidation cycle of ubiquinones in a model of mitochondrial electron transport systems. Biochim Biophys Acta 1988;936:377-85.

32. Tay VK, Wang AS, Leow KY, Ong MM, Wong KP, Boelsterli UA. Mitochondrial permeability transition as a source of superoxide anion induced by the nitroaromatic drug nimesulide in vitro. Free Radic Biol Med 2005;39:949-59.

33. Davis HL, Davis TE. Daunorubicin and adriamycin in cancer treatment: an analysis of their roles and limitations. Cancer Treat Rep 1979;63:809-15.

34. Dancey J, Eisenhauer EA. Current perspectives on camptothecins in cancer treatment. Br J Cancer 1996;74:327-38.

35. Ye J, Ding M, Leonard SS, et al. Vanadate induces apoptosis in epidermal JB6 P+ cells via hydrogen peroxide-mediated reactions. Mol Cell Biochem 1999;202:9-17.

36. Simizu S, Imoto M, Masuda N, Takada M, Umezawa K. Involvement of hydrogen peroxide production in erbstatin-induced apoptosis in human small cell lung carcinoma cells. Cancer Res 1996;56:4978-82.

37. Simizu S, Takada M, Umezawa K, Imoto M. Requirement of caspase-3(-like) protease-mediated hydrogen peroxide production for apoptosis induced by various anticancer drugs. J Biol Chem 1998;273:26900-7.

Chapter 6: The RBS can detect caspase-independent PCD through pathways involving ROS production, Bcl-2 downregulation and mitochondrial membrane permeabilization

6.1 Abstract

A variety of cancer phenotypes possess the ability to evade caspase activation and this can result in both tumorigenesis and anticancer drug resistance, especially if the drugs are designed to induce caspase-dependent PCD. Accordingly, the development of drugs that induce caspase-independent PCD has been garnering much attention in the scientific community. It is envisioned that the ability to monitor caspase-independent PCD through molecular imaging would undoubtedly lead to both novel and improved cancer therapeutics. In this chapter, we show that the RBS is capable of detecting caspase-independent PCD induced by different compounds that act through distinct pathways.

6.2 Introduction

While caspase-3 activation is considered a gold-standard for the identification of cells undergoing programmed cell death (PCD), caspase-independent PCD has recently been attracting attention in regards to cancer drug development. Anticancer drug resistance and tumorigenesis have been linked to the ability of certain cancer types to

evade caspase activation(1, 2). Thus, it is envisioned that cancer therapeutics that induce caspase-independent PCD could have widespread impact.

In one study, caspase-independent PCD was induced in HeLa cells treated with sodium selenite (SSe)(3). Here, it was deduced that p53 and p38 were activated independently of caspases through an oxidative stress mediated process. It has also been shown that resveratrol induces caspase-independent PCD in MCF7 cells through Bcl-2 downregulation, mitochondrial membrane permeabilization and ROS production without caspase 3 activation, PARP cleavage or cytochrome c release(4). In another study, various microtubule stabilizing agents (MSAs) induced caspase-independent PCD in non-small cell lung carcinoma (NSCLC) cells and it was found that cathepsin B played a pivotal role(5). Additionally, paclitaxel, a type of MSA(6), has been shown to induce caspase-independent PCD in ovarian cancer cells through an apoptosis inducing factor (AIF) mechanism(7). Other groups have reported caspase-independent PCD in arsenic trioxide-treated myeloma cells(8), vitamin D-treated breast cancer cells(9, 10), and flavopiridol-treated glioma cells(11).

The therapeutic need for agents that induce caspase-independent PCD gives rise to the necessity of assays that can detect this phenomenon. Additionally, current studies involving these types of agents will likely warrant assays that can be extended to animal models. Currently, not all PCD sensors rely on caspase activity as a metric for PCD. The terminal deoxynucleotidyl transferase dUTP nick end labeling (TUNEL) assay, first developed in 1992(12), detects DNA strand breaks after terminal deoxynucleotidyl transferase (TdT) incorporates labeled dUTP at break sites; DNA fragmentation is a hallmark of cells undergoing PCD(13). CytoTox Glo is a bioluminescent assay that

measures the activity of certain intracellular proteases (dead-cell proteases) that are released from cells with compromised membranes. Additionally, assays that measure the reduction of various tetrazolium salts, such as MTT(14), XTT(15) and WST-1(16), by intracellular dehydrogenases active only in living cells are commonly used. However, it is important to note that these reduction assays are actually a measure of cell viability as opposed to cell death. Although all of these assays clearly have utility in measuring PCD in cell culture, most of them are not appropriate for real-time imaging/detection and/or imaging in animal models of disease. These limitations arise from the need for cell lysis, the use of membrane impermeable substrates, and/or the use of green fluorescent dyes, which are generally masked by autofluorescence *in vivo*.

Notably, many instances of caspase-independent PCD involve an increase in the intracellular level of reactive oxygen species (ROS)(1-3, 17). Therefore, imaging agents that specifically detect ROS could potentially be used to identify cells undergoing caspase-independent cell death. In this chapter, we show that the RBS is able to detect caspase-independent PCD with inducers that involve distinct pathways, and that this detection corresponds with intracellular H_2O_2 levels.

6.3 Results

To test the hypothesis that the RBS may be able to provide insight into cells undergoing caspase-independent PCD, RBS-HeLa cells were treated with sodium selenite (SSe). This compound has been shown to induce caspase-independent PCD in HeLa cells through oxidative stress mediated activation of p53 and p38(3). When RBS-HeLa cells were treated with a dosage range of SSe for 24 hours, the RLuc8:fLuc ratio increased

(Figure 6.1A), while caspases 3 and 7 remained relatively inactive (Figure 6.1B). Under the same conditions, the intracellular H_2O_2 levels also rose appreciably (Figure 6.1C). Additionally, to examine whether or not SSe caused cell death, a TUNEL assay was performed. As seen in Figure 6.1D, DNA fragmentation increased with SSe treatment.

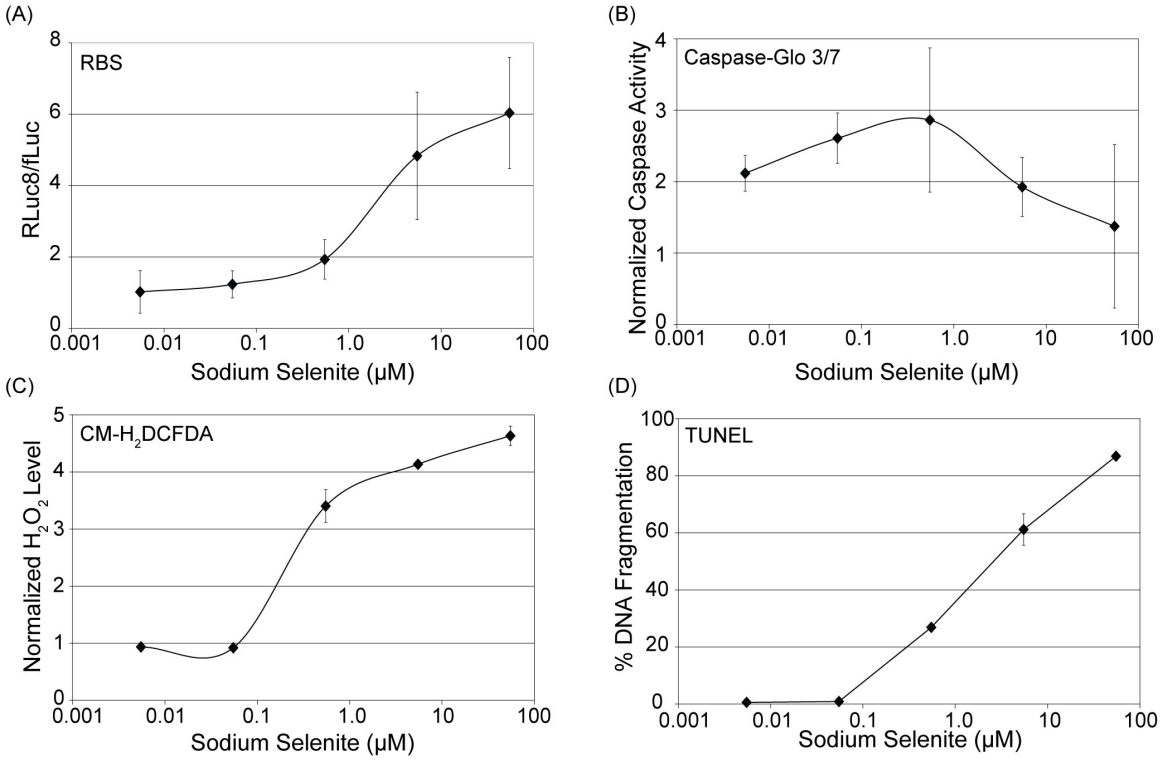

Figure 6.1. Response of RBS-HeLa cells to increasing doses of sodium selenite. Sodium selenite (SSe) was added to RBS-HeLa cells at a concentration range of 0-55 μM for 24 hours. (A) RLuc8:fLuc ratios were calculated for treated RBS-HeLa cells. (B) Caspase activity in treated RBS-HeLa cells was measured using Caspase 3/7 Glo. (C) Intracellular H_2O_2 measurements in treated RBS-HeLa cells were obtained using CM-H_2DCFDA. (D) A TUNEL assay for DNA fragmentation was performed on treated RBS-HeLa cells. In all studies (except TUNEL assays, which provide an absolute measure of cell death), measurements were normalized to control (0 μM SSe).

Parallel studies were performed on RBS-MCF7 cells using SSe; the pathway in which SSe induces PCD in MCF7 cells remains unknown, however it has been shown to decrease viability in these cells(18). With increasing SSe dosage (0 – 55 μM), the RLuc8:fLuc ratio of the RBS increased (Figure 6.2A), caspase-3 activation was not observed (Figure 6.2B), and intracellular H_2O_2 and DNA fragmentation levels (Figure 6.2C and 6.2D, respectively) increased.

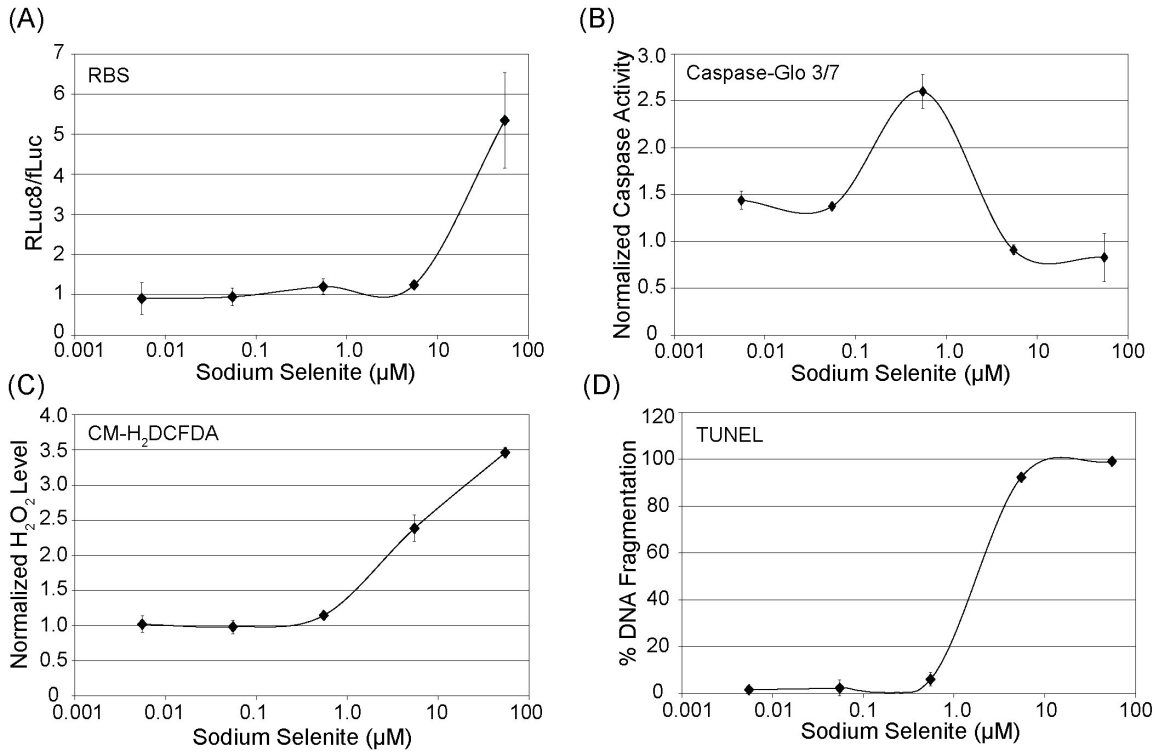

Figure 6.2. Response of RBS-MCF7 cells to increasing doses of sodium selenite. Sodium selenite (SSe) was added to RBS-MCF7 cells at a concentration range of 0-55 μM for 48 hours. (A) Bioluminescent measurements of RLuc8 and fLuc were acquired at each SSe concentration and the RLuc8:fLuc ratios were subsequently calculated. (B) A Caspase 3/7 Glo assay was performed to measure caspase activity at each SSe concentration. (C) Intracellular H_2O_2 levels were assessed using CM-H_2DCFDA at each SSe concentration. (D) A TUNEL assay for DNA fragmentation was performed at each STS concentration. In all studies (except TUNEL assays, which provide an absolute measure of cell death), measurements were normalized to control (0 μM SSe).

To further examine the detection of caspase-independent PCD by the RBS, resveratrol was used as a cell death inducer in RBS-MCF7 cells. Resveratrol has been shown to induce caspase-independent PCD in MCF7 cells through Bcl-2 downregulation, mitochondrial membrane permeabilization and ROS production without caspase 3 activation, PARP cleavage or cytochrome c release(4). As shown in Figure 6.3A, when RBS-MCF7 cells were treated with increasing dosages of resveratrol for 24 hours, the RLuc8:fLuc ratio increased. Similarly to the SSe studies, caspases remained relatively inactive while intracellular H_2O_2 and DNA fragmentation levels increased (Figure 6.3B-D).

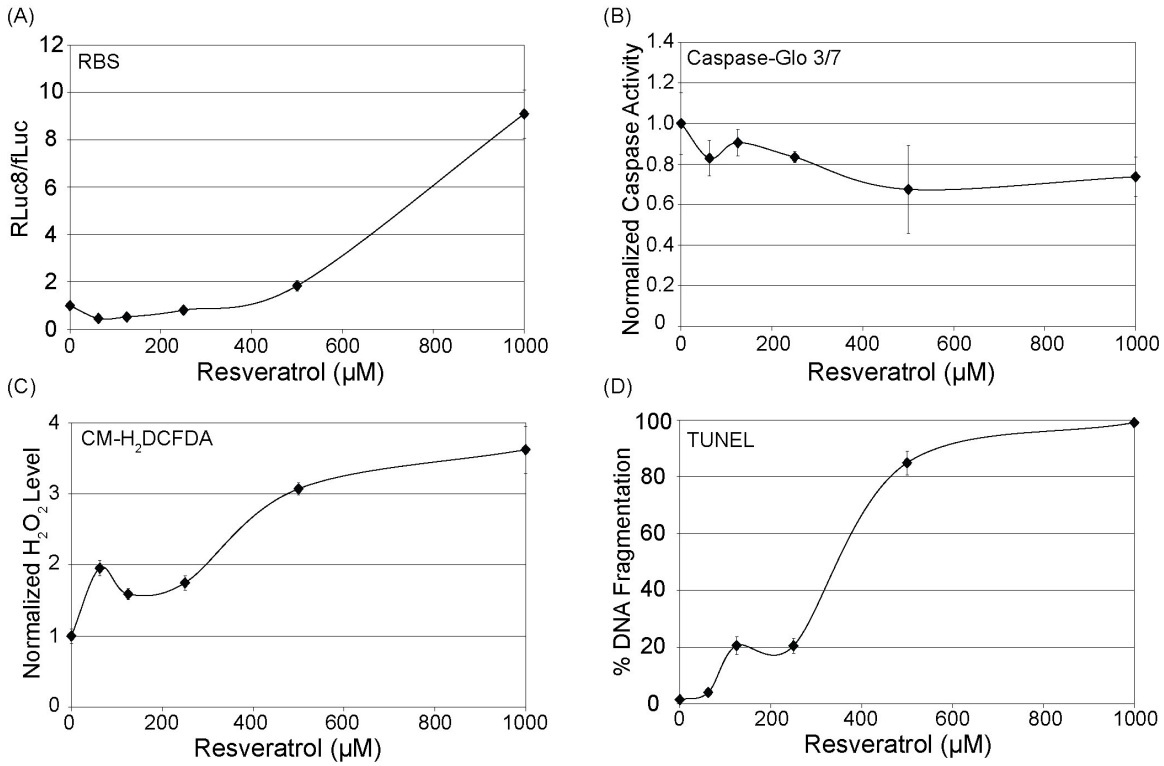

Figure 6.3. Response of RBS-MCF7 cells to increasing doses of resveratrol. Resveratrol (Res) was added to RBS-MCF7 cells at a concentration range of 0-1000 μM for 24 hours. (A) RLuc8:fLuc ratios were calculated for treated RBS-MCF7 cells. (B) Caspase activity in treated RBS-MCF7 cells was measured using Caspase 3/7 Glo. (C) Intracellular H_2O_2 measurements in treated RBS-MCF7 cells were obtained using CM-H_2DCFDA. (D) A TUNEL assay for DNA fragmentation was performed on treated RBS-MCF7 cells. In all studies (except TUNEL assays, which provide an absolute measure of cell death), measurements were normalized to control (0 μM Res).

As with previous studies with cell death inducers, allopurinol was used as an inhibitor of xanthine oxidase in order to reduce intracellular H_2O_2 on both RBS-HeLa and RBS-MCF7 cells treated with 55 μM SSe and RBS-MCF7 cells treated with 1 mM Res. RBS-HeLa cells pretreated with 100 μM allopurinol for 1 hour prior to 55 μM SSe treatment for 24 hours exhibited significant decreases ($p<0.05$) in both RLuc8:fLuc ratio and intracellular H_2O_2 levels (Figure 6.4A and 6.4B, respectively), compared to PBS pretreated controls. Similarly, when RBS-MCF7 cells were pretreated with 100 μM STS for 1 hour before the addition of 55 μM SSe, there was a significant ($p<0.05$) decrease in the RLuc8:fLuc ratio and intracellular H_2O_2 levels compared to PBS pretreated controls after 48 hours, as seen in Figure 4C and 4D, respectively. Finally, Res-treated RBS-MCF7 cells that were subjected to allopurinol pretreatment also demonstrated significant ($p<0.01$) reductions in both RLuc8:fLuc (Figure 6.4E) and intracellular H_2O_2 levels (Figure 6.4F) after 24 hours.

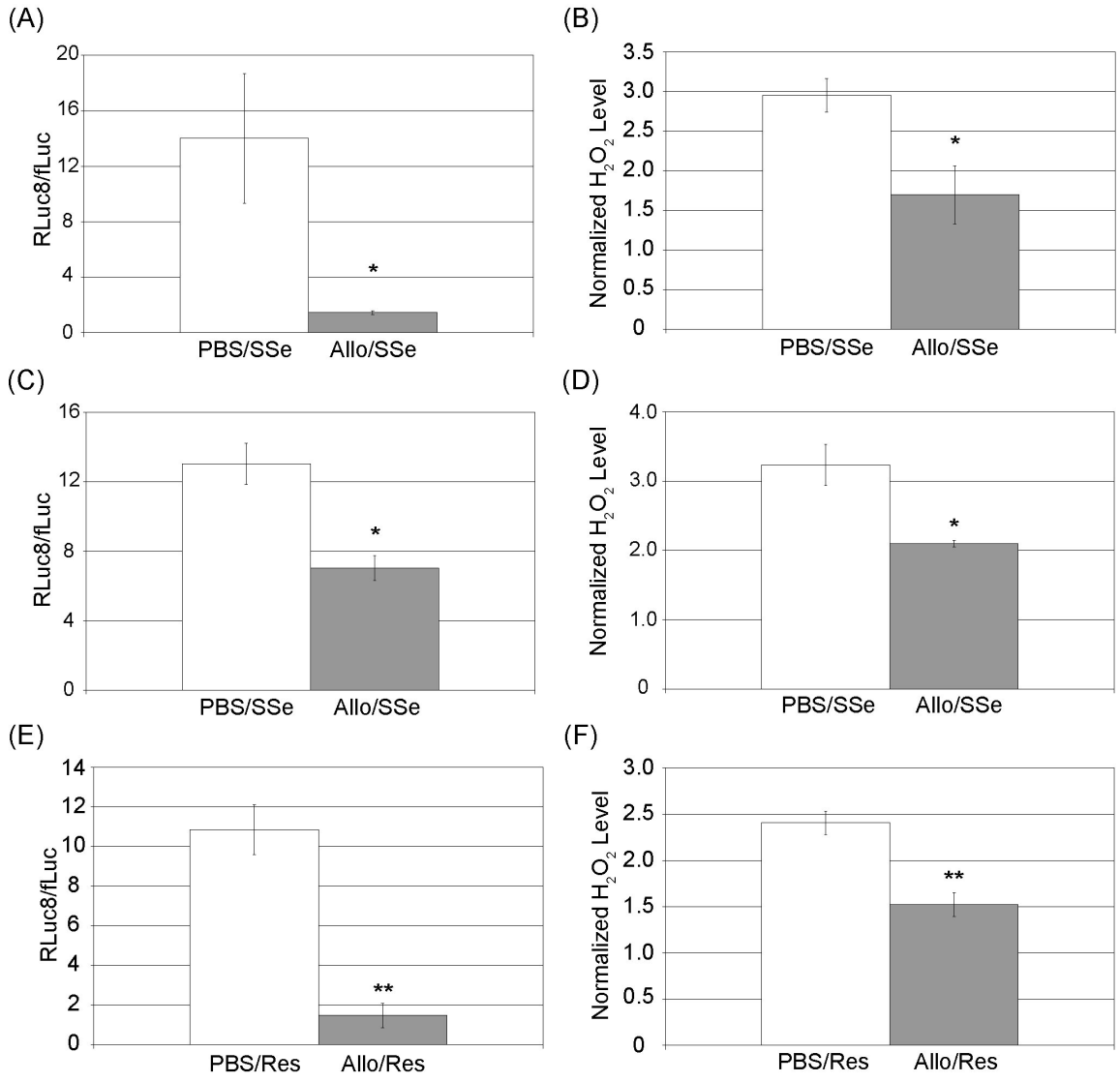

Figure 6.4. Effect of allopurinol on RBS-HeLa and RBS-MCF7 cells treated with SSe and RBS-MCF7 cells treated with Res. PBS or 100 μM allopurinol was added to cells for 1 hour prior to drug treatment. RLuc8 and fLuc bioluminescence measurements were acquired and the RLuc8:fLuc ratios were calculated and reported for (A) RBS-HeLa cells treated with 55 μM SSe for 24 hours, (C) RBS-MCF7 cells treated with 55 μM SSe for 48 hours, (E) RBS-MCF7 cells treated with 1 mM Res. Intracellular H_2O_2 levels were determined using CM-H_2DCFDA for (B) RBS-HeLa cells treated with 55 μM SSe for 24 hours, (D) RBS-MCF7 cells treated with 55 μM SSe for 48 hours, (F) RBS-MCF7 cells treated with 1 mM Res. All reported values were normalized to untreated controls. Statistical significance: *($p<0.05$), **($p<0.01$).

When RBS-HeLa cells were pretreated with allopurinol for one hour prior to 55 μM SSe treatment for 24 hours, the extent of PCD remained unchanged compared to PBS pretreatment according to the DNA fragmentation levels reported by the TUNEL assay (Figure 6.5A). DNA fragmentation percentage remained unchanged between PBS and allopurinol pretreated RBS-MCF7 cells after the application of 55 μM SSe for 48 hours (Figure 6.5B). Additionally, allopurinol pretreatment conferred no rescue from cell death when RBS-MCF7 cells were treated with 1 mM Res, compared to PBS pretreated control (Figure 6.5C).

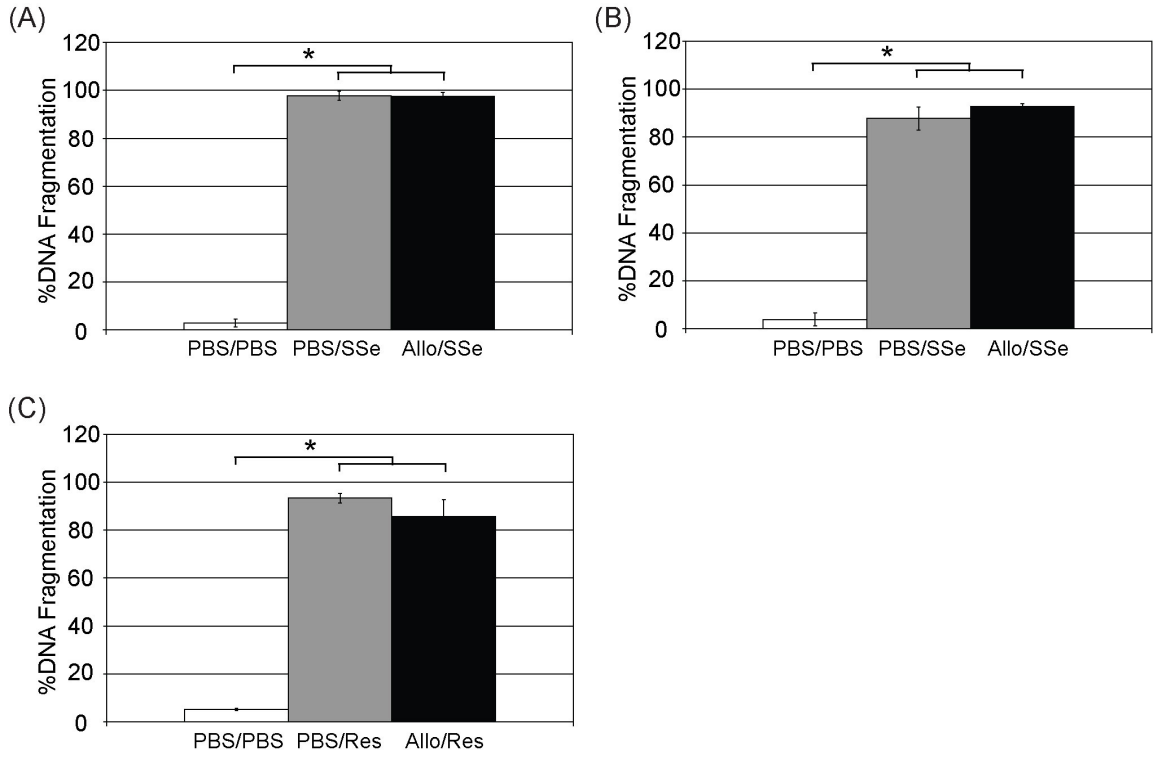

Figure 6.5. Extent of DNA fragmentation in RBS cells pretreated with allopurinol prior to the addition of SSe or Res. PBS or 100 μM allopurinol was used as a pretreatment for 1 hour prior to adding (A) PBS or 55 μM SSe to RBS-HeLa cells for 24 hours, (B) PBS or 55 μM SSe to RBS-MCF7 cells for 48 hours, or (C) PBS or 1 mM Res to RBS-MCF7 cells for 24 hours. Statistical significance: *($p<0.01$).

6.4 Discussion

Given the disparities seen in previous chapters where caspase-3 activity levels did not exhibit the same trends as DNA fragmentation levels, it was hypothesized that the RBS could be used to detect caspase-independent PCD. When both RBS-HeLa and RBS-MCF7 cells were treated with SSe, the RLuc8:fLuc ratio, percent DNA fragmentation and intracellular H_2O_2 levels increased while caspase-3/7 activity levels remained relatively unchanged. The increase in DNA fragmentation along with the lack of appreciable caspase activation show that SSe induces caspase-independent PCD and that this form of cell death can be detected by the RBS sensor in HeLa and MCF7 cells.

Resveratrol application to RBS-MCF7 cells produced results comparable to RBS-HeLa and RBS-MCF7 cells treated with SSe, further attesting to the impact the RBS may have on caspase-independent PCD research. Given the reported effects of resveratrol on the mitochondria and the associated increase in ROS(4), the RBS may be particularly useful in studies investigating the targeting of this organelle in cancer therapy(19). In fact, many compounds that target the mitochondria for this purpose create excessive amounts of ROS(20-24).

When cells were pretreated with allopurinol for one hour prior to SSe (RBS-HeLa and RBS-MCF7) or resveratrol (RBS-MCF7), the RLuc8:fLuc ratios were significantly decreased ($p<0.05$ for SSe, $p<0.01$ for resveratrol) compared to cells pretreated with PBS. As shown in previous chapters, this decrease corresponds to a decrease in intracellular H_2O_2. These results provide strong evidence that the RBS is specifically

responsive to the increasing H_2O_2 levels in SSe/Resveratrol-treated cells. However, even though the RBS is specifically responsive to intracellular H_2O_2 in cells treated with SSe and Res, allopurinol pretreatment did not protect these cells from undergoing PCD, according to the TUNEL assay. Previously, it was reported that these inducers trigger PCD through ROS in some manner; however, it is likely that H_2O_2 is not the catalyst since its removal does not prevent PCD, even in cases of caspase-independent cell death. This suggests that increasing H_2O_2 levels are a consequence of cell death. In spite of these results, we still believe that the RBS will prove to be an informative tool in studies investigating caspase-independent PCD, given that we and others have shown increases in intracellular H_2O_2 levels in wide varieties of cell types and death inducing conditions(25-27).

Extensive testing of the RBS across different cell lines and with multiple cell death inducers has shown that the RBS may be a useful tool in the investigation of cancer therapeutics that focus on either caspase-dependent or caspase-independent PCD. The consistent correlation between the RLuc8:fLuc ratio and intracellular H_2O_2 concentration, along with the reduction in the RLuc8:fLuc ratio by allopurinol strongly indicate that the RBS detects multiple types of PCD through an ROS (or more specifically, H_2O_2) dependent manner. This is not entirely surprising, given the reported increases in ROS in both caspase-dependent and caspase-independent PCD(1-3, 17, 28). The intracellular H_2O_2 trends reported here under all cell death inducing conditions tested suggest that the RBS will likely perform well in a wide range of PCD-inducing conditions.

6.5 References

1. Martinvalet D, Dykxhoorn DM, Ferrini R, Lieberman J. Granzyme A cleaves a mitochondrial complex I protein to initiate caspase-independent cell death. Cell 2008;133:681-92.

2. Parreno M, Vaque JP, Casanova I, et al. Novel triiodophenol derivatives induce caspase-independent mitochondrial cell death in leukemia cells inhibited by Myc. Mol Cancer Ther 2006;5:1166-75.

3. Rudolf E, Rudolf K, Cervinka M. Selenium activates p53 and p38 pathways and induces caspase-independent cell death in cervical cancer cells. Cell Biol Toxicol 2008;24:123-41.

4. Pozo-Guisado E, Merino JM, Mulero-Navarro S, et al. Resveratrol-induced apoptosis in MCF-7 human breast cancer cells involves a caspase-independent mechanism with downregulation of Bcl-2 and NF-kappaB. Int J Cancer 2005;115:74-84.

5. Broker LE, Huisman C, Span SW, Rodriguez JA, Kruyt FA, Giaccone G. Cathepsin B mediates caspase-independent cell death induced by microtubule stabilizing agents in non-small cell lung cancer cells. Cancer Res 2004;64:27-30.

6. Schiff PB, Horwitz SB. Taxol stabilizes microtubules in mouse fibroblast cells. Proc Natl Acad Sci U S A 1980;77:1561-5.

7. Ahn HJ, Kim YS, Kim JU, Han SM, Shin JW, Yang HO. Mechanism of taxol-induced apoptosis in human SKOV3 ovarian carcinoma cells. J Cell Biochem 2004;91:1043-52.

8. McCafferty-Grad J, Bahlis NJ, Krett N, et al. Arsenic trioxide uses caspase-dependent and caspase-independent death pathways in myeloma cells. Mol Cancer Ther 2003;2:1155-64.

9. Mathiasen IS, Lademann U, Jaattela M. Apoptosis induced by vitamin D compounds in breast cancer cells is inhibited by Bcl-2 but does not involve known caspases or p53. Cancer Res 1999;59:4848-56.

10. Mathiasen IS, Sergeev IN, Bastholm L, Elling F, Norman AW, Jaattela M. Calcium and calpain as key mediators of apoptosis-like death induced by vitamin D compounds in breast cancer cells. J Biol Chem 2002;277:30738-45.

11. Alonso M, Tamasdan C, Miller DC, Newcomb EW. Flavopiridol induces apoptosis in glioma cell lines independent of retinoblastoma and p53 tumor suppressor pathway alterations by a caspase-independent pathway. Mol Cancer Ther 2003;2:139-50.

12. Gavrieli Y, Sherman Y, Ben-Sasson SA. Identification of programmed cell death in situ via specific labeling of nuclear DNA fragmentation. J Cell Biol 1992;119:493-501.

13. Williams JR, Little JB, Shipley WU. Association of mammalian cell death with a specific endonucleolytic degradation of DNA. Nature 1974;252:754-5.

14. Mosmann T. Rapid colorimetric assay for cellular growth and survival: application to proliferation and cytotoxicity assays. J Immunol Methods 1983;65:55-63.

15. Scudiero DA, Shoemaker RH, Paull KD, et al. Evaluation of a soluble tetrazolium/formazan assay for cell growth and drug sensitivity in culture using human and other tumor cell lines. Cancer Res 1988;48:4827-33.

16. Hamasaki K, Kogure K, Ohwada K. A biological method for the quantitative measurement of tetrodotoxin (TTX): tissue culture bioassay in combination with a water-soluble tetrazolium salt. Toxicon 1996;34:490-5.

17. Franke JC, Plotz M, Prokop A, Geilen CC, Schmalz HG, Eberle J. New caspase-independent but ROS-dependent apoptosis pathways are targeted in melanoma cells by an iron-containing cytosine analogue. Biochem Pharmacol;79:575-86.

18. Watrach AM, Milner JA, Watrach MA, Poirier KA. Inhibition of human breast cancer cells by selenium. Cancer Lett 1984;25:41-7.

19. Fulda S, Galluzzi L, Kroemer G. Targeting mitochondria for cancer therapy. Nat Rev Drug Discov;9:447-64.

20. Maeda H, Hori S, Ohizumi H, et al. Effective treatment of advanced solid tumors by the combination of arsenic trioxide and L-buthionine-sulfoximine. Cell Death Differ 2004;11:737-46.

21. Trachootham D, Zhou Y, Zhang H, et al. Selective killing of oncogenically transformed cells through a ROS-mediated mechanism by beta-phenylethyl isothiocyanate. Cancer Cell 2006;10:241-52.

22. Magda D, Miller RA. Motexafin gadolinium: a novel redox active drug for cancer therapy. Semin Cancer Biol 2006;16:466-76.

23. Dragovich T, Gordon M, Mendelson D, et al. Phase I trial of imexon in patients with advanced malignancy. J Clin Oncol 2007;25:1779-84.

24. Bey EA, Bentle MS, Reinicke KE, et al. An NQO1- and PARP-1-mediated cell death pathway induced in non-small-cell lung cancer cells by beta-lapachone. Proc Natl Acad Sci U S A 2007;104:11832-7.

25. Simizu S, Imoto M, Masuda N, Takada M, Umezawa K. Involvement of hydrogen peroxide production in erbstatin-induced apoptosis in human small cell lung carcinoma cells. Cancer Res 1996;56:4978-82.

26. Simizu S, Takada M, Umezawa K, Imoto M. Requirement of caspase-3(-like) protease-mediated hydrogen peroxide production for apoptosis induced by various anticancer drugs. J Biol Chem 1998;273:26900-7.

27. Ye J, Ding M, Leonard SS, et al. Vanadate induces apoptosis in epidermal JB6 P+ cells via hydrogen peroxide-mediated reactions. Mol Cell Biochem 1999;202:9-17.

28. Gil J, Almeida S, Oliveira CR, Rego AC. Cytosolic and mitochondrial ROS in staurosporine-induced retinal cell apoptosis. Free Radic Biol Med 2003;35:1500-14.

Chapter 7: The RBS detects programmed cell death *in vivo*

7.1 Abstract

In regards to optical imaging modalities for *in vivo* research endeavors investigating cancer therapeutics, bioluminescence imaging (BLI) is an attractive choice given its simplicity, cost-effectiveness, sensitivity and spatiotemporal imaging abilities. There are currently only a few bioluminescent sensors designed to detect PCD, and of these, none can specifically detect caspase-independent PCD. Anticancer drug resistance and tumorigenesis have been attributed to the evasion of caspase activation, making caspase-independent PCD a new target for cancer therapeutic development. In this chapter, we show that the RBS, which has previously been shown to detect caspase-dependent and –independent PCD, can detect PCD in murine tumor models, and that this detection is related to intracellular levels of H_2O_2.

7.2 Introduction

Bioluminescence imaging (BLI) has emerged as a powerful molecular imaging tool to investigate diverse cellular processes non-invasively and in real-time. While its *in vitro* utility should not be discounted, its ability to relay physiological information in animal models makes it an attractive choice for many research endeavors. The optical properties of some bioluminescent proteins allow for depths of up to a few centimeters to be imaged *in vivo*(1, 2). The emission wavelength of fLuc is ~600 nm, making it less likely to be attenuated in animal tissue. Cancer cells expressing fLuc have been imaged in rat colon(1) and mouse lungs(2), illustrating the potential of BLI to image beyond

superficial depths in animal models. Also, the intrinsically low bioluminescence of tissues allows for greater signal-to-background ratios, as opposed to fluorescence, for example, where the autofluorescence of tissues causes unwanted background signal, effectively reducing this ratio.

In addition to its cost-effectiveness, robustness and simplicity, BLI has recently proven to be quite useful in high-throughput screening (HTS) assays(3-5). An advantage of using BLI in HTS assays is that lead compounds can be applied to *in vivo* models that utilize the same bioluminescent cellular targets originally tested, thus accelerating the translation from bench to clinic. HTS assays have been employed to identify compounds that induce programmed cell death (PCD) in many types of cancer cells including retinoblastoma(6), lymphoma(7) and breast cancer stem cells (8), a subpopulation of tumor cells that have been shown to drive tumor growth/recurrence (see (9) for review) and are resistant to many cancer treatments(10). It is envisioned that bioluminescent probes that detect PCD through cellular and *in vivo* HTS assays could improve the cancer therapeutic milieu.

Several bioluminescent sensors for PCD have been developed recently and they all target caspase-3, a protease critical for certain manifestations of PCD(11). In general, these sensors have utilized the cleavage of the caspase-3 recognition sequence, DEVD, as a catalyst for luciferin (substrate) recognition(12, 13), removal of steric hindrance(14), or protein fragment complementation(15). However, tumorigenesis and anticancer drug resistance have been attributed to the ability of cancer cells to evade caspase activation and thus caspase-dependent PCD(16, 17). This phenomenon has led to the investigation of therapeutics that induce caspase-independent cell death, for example sodium

selenite(18), resveratrol(19) and various microtubule stabilizing agents(20, 21). The lack of caspase activity here deems the aforementioned sensors ineffective in research efforts involving this mechanism of PCD.

We have shown previously that the Ratiometric Bioluminescent Sensor (RBS) is capable of detecting caspase-dependent and caspase-independent PCD in multiple cell lines. Additionally it was shown that the response level of the RBS was directly related to intracellular hydrogen peroxide (H_2O_2) levels. In this chapter, we show that the RBS is capable of detecting PCD in murine tumor models of cervical cancer and that this detection correlates with H_2O_2 levels.

7.3 Results

To investigate the capability of the RBS to provide information on cell death *in vivo*, RBS-HeLa tumor xenografts were grown in nude mice (n = 3 per group). Tumors were initially treated with PBS or Allopurinol as an inhibitor, followed by PBS or STS 1 hour later. As seen in Figure 7.1A, control mice that were treated with PBS as an inhibitor and PBS as treatment (PBS/PBS) exhibited little change in RLuc8 bioluminescence after 24 hours (top panel). Similarly, the fLuc bioluminescence also did not change significantly in PBS/PBS-treated mice (Figure 7.1A, bottom panel). In contrast, in PBS/STS-treated mice, the RLuc8 bioluminescence remained stable (Figure 7.1B, top panel), but the fLuc bioluminescence was significantly diminished after 24 hours (Figure 7.1B, bottom panel). When mice were treated with inhibitor alone (Allo/PBS), the tumors again exhibited little change in RLuc8 bioluminescence (Figure 7.1C, top panel), but there was a slight increase in fLuc bioluminescence (Figure 7.1C,

bottom panel) after 24 hours. Finally, when mice were treated with the inhibitor and the cell death inducer (Allo/STS), tumors showed little change in bioluminescence for RLuc8 (Figure 7.1D, top panel) and fLuc (Figure 7.1D, bottom panel).

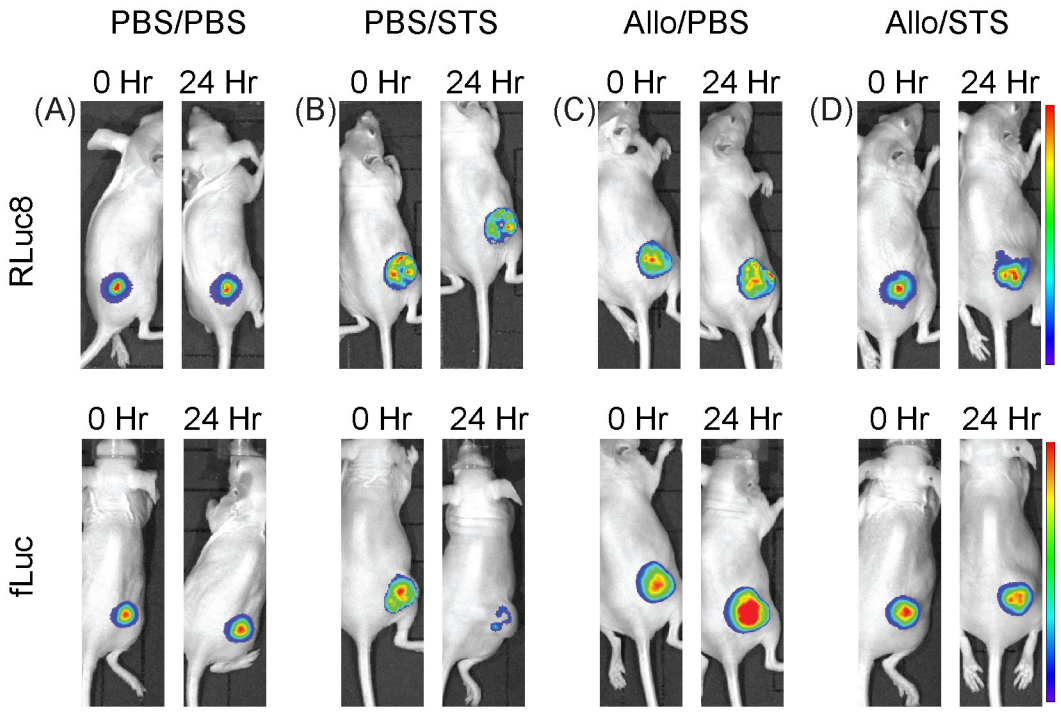

Figure 7.1. Assessment of RBS performance *in vivo*. Female nude mice bearing RBS-HeLa tumor xenografts were imaged prior to and 24 hours after the following inhibitor/drug treatment regiment: (A) PBS/PBS, (B) PBS/STS, (C) Allo/PBS, and (D) Allo/STS. Inhibitors were administered 1 hour prior to drug treatment.

The bioluminescence values were quantified for each group of animals and the RLuc8:fLuc ratio values are reported in Figure 7.2. Consistent with previous cell culture studies, the ratio increased significantly ($p < 0.01$) between the PBS/PBS and PBS/STS groups. The RLuc8:fLuc ratio decreased slightly from the PBS/PBS groups to the Allo/PBS groups; however, the change was not statistically significant. A significant

reduction in the RLuc8:fLuc ratio ($p < 0.05$) was observed between the PBS/STS and Allo/STS groups.

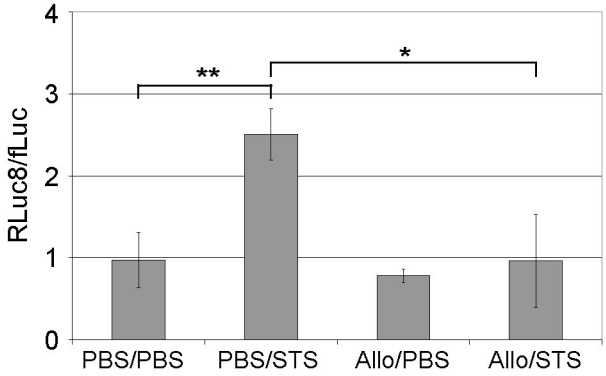

Figure 7.8. Quantitative analysis of RBS in live animals. RLuc8 and fLuc bioluminescence counts were obtained from mice bearing RBS-HeLa tumor xenografts and treated with PBS/PBS, PBS/STS, Allo/PBS, and Allo/STS. All images were analyzed using Living Image Software. Following background subtraction, the RLuc8:fLuc ratios were calculated and normalized to day 1 values. Statistical significance: * ($p<0.05$), ** ($p<0.01$).

7.4 Discussion

The RBS was tested for its ability to detect PCD in murine tumor models using STS. RBS-HeLa tumors were subjected to one of four conditions: PBS/PBS, PBS/STS, Allopurinol/PBS or Allopurinol/STS. The inhibitor (or control of PBS) was administered 1 hour prior to drug treatment (or control of PBS). Representative bioluminescence images of each treatment for RLuc8 and fLuc mimicked *in vitro* results when the same cell line (HeLa) and treatment (STS) was investigated (Chapter 3). The fLuc bioluminescence was noticeably diminished in the PBS/STS tumor, while the RLuc8 bioluminescence remained stable. Additionally, when tumors were pretreated with

allopurinol before STS, little change in either signal was observed after 24 hours. Interestingly, in the tumors pretreated with allopurinol prior to PBS, an increase in fLuc bioluminescence was observed after 24 hours that was not seen with RLuc8. This could be attributed to elevated levels of H_2O_2 within the hypoxic cores of tumors (see (22) for review); after 24 hours of allopurinol treatment, H_2O_2 levels may be reduced, thus restoring the bioluminescence of fLuc. The quantification of the bioluminescence images revealed that the RLuc8:fLuc ratio was significantly increased in the PBS/STS group compared to PBS/PBS ($p<0.01$) and that this ratio was significantly decreased in the Allo/STS group compared to PBS/STS ($p<0.01$). These results were somewhat expected, given the past performance of the RBS in PCD-inducing conditions, both with and without allopurinol. These results provide evidence that the RBS is capable of detecting PCD *in vivo* in an H_2O_2-related manner.

We have shown in this body of work that the RBS detects PCD *in vitro* and *in vivo*. Taken together, it is envisioned that the same RBS could be used in HTS assays to screen for PCD-inducing drugs, *in vitro* assays to validate lead compounds and *in vivo* assays to ensure efficacy with minimal toxicity, which would be necessary prior to clinical trials. The *in vivo* imaging capability of the RBS would potentially allow for a more streamlined transition from the initial screen to animal models, given that it has been shown to function both *in vitro* and *in vivo*.

In addition to screens for PCD-inducing compounds, the RBS could be utilized in HTS assays that try to identify antioxidant compounds. An example of this involves the burgeoning area of cancer stem cells (CSCs). This subset of cells within a tumor are often resistant to chemotherapeutics (10) and ionizing radiation(23, 24). This resistance

in mammary CSCs has recently been attributed to the lower ROS levels present in these cells compared to non-tumorigenic cells(25), since ROS are essential elements involved in ionization-mediated PCD(26, 27). To increase intracellular ROS levels of the mammary CSCs, a glutathione (GSH)-depleting agent has been used to decrease intracellular levels of the antioxidant GSH. After GSH depletion, the mammary CSCs exhibited higher ROS levels, and thus higher radiosensitization compared to cells with normal GSH levels(25). It can be imagined that the RBS would prove to be useful in screens of other compounds that possess the capability of increasing or decreasing intracellular antioxidant levels in this system.

In summary, we have shown that the RBS is capable of detecting PCD in a murine tumor model. Inhibition studies using allopurinol demonstrated that the RBS is likely responsive to intracellular H_2O_2 levels. Thus it is envisioned that the RBS may be a useful tool in research endeavors involving caspase-dependent or caspase-independent PCD as a target for cancer therapeutics.

7.5 References

1. Contag CH, Spilman SD, Contag PR, et al. Visualizing gene expression in living mammals using a bioluminescent reporter. Photochem Photobiol 1997;66:523-31.

2. Edinger M, Sweeney TJ, Tucker AA, Olomu AB, Negrin RS, Contag CH. Noninvasive assessment of tumor cell proliferation in animal models. Neoplasia 1999;1:303-10.

3. McMillin DW, Delmore J, Weisberg E, et al. Tumor cell-specific bioluminescence platform to identify stroma-induced changes to anticancer drug activity. Nat Med;16:483-9.

4. O'Leary DA, Sharif O, Anderson P, et al. Identification of small molecule and genetic modulators of AON-induced dystrophin exon skipping by high-throughput screening. PLoS One 2009;4:e8348.

5. Zhang Y, Byun Y, Ren YR, Liu JO, Laterra J, Pomper MG. Identification of inhibitors of ABCG2 by a bioluminescence imaging-based high-throughput assay. Cancer Res 2009;69:5867-75.

6. Reed D, Shen Y, Shelat AA, et al. Identification and characterization of the first small molecule inhibitor of MDMX. J Biol Chem;285:10786-96.

7. Kim BH, Yin CH, Guo Q, et al. A small-molecule compound identified through a cell-based screening inhibits JAK/STAT pathway signaling in human cancer cells. Mol Cancer Ther 2008;7:2672-80.

8. Gupta PB, Onder TT, Jiang G, et al. Identification of selective inhibitors of cancer stem cells by high-throughput screening. Cell 2009;138:645-59.

9. Stingl J, Caldas C. Molecular heterogeneity of breast carcinomas and the cancer stem cell hypothesis. Nat Rev Cancer 2007;7:791-9.

10. Woodward WA, Chen MS, Behbod F, Alfaro MP, Buchholz TA, Rosen JM. WNT/beta-catenin mediates radiation resistance of mouse mammary progenitor cells. Proc Natl Acad Sci U S A 2007;104:618-23.

11. Nicholson DW, Ali A, Thornberry NA, et al. Identification and inhibition of the ICE/CED-3 protease necessary for mammalian apoptosis. Nature 1995;376:37-43.

12. Kizaka-Kondoh S, Itasaka S, Zeng L, et al. Selective killing of hypoxia-inducible factor-1-active cells improves survival in a mouse model of invasive and metastatic pancreatic cancer. Clin Cancer Res 2009;15:3433-41.

13. Shah K, Tung CH, Breakefield XO, Weissleder R. In vivo imaging of S-TRAIL-mediated tumor regression and apoptosis. Mol Ther 2005;11:926-31.

14. Laxman B, Hall DE, Bhojani MS, et al. Noninvasive real-time imaging of apoptosis. Proc Natl Acad Sci U S A 2002;99:16551-5.

15. Coppola JM, Ross BD, Rehemtulla A. Noninvasive imaging of apoptosis and its application in cancer therapeutics. Clin Cancer Res 2008;14:2492-501.

16. Martinvalet D, Dykxhoorn DM, Ferrini R, Lieberman J. Granzyme A cleaves a mitochondrial complex I protein to initiate caspase-independent cell death. Cell 2008;133:681-92.

17. Parreno M, Vaque JP, Casanova I, et al. Novel triiodophenol derivatives induce caspase-independent mitochondrial cell death in leukemia cells inhibited by Myc. Mol Cancer Ther 2006;5:1166-75.

18. Rudolf E, Rudolf K, Cervinka M. Selenium activates p53 and p38 pathways and induces caspase-independent cell death in cervical cancer cells. Cell Biol Toxicol 2008;24:123-41.

19. Pozo-Guisado E, Merino JM, Mulero-Navarro S, et al. Resveratrol-induced apoptosis in MCF-7 human breast cancer cells involves a caspase-independent mechanism with downregulation of Bcl-2 and NF-kappaB. Int J Cancer 2005;115:74-84.

20. Broker LE, Huisman C, Span SW, Rodriguez JA, Kruyt FA, Giaccone G. Cathepsin B mediates caspase-independent cell death induced by microtubule stabilizing agents in non-small cell lung cancer cells. Cancer Res 2004;64:27-30.

21. Schiff PB, Horwitz SB. Taxol stabilizes microtubules in mouse fibroblast cells. Proc Natl Acad Sci U S A 1980;77:1561-5.

22. Guppy M. The hypoxic core: a possible answer to the cancer paradox. Biochem Biophys Res Commun 2002;299:676-80.

23. Bao S, Wu Q, McLendon RE, et al. Glioma stem cells promote radioresistance by preferential activation of the DNA damage response. Nature 2006;444:756-60.

24. Phillips TM, McBride WH, Pajonk F. The response of CD24(-/low)/CD44+ breast cancer-initiating cells to radiation. J Natl Cancer Inst 2006;98:1777-85.

25. Diehn M, Cho RW, Lobo NA, et al. Association of reactive oxygen species levels and radioresistance in cancer stem cells. Nature 2009;458:780-3.

26. Powell S, McMillan TJ. DNA damage and repair following treatment with ionizing radiation. Radiother Oncol 1990;19:95-108.

27. Ward JF. Biochemistry of DNA lesions. Radiat Res Suppl 1985;8:S103-11.

Chapter 8: Overall discussion, future directions and concluding remarks

8.1 Overall Discussion

8.1.1 Development of the Ratiometric Bioluminescent Sensor (RBS) and its response to cellular stress in HeLa cells

Many optical imaging sensors designed to report on PCD are based on the specific proteolytic cleavage of the amino acid sequence DEVD by caspase-3, the cysteine-aspartic protease that is required for apoptotis(1). However, caspases are not the only proteases that are active during PCD; it has been shown that calpains(2, 3) and cathepsins(4, 5) are upregulated during this process. Additionally, damaging oxidative modifications may result from increases in ROS(6-8) that can occur during PCD(9-11). Thus, information garnered from fluorescent(12-21) and bioluminescent(22-25) sensors for PCD must be scrutinized carefully, given the many opportunities for damage and/or modification.

In order to investigate the sensitivity of bioluminescent proteins during PCD, we began by examining the effects of staurosporine (STS), a PCD-inducing drug(26) that has also been shown to increase intracellular ROS(9), on HeLa cells transiently expressing fLuc or RLuc. Throughout 24 hours of 1 μM STS treatment, both fLuc and RLuc exhibited decreased bioluminescence while a parallel assay indicated that caspase-3 activity was markedly increased over the same time period. The disparity between

diminished fluc/RLuc bioluminescence and elevated caspase-3 activity confirmed that the utilization of these proteins in sensors for PCD must be done with caution, as signals would not only reflect caspase activity, but also other degradation/modification mechanisms within the cell.

These observations led us to investigate methods of increasing the stabilities of fLuc and RLuc. The implementation of phenylbenzothiazole (PBT), a chemical reported to increase the stability of fLuc by preventing its intracellular degradation(27), abrogated the decrease in fLuc bioluminescence previously seen in STS-treated cells. While initially promising, certain limitations prevented PBT from being examined further. First, it was unknown whether this chemical would interfere with other intracellular proteins or exogenously applied PCD-inducing compounds. Second, the use of PBT may not have translated well into *in vivo* models due to issues related to administration and pharmacokinetics. Additionally, PBT derivatives have been reported to exhibit anti-tumor activity(28), which would undoubtedly interfere with both *in vitro* and *in vivo* assays related to PCD. Thus, we investigated two luciferase mutants that have been reported to exhibit increased stability under various stress conditions, fLuc5(29) and RLuc8(30). The bioluminescence of fLuc5 remained more stable compared to wild-type fLuc when transiently expressed in STS-treated HeLa cells. RLuc8 also exhibited improved stability when compared to RLuc under the same conditions, and was the more stable of the two variants tested.

These results led to the hypothesis that if a stable and unstable luciferase were incorporated into one sensor, the resulting bioluminescence ratio (stable bioluminescence:unstable bioluminescence) could be used to report on the extent of PCD

and potentially specific molecular processes associated with PCD (e.g., oxidative stress). RLuc8 was chosen as the stable luciferase element because it possessed the greatest bioluminescence stability when expressed in HeLa cells undergoing PCD. Wild-type fLuc was chosen as the unstable luciferase element. Notably, each of these enzymes utilizes a different substrate, effectively simplifying the distinction between the bioluminescence of fLuc and RLuc8. The sensor incorporating RLuc8 and fLuc was termed the Ratiometric Bioluminescent Sensor, or RBS.

Preliminary examination of the RBS using STS-treated HeLa cells demonstrated that the RLuc8:fLuc ratio, derived from fLuc and RLuc8 bioluminescence measurements, correlated well with both caspase activation and DNA fragmentation, two hallmarks of cells undergoing PCD(1, 31). Representative images from STS-treated RBS-HeLa cells exemplified similar trends to the recorded fLuc and RLuc8 bioluminescence measurements and ratios. These results suggested that the RBS was capable of detecting PCD in STS-treated HeLa cells.

When RBS-HeLa cells were plated at a range of 0 – 20,000 cells/well of a 96-well tissue culture plate, the recorded RLuc8:fLuc ratio was shown to be independent of cell number. Additionally, there was virtually no increase in the RLuc8:fLuc ratio observed in RBS-HeLa cells that were incubated (untreated) over a period of 24 hours. These results highlight the potential transitional use of the RBS, from high-throughput screening where very small samples are used all the way to animal models, where large numbers of cells are usually necessary.

While these initial studies regarding the RBS and its response to PCD induction were promising, the mechanism behind the disparity in fLuc and RLuc8 activity had yet

to be determined. An initial theory involved the use of the IRES sequence in the plasmid DNA vector encoding the RBS. This sequence was incorporated into the plasmid such that it was flanked by RLuc8 and fLuc (RLuc8-IRES-fLuc) in order to allow for protein translation from a single, bicistronic mRNA(32, 33), effectively eliminating any unwanted effects related to altered promoter activity. Since it has been reported that in healthy cells, proteins translated from sequences downstream of the IRES site can be expressed at lower levels compared with upstream sequences(34), a 'reverse RBS' sensor was created (fLuc-IRES-RLuc8) to determine the effects of the positioning of fLuc and RLuc8 relative to the IRES sequence. HeLa cells expressing this sensor exhibited an increase in the RLuc8:fLuc ratio when treated with STS. While this ratio was considerably higher than that of the 'normal' RBS, this can likely be attributed to the transient expression of the 'reverse' sensor compared to the stable expression of the 'normal' sensor, specifically the accelerated loss of fLuc activity owing to, the lack of genomic integration of the 'reverse' RBS plasmid would lead to its dilution through cell division and/or degradation.

After the elimination of the IRES sequence as a source of the explicit differential between fLuc and RLuc8 activity, the mechanism behind this difference remained unknown. There have been various reports indicating that the proteasome(35, 36) and calpain(2, 3) and cathepsin(4, 5) proteases can play significant roles in PCD. Additionally, increases in ROS that can occur in cells undergoing PCD broach the possibility of potentially damaging oxidative modifications to proteins(6-8) and/or RNA(37). In the subsequent determination of the RBS mechanism, the roles of these proteases and ROS, among others, were investigated.

8.1.2 The RBS mechanism relies on ROS, particularly H_2O_2

In order to determine the mechanism behind the bioluminescence disparity between fLuc and RLuc8 in the RBS in cells undergoing PCD, an RT-PCR study was first performed to assess fLuc and RLuc8 mRNA levels in STS treated cells compared to PBS treated cells. This assay revealed that the relative expression of these mRNAs within RBS-HeLa cells did not significantly change regardless of PBS or STS treatment. In contrast, Western blot analysis demonstrated that fLuc protein levels decreased over the time course of STS treatment, while RLuc8 protein levels remained relatively stable. Interestingly, some fLuc staining was observed at higher than expected molecular weights at later time points, which could be indicative of protein cross-links or posttranslational modifications. Taken together, these results suggested that the mechanism of the RBS involved the bioluminescent proteins themselves, rather than mRNA levels.

Next, various inhibition/scavenging studies were performed on targets known to play roles in PCD. It was expected that certain inhibitors would rescue fLuc activity, resulting in a decrease in the RLuc8:fLuc ratio in STS-treated RBS-HeLa cells. Given that the proteasome is responsible for the majority of intracellular protein degradation, it was naturally one of the first targets of the inhibition study. The employment of the proteasome inhibitors MG-132, epoxomicin and lactacystin on STS-treated RBS-HeLa cells did not rescue fLuc activity and actually caused a slight increase in the RLuc8:fLuc ratio. In the case of epoxomicin, this slight increase was statistically significant compared to uninhibited controls. This result is potentially indicative of increased PCD, an effect that has been reported to occur during proteasome inhibition using

epoxomicin(35). Proteasome inhibition has also been shown to increase intracellular ROS levels(9, 38-40), possibly implicating ROS in the RBS mechanism. Nonetheless, these results provided strong evidence that enhanced proteasomal degradation was not likely responsible for the RBS mechanism.

The next group of inhibitors focused on various proteases that are associated with PCD through various mechanisms: calpains, cathepsins and caspases. When STS-treated RBS-HeLa cells were pretreated with Calpain Inhibitor III, the RLuc8:fLuc ratio was not significantly affected compared to PBS pretreated controls. These results suggested that calpains were not involved in the mechanism of the RBS. Interestingly, an increase in the ratio was seen in RBS-HeLa cells treated with PBS following Calpain Inhibitor III. This inhibitor has been shown to decrease the levels of intracellular antioxidant glutathione (GSH) levels, effectively increasing intracellular ROS(41), again potentially implicating ROS in the RBS mechanism.

Two inhibitors for cathepsins were employed: Pepstatin A (inhibits aspartyl proteases) and ammonium chloride (inhibits phagosome-lysosome fustion(42)). Neither of these inhibitors significantly affected the RLuc8:fLuc ratios in STS-treated RBS-HeLa cells and hence they were discounted from the mechanism of the RBS.

Arguably, the most thoroughly characterized proteases involved in PCD are the caspase family of proteases (see (43) for review). To inhibit caspase activity during STS treatment of RBS-HeLa cells, the pan-caspase inhibitor z-vad-fmk was employed, and surprisingly the use of this inhibitor did not affect the RLuc8:fLuc ratio. These results suggested that caspases did not play a significant role in the disparity between fLuc and RLuc8 activity in STS-treated cells.

In addition to proteases, various ROS can contribute to the modification, damage or degradation of proteins in dying cells. Three superoxide ($O_2^{\bullet-}$) scavengers, Tiron, TEMPOL and MnTMPyP, were tested for their ability to reduce the RLuc8:fLuc ratio in STS treated cells. None of these scavengers had any significant effect on the RLuc8:fLuc ratio which led us to conclude that $O_2^{\bullet-}$ alone is not responsible for the trends observed in STS-treated RBS-HeLa cells. This was somewhat expected given the short half-life of $O_2^{\bullet-}$ and its function as a precursor to other oxidizing agents. However, even though the $O_2^{\bullet-}$ scavenging abilities of TEMPOL, Tiron and MnTMPyP were confirmed to be statistically significant by using a dihydroethidium assay, the intracellular levels of $O_2^{\bullet-}$ appeared to be reduced by only ~50%. Therefore, further studies on the effects $O_2^{\bullet-}$ in regards to the RBS mechanism may be warranted. Initial experiments could involve the use of other $O_2^{\bullet-}$ scavengers, such as SOD transgenes(44).

Peroxynitrite (ONOO-) is formed as a result of the reaction between $O_2^{\bullet-}$ and nitric oxide (NO)(45) and specific amino acid residues (methionine, cysteine, tyrosine and tryptophan) are vulnerable to modification by ONOO-(6). To scavenge ONOO-, the scavenger uric acid was used as a pretreatment on STS-treated RBS-HeLa cells. A slight, but insignificant, increase in the RLuc8:fLuc ratio was observed compared to PBS-pretreated controls which suggested that ONOO- does not play a dominant role in the mechanism of the RBS. Even though there currently exists no commerical assays to detect ONOO-, numerous studies have shown that acid is an effective scavenger of ONOO-(46-48).

The agents mannitol, a specific scavenger of $^{\bullet}OH$, deferoxamine (DFO), an iron chelator, and tetraethylenepentamine (TEPA), a copper chelator, were utilized to examine the effects of $^{\bullet}OH$ on the RLuc8:fLuc ratio of RBS-HeLa cells treated with STS. Carbon-centered radical formation via hydroxyl radicals ($^{\bullet}OH$) serves to initiate the oxidative attack of protein radicals(6). This carbon-centered radical can give rise to protein cross-links, peptide-bond cleavage or direct oxidation of amino acids(6). The two metal chelators, alone and in combination, were used to reduce the amounts of metals available for the Fenton reaction ($Fe^{2+} + H_2O_2 \rightarrow Fe^{3+} + {}^{\bullet}OH + OH^-$). None of these compounds significantly reduced the RLuc8:fLuc ratio, and these results effectively eliminated the likelihood that $^{\bullet}OH$ as a direct contributor to the loss in fLuc activity. It may be argued that the slight increase in the RLuc8:fLuc ratio that was observed with TEPA could be a result of excess H_2O_2 buildup from the prevention of the Fenton reaction, however further studies are warranted since the combination of DFO + TEPA did not yield an additive effect. Additionally, it remains unclear as to the effect of metal chelation on the Fenton reaction. It has been reported that iron chelation can serve both antioxidant(49) and prooxidant(50) functions.

Hydrogen peroxide (H_2O_2) is a powerful oxidizing agent that can directly and indirectly modify many amino acids, often creating hydroxyl- or carbonyl-derivatives (see (51) for review). It has been shown that this oxidation can destabilize a protein's native structure and result in activity loss(8, 52). The H_2O_2 inhibitors/scavengers catalase, allopurinol and aspirin were tested for their ability to reduce the RLuc8:fLuc ratio in STS-treated RBS-HeLa cells. The pretreatment of RBS-HeLa cells with these reagents prior to STS treatment conferred a significant reduction ($p<0.01$) in the

RLuc8:fLuc ratio. These findings suggested that fLuc activity could be recovered in STS-treated RBS-HeLa cells through removal of H_2O_2. It should be noted that catalase cannot cross cell membranes, but our results are consistent with previous studies reporting that extracellularly added catalase is effective at removing intracellular H_2O_2(53, 54).

When STS-treated RBS-HeLa cells were subjected to increasing dosages of catalase, allopurinol and aspirin, the RLuc8:fLuc ratio decreased in a dose-dependent manner. These results confirmed that fLuc activity could be recovered by reducing H_2O_2 levels in STS-treated cells. Additionally, Western blot analysis indicated that fLuc protein levels in STS-treated RBS-HeLa cells were rescued slightly when pretreated with each inhibitor compared to PBS-pretreated controls. Therefore, H_2O_2 inhibitors/scavengers were able to reduce the degradation of fLuc in STS-treated RBS-HeLa cells.

Given that the inhibitors/scavengers of H_2O_2 significantly affected the RLuc8:fLuc ratio, additional studies were performed that dealt with H_2O_2 more directly. Intracellular H_2O_2 levels were measured in STS-treated RBS-HeLa cells over a time course of 24 hours and over a dosing range of 0-50 μM. In both cases intracellular H_2O_2 levels increased up to nearly three-fold. Additionally, when RBS-HeLa cells were treated directly with H_2O_2 in fully supplemented culture medium, the RLuc8:fLuc ratios exhibited striking increases. These results further supported the intrinsic involvement of H_2O_2 in the RBS mechanism.

It may be argued that the concentrations of H_2O_2 used in both the cellular and *in vitro* assays was too high to be biologically relevant. However, recent studies

investigating oxidative stress have employed similar concentrations of H_2O_2(55, 56). Nonetheless, an immunohistochemical analysis of RLuc8 and fLuc proteins in control and STS-treated cells may provide insight into any preferential localization of these proteins to sites of increased ROS (e.g. peroxisomes) during cell death. Peroxisomes contain ROS and enzymes that generate these species, e.g., xanthine oxidase (see (57) for review), thus it can be envisioned that localization of proteins to this organelle could be a source excessive ROS exposure that would subsequently modify/damage fLuc.

The highest level of fLuc rescue in STS-treated RBS-HeLa cells was exhibited when allopurinol, an XO inhibitor, was employed as a pretreatment. Therefore, RBS-HeLa cells were subjected to an HX-XO reaction, which has been shown to produce H_2O_2 as the dominant oxidant(58). After 24 hours, a significant ($p<0.01$) increase in the RLuc8:fLuc ratio was observed. The magnitude of this increase was above that seen with STS treatment, but lower than with direct H_2O_2 treatment, which was expected given that this reaction produces H_2O_2 more directly than STS, but is obviously not as harsh as direct H_2O_2 application. When purified RLuc8 and fLuc proteins were subjected to the HX-XO reaction, the RLuc8:fLuc ratio increased significantly ($p<0.01$). These findings suggested that the RBS may be specifically responsive to intracellularly produced H_2O_2 alone, and not other upstream or downstream reactions involving other ROS or enzymes.

We recently measured the amount of H_2O_2 generated by the HX-XO system we employed and it was determined that the concentration was ~5 μM. However, when both RBS-HeLa cells and pure fLuc and RLuc8 proteins were subjected to 5 μM H_2O_2, no differences in the RLuc8:fLuc ratio or activity were observed. This could be explained by degradation of the acutely applied H_2O_2 at the initial time points of the assays, as

opposed to the chronic generation of H_2O_2 via the HX-XO reaction. Alternatively, the XO enzyme itself contains 4 iron atoms. The reaction of both $O_2^{\bullet-}$ and H_2O_2 with iron can generate damaging $^{\bullet}OH$, potentially leading to protein crosslinks, peptide bond cleavage and amino acid modifications(6).

When RBS-HeLa cells were pretreated with allopurinol prior to STS, no changes in DNA fragmentation levels were observed. However, in parallel assays, this pretreatment significantly ($p<0.01$) decreased both the RLuc8:fLuc ratio and intracellular H_2O_2 levels. This correlation supported earlier findings that the RBS is specifically responsive to H_2O_2 during cell death and not other degradation pathways associated with PCD. Further, the ability of allopurinol to reduce H_2O_2 levels without affecting cell death implicated H_2O_2 production as a consequence of, rather than a catalyst for, cell death.

In order to obtain a more definitive understanding of the role of H_2O_2 in the RBS mechanism, purified RLuc8 and fLuc proteins were exposed to a range of H_2O_2 concentrations. Analysis of both SDS-PAGE and bioluminescence measurements indicated that when the proteins were treated with H_2O_2, fLuc bioluminescence and protein levels decreased, while RLuc8 bioluminescence and protein levels remained relatively stable over the time course for all doses tested. Additionally, smearing of the fLuc protein was observed for most H_2O_2 concentrations, indicative of possible modifications or degradation. Interestingly, fLuc bioluminescence appeared to decay more rapidly and to a greater extent than fLuc protein levels at all concentrations tested. These observations indicate that H_2O_2 may have oxidatively modified or damaged the fLuc proteins, rendering them inactive, prior to degradation/protein loss. This conclusion would also support the Western blot analysis where fLuc protein levels were rescued by

the H_2O_2 inhibitors/scavengers. Since oxidatively modified/damaged proteins are often targets for proteasomal degradation(59, 60), it can be hypothesized that the H_2O_2 inhibitors scavengers prevented oxidative modifications of fLuc that would normally trigger proteasomal degradation of the protein.

H_2O_2 may modify the fluc protein through carbonylation; protein carbonylation is irreversible(61), can cause protein aggregates to form(51, 62) and targets damaged proteins for degradation(63). When STS-treated RBS-HeLa cells were analyzed for protein carbonylation, a substantial increase in this phenomenon was seen when compared to PBS treated controls. Furthermore, when H_2O_2-treated purified fLuc and RLuc8 proteins were subjected to the carbonylation assay, fLuc became extensively more carbonylated versus RLuc8, compared to PBS-treated controls. These results implicated protein carbonylation as one of the potential modifications to fLuc in STS-treated RBS-HeLa cells, especially since it has been shown that H_2O_2 can cause protein carbonylation(51).

Investigation into the crystal structures of fLuc and RLuc8 may provide insight into the activity disparity between fLuc and RLuc8 in stressed cells as well. Given that certain amino acid residues, namely lysine, arginine, proline, methionine, cysteine and tyrosine are preferentially oxidatively modified(6, 64, 65), the relative locations of these residues (i.e. on the surface or buried) might explain the differential in oxidative modifications leading to fLuc protein activity loss.

While the precise mechanism behind the ROS-mediated activity of the RBS has yet to be determined, we have shown that it is primarily responsive to intracellular H_2O_2

levels. Thus, it is envisioned that the RBS will be useful as a sensor for PCD, since many instances of PCD are accompanied by ROS production(11, 66-74).

8.1.3 The RBS can detect caspase-dependent PCD in multiple cell lines using multiple inducers

Many therapies that have been developed to treat cancer involve inducing apoptosis, a type of PCD, that is mechanistically characterized by a proteolytic cascade involving caspases (See (43) for comprehensive review). Accordingly, a variety of sensors have been developed to image and monitor apoptosis, or more specifically caspase-3 activity, to further assist in the discovery, development, and evaluation of apoptosis-inducing agents. These sensors detect caspase-3 by the recognition and cleavage of the amino acid sequence DEVD and are either fluorescent(12-21) or bioluminescent(22-25) in nature. However, we have shown caspase-3 activity is not always elevated in apoptotic cells (Chapter 3). Another confounding factor in regarding sensors for caspase-3 is that caspase-7 recognizes and cleaves the same amino acid sequence (DEVD) as caspase-3. Thus, sensors designed specifically for caspase-3 activity as a biomarker for apoptosis may not accurately report on the extent of cell death.

As shown in chapter 3, the RBS is responsive to cell death induced by STS in HeLa cells. To begin to investigate the span of cell types in which the RBS could function, RBS-MCF7 cells were treated with a dosage range of STS (0 – 50 μM) for 6 hours. Here, fLuc bioluminescence decreased by up to 90% while RLuc8 remained relatively insensitive to the treatment and only decreasing by 20%. Accordingly, the RLuc8:fLuc ratio increased with increasing STS dose. Additionally, intracellular H_2O_2

levels, caspase-3 activity and DNA fragmentation levels all increased with STS dosage in RBS-MCF7 cells, consistent with the notion that the RBS detects PCD through a H_2O_2-related mechanism. When RBS-293T/17 cells were treated with the same STS dosage range for 6 hours, increases were also seen in the RLuc8:fLuc ratio, intracellular H_2O_2 levels, caspase-3 activity and DNA fragmentation levels. The ability of the RBS to relay information on cell death in MCF7 and 293T/17 cells in addition to HeLa cells indicates its versatility and potential for utilization over a wide range of cellular research endeavors.

The treatment of RBS-MCF7 and 293T/17 cells with allopurinol for 1 hour prior to 10 μM STS for 6 hours effectively reduced the RBS ratio and intracellular H_2O_2 levels, while leaving caspase-3 activity and DNA fragmentation unchanged. The trends in RLuc8:fLuc ratio and intracellular H_2O_2 reduction with allopurinol pretreatment further supported the theory that the RBS is specifically responsive to H_2O_2 during cell death. Also, these results further confirm that H_2O_2 elevation is a consequence of cell death, rather than a catalyst for cell death in STS-treated RBS-MCF7 cells.

The STS studies on RBS-MCF7 cells were expanded to a time course of 24 hours using 10 μM STS. Under these conditions, the RLuc8:fLuc ratio increased dramatically compared to PBS-treated controls. The intracellular H_2O_2 levels also increased under this conditions while the caspase-3 activity actually peaked at the 6 hour time point and returned to control levels by 24 hours. The TUNEL assay revealed that DNA fragmentation remained elevated throughout the entire time course. These results introduced an interesting disparity between caspase-3 activity and DNA fragmentation, RBS ratio and intracellular H_2O_2 levels; namely, caspase-3 activity returned to near-

control levels while the remaining three parameters remained elevated. These results highlighted how the use of caspase-3 activity as a biomarker for cell death could potentially lead to ambiguous findings, due to the transient nature of its activation. Here, the RBS may hold an advantage over traditional cell death assays, since it is capable of detecting cell death when caspase activity assays cannot and possesses real-time and *in vivo* capabilities that are not characteristic of the TUNEL assay. Additionally, the correlation between the TUNEL assay and the RBS, even in the absence of caspase activity, suggests that the RBS may be able to provide insight on cells undergoing caspase-independent PCD. This would not be entirely surprising considering that many previous studies have shown that caspase-independent cell death pathways can involve ROS(11, 68, 69, 74-76).

Even though caspase-independent PCD research is gaining in popularity, caspase-dependent cell death remains a prominent area of interest regarding cancer therapeutics, whether by inducing PCD on their own(77-79) or in combination with other drugs(80, 81). Two drugs that induce apoptosis in HeLa cells are doxorubicin (DOX, (82)) and camptothecin (Cpt, (83)). When RBS-HeLa cells were treated with 1 μM DOX or 10 μM Cpt over the course of 48 hours, the RLuc8:fLuc ratio increased compared to PBS-treated controls. In addition, the intracellular H_2O_2 levels increased compared to untreated control and the RLuc8:fLuc ratio was significantly decreased when the cells were pretreated with 100 μM allopurinol (DOX, $p<0.05$, Cpt, $p<0.01$). Parallel caspase activity and DNA fragmentation assays indicated that PCD was occurring under DOX and Cpt treatment. The overall increasing trend in RLuc8:fLuc ratio, DNA fragmentation and H_2O_2 levels following DOX- and CPT-treatment suggests that the RBS will likely

detect cell death under a vast array of induction methods, since many are accompanied by an increase in H_2O_2 levels. For example, it has been shown that murine epidermal cells treated with vanadate undergo apoptosis and exhibit an increase in intracellular H_2O_2 cells(84). Similarly, apoptosis induced by erbstatin(85), vinblastine and inostamycin(86) in human small cell lung carcinoma cells is also accompanied by increased intracellular H_2O_2 levels.

While the ability of the RBS to detect caspase-dependent PCD should not be discounted, it would be interesting to determine whether it would be responsive in oxidatively stressed cells that are not undergoing PCD. This could be accomplished by treating RBS-cells with tumor necrosis factor (TNF) alpha or various antioxidant inhibitors. Additionally, expressing the RBS in immune cells, such as neutrophils, that exhibit a characteristic 'oxidative burst' may provide more insight into the response of the RBS to oxidative stress induction.

8.1.4 The RBS can detect caspase-independent PCD through pathways involving ROS production, Bcl-2 downregulation and mitochondrial membrane permeabilization

Anticancer drug resistance and tumorigenesis have been attributed to the ability of certain cancers to evade caspase activation(87, 88). It is envisioned that cancer therapeutics that induce PCD through a caspase-independent mechanism could have widespread impact. The therapeutic need for agents that induce caspase-independent PCD gives rise to the necessity of assays that can detect this phenomenon; thus, the RBS was examined for its potential to report on caspase-independent PCD.

When RBS-HeLa cells were treated with a dosage range (0-55 μM) of sodium selenite (SSe), a compound that has been shown to induce caspase-independent PCD in HeLa cells through oxidative stress mediated activation of p53 and p38(89), the RLuc8:fLuc ratio increased. Under the same conditions, caspase-3 remained relatively inactive, while intracellular H_2O_2 and DNA fragmentation levels increased. RBS-MCF7 cells were subjected to the same SSe dosage conditions for 48 hours. The exact pathway by which SSe induces caspase-independent PCD in MCF7 cells is unknown, however it has been shown to decrease viability in this cell type(90). Similarly to RBS-HeLa cells, the RLuc8:fLuc ratio, intracellular H_2O_2 levels and DNA fragmentation levels increased, while caspase activity remained unchanged, as the SSe dosage increased. In both of these studies, the increase in DNA fragmentation along with the lack of appreciable caspase activity show that SSe induces caspase-independent PCD and that it can be detected by the RBS. Also, the correlation between levels of intracellular H_2O_2 and the RLuc8:fLuc ratio suggested that the RBS was responsive to H_2O_2 in these instances of PCD.

To further investigate the detection of caspase-independent PCD by the RBS, resveratrol was used as a PCD inducer in RBS-MCF7 cells. Resveratrol has been shown to induce PCD in MCF7 cells through Bcl-2 downregulation, mitochondrial membrane permeabilization and ROS production without caspase-3 activation, PARP cleavage or cytochrome c release(91). With increased resveratrol dosage (0-1 mM), the RLuc8:fLuc ratio increased, while caspase activity remained unchanged. Additionally, intracellular H_2O_2 and DNA fragmentation levels increased as the resveratrol dose increased. Taken together, the studies that used SSe and Res further attested to the impact the RBS may have on research endeavors involving caspase-independent PCD. The RBS may be

particularly useful in studies involving the targeting of mitochondria in cancer therapy, given the reported effects of resveratrol on the mitochondria and the associated increase in ROS(91). In fact, many compounds that target the mitochondria for this purpose generate excessive amounts of ROS(92-96).

To examine the role of H_2O_2 in these caspase-independent PCD processes, allopurinol was used as an inhibitor for one hour prior to the application of SSe (RBS-HeLa and RBS-MCF7) and resveratrol (RBS-MCF7). RBS-HeLa and RBS-MCF7 cells pretreated with 100 μM allopurinol for 1 hour prior to treatment with 55 μM SSe exhibited significant decreases ($p<0.05$) in the RLuc8:fLuc ratio and intracellular H_2O_2 levels, compared to cells pretreated with PBS. Similarly, allopurinol pretreatment for 1 hour prior to 1 mM resveratrol application for 24 hours on RBS-MCF7 cells conferred significant ($p<0.01$) reductions in the RLuc8:fLuc ratio and levels of intracellular H_2O_2. These results provided strong evidence that the RBS is specifically responsive to the increasing H_2O_2 levels seen in SSe/resveratrol-treated cells.

Allopurinol pretreatment did not protect either of the cell types from PCD compared to PBS pretreatment, as indicated by a TUNEL assay. Previous reports have indicated that the mechanisms of PCD induced by SSe and resveratrol involve ROS in some manner(89, 91); however, it is unlikely that H_2O_2 is the catalyst because its removal does not prevent PCD. These results suggested that increasing levels of H_2O_2 are thus a consequence of cell death.

We have shown through extensive testing of multiple compounds on multiple cell lines that the RBS may be a useful tool in the development and testing of cancer therapeutics designed to induce caspase-independent PCD. There was a consistent

correlation between the RLuc8:fLuc ratio and levels of intracellular H_2O_2. Further, the RLuc8:fLuc ratio was reduced in drug-treated cells when pretreated with allopurinol. The trends reported here suggest that the RBS will likely perform well in a wide range of PCD-inducing conditions.

8.1.5 The RBS detects programmed cell death *in vivo*

We have acquired evidence that the RBS is capable of detecting caspase-dependent and caspase-independent PCD in multiple cell lines. Additionally it was shown that the response level of the RBS was directly related to intracellular H_2O_2 levels. To test the *in vivo* imaging capability of the RBS, a murine tumor model was employed.

Nude mice bearing RBS-HeLa tumors (n = 3 per group) were imaged at time 0 hours to obtain fLuc and RLuc8 bioluminescence images. Immediately following the second imaging session, tumors were treated with either PBS or allopurinol as inhibitors for one hour prior to PBS or STS administration. After 24 hours, the animals were imaged again. The animals treated with PBS as an inhibitor and as a drug treatment (PBS/PBS) exhibited little change in either RLuc8 or fLuc bioluminescence after 24 hours. The group treated with PBS followed by STS (PBS/STS) retained RLuc8 bioluminescence after 24 hours, while fLuc bioluminescence diminished considerably. When tumors were treated with allopurinol followed by PBS (Allo/PBS), the RLuc8 bioluminescence did not change and fLuc demonstrated a slight increase in bioluminescence after 24 hours. Finally, STS treatment following allopurinol pretreatment (Allo/STS) conferred little change in RLuc8 bioluminescence and a slight decrease in fLuc bioluminescence after 24 hours. Following bioluminescence image

quantification, it was found that the RLuc8:fLuc ratio increased significantly ($p<0.01$) for the PBS/STS group compared to the PBS/PBS control. Additionally, the ratio significantly decreased ($p<0.05$) for the Allo/STS group compared to the PBS/STS group. These results indicated that the RBS was capable of detecting PCD *in vivo*.

After 24 hours, the tumors treated with Allo/STS exhibited an increase in fLuc bioluminescence that was not observed with RLuc8. This could be attributed to the elevated levels of H_2O_2 within the hypoxic cores of tumors (see (97) for review). Intrinsically high levels of H_2O_2 levels within these tumors were likely reduced after 24 hours of allopurinol treatment, thus restoring fLuc bioluminescence.

In summary, we have shown that the RBS is capable of detecting PCD *in vivo* through a murine tumor model. Using allopurinol as an inhibitor demonstrated that the RBS is likely responsive to intracellular H_2O_2 levels. Together with previous *in vitro* results, it is envisioned that the RBS will be a useful tool in research endeavors involving caspase-dependent and caspase-independent cell death.

8.2 Future Directions

Intracellular H_2O_2 levels are generally accepted to lie in the nM-μM range, depending on health status. However, the levels of exogenously applied H_2O_2 in our studies were in the mM range. Thus, this concentration discrepancy should be further examined. When we treated both RBS-HeLa cells and purified proteins with the HX-XO reaction, we also observed that fLuc activity decreased significantly, while the RLuc8 activity remained stable. Interestingly, when the H_2O_2 concentration generated by this

HX-XO reaction was measured using Amplex Red, it was found to be ~5 μM. The HX-XO reaction generates H_2O_2 in a continuous manner, until the compounds are exhausted. Conversely, the exogenously applied H_2O_2 could be degraded over time, which could account for the mM levels of H_2O_2 used to activate the RBS. It has been shown that exogenously applied H_2O_2 can decrease by ~67% after 20 minutes in fully supplemented cell culture medium(98). To explore this further, additional studies could be performed to more accurately quantify H_2O_2 levels as a function of time during both the HX-XO reaction and acute H_2O_2 application on both cells and purified proteins.

The SDS-PAGE and bioluminescence assays performed on purified proteins demonstrated that, when treated with H_2O_2, the fLuc protein exhibited activity loss at a higher rate and to a greater extent than protein degradation. This suggests that the oxidative modification of the fLuc protein may be primarily responsible for its activity loss and that degradation only occurs at a later stage. This would be consistent with current observations that oxidatively modified/damaged proteins are targeted for proteasomal degradation(59, 60, 99). In order to further examine these processes, a Western blot could be performed on PBS and STS-treated RBS-cells that were pretreated with PBS or proteasome inhibitors. It would be expected that the inhibitor pretreated STS-treated RBS-cells would exhibit higher fLuc protein levels even if cells under the same treatment conditions exhibited low bioluminescence activity. These blots may also reveal altered band staining accounting for damage/modification. The lysates from these cells could also be subjected to a protein carbonylation assay to assess the levels of carbonyl-derivative formation. Presumably, these proteins would be carbonylated, but not degraded due to proteasome inhibition. To specifically investigate carbonylation

levels of fLuc and RLuc8 in these cells, the carbonylation assay could be performed on immunoprecipitated fLuc and RLuc8 proteins.

While many commercial assays for ROS are unable to be used in animal models of disease, they often possess high *in vitro* sensitivity. To improve the sensitivity of the RBS, additional luciferases (e.g. gaussia, cbRed, cbGreen) or randomly mutated fLuc could be examined for their sensitivity to inactivation in stressed cells. It also may be worthwhile to investigate fLuc variants that are engineered to be even less stable than wild-type fLuc. For example, a fLuc variant containing a 'PEST' sequence from mouse ornithine decarboxylase targets the protein for proteolytic degradation, effectively reducing its half-life to less than 1 hour, compared to ~3.5 hours for wild-type fLuc(100). The use of this fLuc variant in the RBS could result in a faster stress response given the higher rate of protein turnover.

Intriguingly, the wild-type fLuc sequence from the popular pGL3 basic vector (also used in this dissertation) was actually engineered to remove a peroxisomal targeting sequence(101) (discovered to be the C-terminal sequence -Ser-Lys-Leu(102)). It was thought the peroxisomal targeting of fLuc could interfere with normal cell functions, contribute to its degradation and/or reduce cofactor availability. With the exception of interfering with basic cellular processes, the remaining two consequences could prove to be beneficial in the context of the RBS.

Additionally, many *in vivo* assays for PCD in regards to cancer therapeutic development occur over many weeks. Thus if the wild-type fLuc of the RBS was replaced with a slightly more stable variant of fLuc, the resulting sensor may prove to be more useful in studies of this nature. We have shown that the fLuc variant, fLuc5,

exhibits improved stability over wild-type fLuc, but not to the extent of RLuc8. Although further testing is warranted, the combination of fLuc5 and RLuc8 could improve upon the functional lifespan of the RBS.

Even though RLuc8 is 4 times brighter than native RLuc, its emitted wavelength of light (480 nm) is greatly attenuated in animal tissue, resulting in low bioluminescence signal measurements during *in vivo* imaging studies. The RBS sensor may be improved by incorporating red-shifted luciferase variants. Recently, a variant of RLuc8 was developed, RLuc8.6, that exhibits a red-shifted bioluminescence compared to both wild-type RLuc and RLuc8(103). It is envisioned that this variant could be utilized in the RBS in two ways. First, it could be combined with wild-type fLuc to create essentially a red-shifted RBS, wherein the bioluminescence signals from fLuc and RLuc8.6 would be distinguished by their different substrates, but the RLuc8.6 would likely exhibit less signal attenuation *in vivo*. A second RBS variant could involve wild-type RLuc and RLuc8.6. In this case, emission filters would be absolutely required in order to distinguish the bioluminescence signals from each enzyme as they catalyze the same substrate, coelenterazine. However, the need for only one substrate administration/imaging session could save considerable time, reagents and financial resources.

8.3 Concluding remarks

This body of work involved the development, characterization and implementation of an ROS-responsive Ratiometric Bioluminescent Sensor (RBS). It was

hypothesized that the RBS could serve as a metric for intracellular stresses involved in PCD, as many instances of PCD are associated with elevated levels of ROS. While the exact mechanism behind the disparity in bioluminescence activity between RLuc8 and fLuc has yet to be elucidated, we have shown that ROS, namely H_2O_2, play a significant role. The RBS was implemented in various models of PCD, both *in vitro* and *in vivo* and proved to be responsive in any instances of PCD that involved increased ROS levels. It is envisioned that the RBS could prove to be quite useful in research endeavors investigating PCD, and its related molecular processes (e.g. oxidative stress). Ultimately, the RBS could have widespread impact in the development, evaluation and/or improvement of therapeutics intended to combat many, often devastating pathologies related to these molecular processes, such as cancer, Alzheimer's disease, autoimmune disorders, type-2 diabetes and AIDS.

8.4 References

1. Nicholson DW, Ali A, Thornberry NA, et al. Identification and inhibition of the ICE/CED-3 protease necessary for mammalian apoptosis. Nature 1995;376:37-43.

2. Aw TY, Nicotera P, Manzo L, Orrenius S. Tributyltin stimulates apoptosis in rat thymocytes. Arch Biochem Biophys 1990;283:46-50.

3. McConkey DJ, Hartzell P, Amador-Perez JF, Orrenius S, Jondal M. Calcium-dependent killing of immature thymocytes by stimulation via the CD3/T cell receptor complex. J Immunol 1989;143:1801-6.

4. Guenette RS, Mooibroek M, Wong K, Wong P, Tenniswood M. Cathepsin B, a cysteine protease implicated in metastatic progression, is also expressed during regression of the rat prostate and mammary glands. Eur J Biochem 1994;226:311-21.

5. Sensibar JA, Liu XX, Patai B, Alger B, Lee C. Characterization of castration-induced cell death in the rat prostate by immunohistochemical localization of cathepsin D. Prostate 1990;16:263-76.

6. Berlett BS, Stadtman ER. Protein oxidation in aging, disease, and oxidative stress. J Biol Chem 1997;272:20313-6.

7. Davies KJ. Protein damage and degradation by oxygen radicals. I. general aspects. J Biol Chem 1987;262:9895-901.

8. Volkin DB, Mach H, Middaugh CR. Degradative covalent reactions important to protein stability. Mol Biotechnol 1997;8:105-22.

9. Gil J, Almeida S, Oliveira CR, Rego AC. Cytosolic and mitochondrial ROS in staurosporine-induced retinal cell apoptosis. Free Radic Biol Med 2003;35:1500-14.

10. Prehn JH, Jordan J, Ghadge GD, et al. Ca2+ and reactive oxygen species in staurosporine-induced neuronal apoptosis. J Neurochem 1997;68:1679-85.

11. Tay VK, Wang AS, Leow KY, Ong MM, Wong KP, Boelsterli UA. Mitochondrial permeability transition as a source of superoxide anion induced by the nitroaromatic drug nimesulide in vitro. Free Radic Biol Med 2005;39:949-59.

12. Ai HW, Hazelwood KL, Davidson MW, Campbell RE. Fluorescent protein FRET pairs for ratiometric imaging of dual biosensors. Nat Methods 2008;5:401-3.

13. Bullok K, Piwnica-Worms D. Synthesis and characterization of a small, membrane-permeant, caspase-activatable far-red fluorescent peptide for imaging apoptosis. J Med Chem 2005;48:5404-7.

14. Hug H, Los M, Hirt W, Debatin KM. Rhodamine 110-linked amino acids and peptides as substrates to measure caspase activity upon apoptosis induction in intact cells. Biochemistry 1999;38:13906-11.

15. Leytus SP, Melhado LL, Mangel WF. Rhodamine-based compounds as fluorogenic substrates for serine proteinases. Biochem J 1983;209:299-307.

16. Liu J, Bhalgat M, Zhang C, Diwu Z, Hoyland B, Klaubert DH. Fluorescent molecular probes V: a sensitive caspase-3 substrate for fluorometric assays. Bioorg Med Chem Lett 1999;9:3231-6.

17. Packard BZ, Toptygin DD, Komoriya A, Brand L. Profluorescent protease substrates: intramolecular dimers described by the exciton model. Proc Natl Acad Sci U S A 1996;93:11640-5.

18. Takemoto K, Nagai T, Miyawaki A, Miura M. Spatio-temporal activation of caspase revealed by indicator that is insensitive to environmental effects. J Cell Biol 2003;160:235-43.

19. Tung CH. Fluorescent peptide probes for in vivo diagnostic imaging. Biopolymers 2004;76:391-403.

20. Tyas L, Brophy VA, Pope A, Rivett AJ, Tavare JM. Rapid caspase-3 activation during apoptosis revealed using fluorescence-resonance energy transfer. EMBO Rep 2000;1:266-70.

21. Zhang HZ, Kasibhatla S, Guastella J, Tseng B, Drewe J, Cai SX. N-Ac-DEVD-N'-(Polyfluorobenzoyl)-R110: novel cell-permeable fluorogenic caspase substrates for the detection of caspase activity and apoptosis. Bioconjug Chem 2003;14:458-63.

22. Coppola JM, Ross BD, Rehemtulla A. Noninvasive imaging of apoptosis and its application in cancer therapeutics. Clin Cancer Res 2008;14:2492-501.

23. Kizaka-Kondoh S, Itasaka S, Zeng L, et al. Selective killing of hypoxia-inducible factor-1-active cells improves survival in a mouse model of invasive and metastatic pancreatic cancer. Clin Cancer Res 2009;15:3433-41.

24. Laxman B, Hall DE, Bhojani MS, et al. Noninvasive real-time imaging of apoptosis. Proc Natl Acad Sci U S A 2002;99:16551-5.

25. Shah K, Tung CH, Breakefield XO, Weissleder R. In vivo imaging of S-TRAIL-mediated tumor regression and apoptosis. Mol Ther 2005;11:926-31.

26. Jarvis WD, Turner AJ, Povirk LF, Traylor RS, Grant S. Induction of apoptotic DNA fragmentation and cell death in HL-60 human promyelocytic leukemia cells by pharmacological inhibitors of protein kinase C. Cancer Res 1994;54:1707-14.

27. Thompson JF, Hayes LS, Lloyd DB. Modulation of firefly luciferase stability and impact on studies of gene regulation. Gene 1991;103:171-7.

28. Kadri H, Matthews CS, Bradshaw TD, Stevens MF, Westwell AD. Synthesis and antitumour evaluation of novel 2-phenylbenzimidazoles. J Enzyme Inhib Med Chem 2008;23:641-7.

29. Law GH, Gandelman OA, Tisi LC, Lowe CR, Murray JA. Mutagenesis of solvent-exposed amino acids in Photinus pyralis luciferase improves thermostability and pH-tolerance. Biochem J 2006;397:305-12.

30. Loening AM, Fenn TD, Wu AM, Gambhir SS. Consensus guided mutagenesis of Renilla luciferase yields enhanced stability and light output. Protein Eng Des Sel 2006;19:391-400.

31. Williams JR, Little JB, Shipley WU. Association of mammalian cell death with a specific endonucleolytic degradation of DNA. Nature 1974;252:754-5.

32. Jackson RJ, Howell MT, Kaminski A. The novel mechanism of initiation of picornavirus RNA translation. Trends Biochem Sci 1990;15:477-83.

33. Jang SK, Davies MV, Kaufman RJ, Wimmer E. Initiation of protein synthesis by internal entry of ribosomes into the 5' nontranslated region of encephalomyocarditis virus RNA in vivo. J Virol 1989;63:1651-60.

34. Houdebine LM, Attal J. Internal ribosome entry sites (IRESs): reality and use. Transgenic Res 1999;8:157-77.

35. Concannon CG, Koehler BF, Reimertz C, et al. Apoptosis induced by proteasome inhibition in cancer cells: predominant role of the p53/PUMA pathway. Oncogene 2007;26:1681-92.

36. Grimm LM, Goldberg AL, Poirier GG, Schwartz LM, Osborne BA. Proteasomes play an essential role in thymocyte apoptosis. EMBO J 1996;15:3835-44.

37. Martinet W, de Meyer GR, Herman AG, Kockx MM. Reactive oxygen species induce RNA damage in human atherosclerosis. Eur J Clin Invest 2004;34:323-7.

38. Alexandrova A, Petrov L, Georgieva A, Kirkova M, Kukan M. Effects of proteasome inhibitor, MG132, on proteasome activity and oxidative status of rat liver. Cell Biochem Funct 2008;26:392-8.

39. Kikuchi S, Shinpo K, Tsuji S, et al. Effect of proteasome inhibitor on cultured mesencephalic dopaminergic neurons. Brain Res 2003;964:228-36.

40. Wu HM, Chi KH, Lin WW. Proteasome inhibitors stimulate activator protein-1 pathway via reactive oxygen species production. FEBS Lett 2002;526:101-5.

41. Han YH, Kim SH, Kim SZ, Park WH. Intracellular GSH levels rather than ROS levels are tightly related to AMA-induced HeLa cell death. Chem Biol Interact 2008;171:67-78.

42. Rote KV, Rechsteiner M. Degradation of microinjected proteins: effects of lysosomotropic agents and inhibitors of autophagy. J Cell Physiol 1983;116:103-10.

43. Nunez G, Benedict MA, Hu Y, Inohara N. Caspases: the proteases of the apoptotic pathway. Oncogene 1998;17:3237-45.

44. St Clair DK, Oberley TD, Ho YS. Overproduction of human Mn-superoxide dismutase modulates paraquat-mediated toxicity in mammalian cells. FEBS Lett 1991;293:199-203.

45. Beckman JS, Beckman TW, Chen J, Marshall PA, Freeman BA. Apparent hydroxyl radical production by peroxynitrite: implications for endothelial injury from nitric oxide and superoxide. Proc Natl Acad Sci U S A 1990;87:1620-4.

46. Foresti R, Sarathchandra P, Clark JE, Green CJ, Motterlini R. Peroxynitrite induces haem oxygenase-1 in vascular endothelial cells: a link to apoptosis. Biochem J 1999;339 (Pt 3):729-36.

47. Kooy NW, Royall JA. Agonist-induced peroxynitrite production from endothelial cells. Arch Biochem Biophys 1994;310:352-9.

48. Regoli F, Winston GW. Quantification of total oxidant scavenging capacity of antioxidants for peroxynitrite, peroxyl radicals, and hydroxyl radicals. Toxicol Appl Pharmacol 1999;156:96-105.

49. Dendorfer A, Heidbreder M, Hellwig-Burgel T, Johren O, Qadri F, Dominiak P. Deferoxamine induces prolonged cardiac preconditioning via accumulation of oxygen radicals. Free Radic Biol Med 2005;38:117-24.

50. Borg DC, Schaich KM. Prooxidant action of desferrioxamine: Fenton-like production of hydroxyl radicals by reduced ferrioxamine. J Free Radic Biol Med 1986;2:237-43.

51. Grune T, Reinheckel T, Davies KJ. Degradation of oxidized proteins in mammalian cells. FASEB J 1997;11:526-34.

52. Gao J, Yin DH, Yao Y, et al. Loss of conformational stability in calmodulin upon methionine oxidation. Biophys J 1998;74:1115-34.

53. Herve-Grepinet V, Veillard F, Godat E, Heuze-Vourc'h N, Lecaille F, Lalmanach G. Extracellular catalase activity protects cysteine cathepsins from inactivation by hydrogen peroxide. FEBS Lett 2008;582:1307-12.

54. Preston TJ, Muller WJ, Singh G. Scavenging of extracellular H2O2 by catalase inhibits the proliferation of HER-2/Neu-transformed rat-1 fibroblasts through the induction of a stress response. J Biol Chem 2001;276:9558-64.

55. Atochina EN, Balyasnikova IV, Danilov SM, Granger DN, Fisher AB, Muzykantov VR. Immunotargeting of catalase to ACE or ICAM-1 protects perfused rat lungs against oxidative stress. Am J Physiol 1998;275:L806-17.

56. Chorny M, Hood E, Levy RJ, Muzykantov VR. Endothelial delivery of antioxidant enzymes loaded into non-polymeric magnetic nanoparticles. J Control Release.

57. Angermuller S, Islinger M, Volkl A. Peroxisomes and reactive oxygen species, a lasting challenge. Histochem Cell Biol 2009;131:459-63.

58. Fatokun AA, Stone TW, Smith RA. Hydrogen peroxide mediates damage by xanthine and xanthine oxidase in cerebellar granule neuronal cultures. Neurosci Lett 2007;416:34-8.

59. Carbone DL, Doorn JA, Petersen DR. 4-Hydroxynonenal regulates 26S proteasomal degradation of alcohol dehydrogenase. Free Radic Biol Med 2004;37:1430-9.

60. Friguet B. Oxidized protein degradation and repair in ageing and oxidative stress. FEBS Lett 2006;580:2910-6.

61. Dalle-Donne I, Giustarini D, Colombo R, Rossi R, Milzani A. Protein carbonylation in human diseases. Trends Mol Med 2003;9:169-76.

62. Bota DA, Davies KJ. Lon protease preferentially degrades oxidized mitochondrial aconitase by an ATP-stimulated mechanism. Nat Cell Biol 2002;4:674-80.

63. Grune T, Merker K, Sandig G, Davies KJ. Selective degradation of oxidatively modified protein substrates by the proteasome. Biochem Biophys Res Commun 2003;305:709-18.

64. Link G, Pinson A, Hershko C. Iron loading of cultured cardiac myocytes modifies sarcolemmal structure and increases lysosomal fragility. J Lab Clin Med 1993;121:127-34.

65. Mak IT, Weglicki WB. Characterization of iron-mediated peroxidative injury in isolated hepatic lysosomes. J Clin Invest 1985;75:58-63.

66. Bellosillo B, Villamor N, Lopez-Guillermo A, et al. Complement-mediated cell death induced by rituximab in B-cell lymphoproliferative disorders is mediated in vitro by a caspase-independent mechanism involving the generation of reactive oxygen species. Blood 2001;98:2771-7.

67. Berneis K, Kofler M, Bollag W, Kaiser A, Langemann A. The degradation of deoxyribonucleic acid by new tumour inhibiting compounds: the intermediate formation of hydrogen peroxide. Experientia 1963;19:132-3.

68. Carmody RJ, Cotter TG. Signalling apoptosis: a radical approach. Redox Rep 2001;6:77-90.

69. Kim R, Emi M, Tanabe K, Murakami S, Uchida Y, Arihiro K. Regulation and interplay of apoptotic and non-apoptotic cell death. J Pathol 2006;208:319-26.

70. Mahmutoglu I, Kappus H. Oxy radical formation during redox cycling of the bleomycin-iron (III) complex by NADPH-cytochrome P-450 reductase. Biochem Pharmacol 1985;34:3091-4.

71. Muller I, Niethammer D, Bruchelt G. Anthracycline-derived chemotherapeutics in apoptosis and free radical cytotoxicity (Review). Int J Mol Med 1998;1:491-4.

72. Pei XY, Dai Y, Grant S. Synergistic induction of oxidative injury and apoptosis in human multiple myeloma cells by the proteasome inhibitor bortezomib and histone deacetylase inhibitors. Clin Cancer Res 2004;10:3839-52.

73. Shanafelt TD, Lee YK, Bone ND, et al. Adaphostin-induced apoptosis in CLL B cells is associated with induction of oxidative stress and exhibits synergy with fludarabine. Blood 2005;105:2099-106.

74. Sugioka K, Nakano M, Totsune-Nakano H, Minakami H, Tero-Kubota S, Ikegami Y. Mechanism of O2- generation in reduction and oxidation cycle of ubiquinones in a model of mitochondrial electron transport systems. Biochim Biophys Acta 1988;936:377-85.

75. Erdal H, Berndtsson M, Castro J, Brunk U, Shoshan MC, Linder S. Induction of lysosomal membrane permeabilization by compounds that activate p53-independent apoptosis. Proc Natl Acad Sci U S A 2005;102:192-7.

76. Kanzawa T, Germano IM, Komata T, Ito H, Kondo Y, Kondo S. Role of autophagy in temozolomide-induced cytotoxicity for malignant glioma cells. Cell Death Differ 2004;11:448-57.

77. Bykov VJ, Zache N, Stridh H, et al. PRIMA-1(MET) synergizes with cisplatin to induce tumor cell apoptosis. Oncogene 2005;24:3484-91.

78. Pitti RM, Marsters SA, Ruppert S, Donahue CJ, Moore A, Ashkenazi A. Induction of apoptosis by Apo-2 ligand, a new member of the tumor necrosis factor cytokine family. J Biol Chem 1996;271:12687-90.

79. Wiley SR, Schooley K, Smolak PJ, et al. Identification and characterization of a new member of the TNF family that induces apoptosis. Immunity 1995;3:673-82.

80. Gerber DE, Choy H. Cetuximab in combination therapy: from bench to clinic. Cancer Metastasis Rev;29:171-80.

81. Micallef IN, Kahl BS, Maurer MJ, et al. A pilot study of epratuzumab and rituximab in combination with cyclophosphamide, doxorubicin, vincristine, and prednisone chemotherapy in patients with previously untreated, diffuse large B-cell lymphoma. Cancer 2006;107:2826-32.

82. Skladanowski A, Konopa J. Adriamycin and daunomycin induce programmed cell death (apoptosis) in tumour cells. Biochem Pharmacol 1993;46:375-82.

83. Whitacre CM, Berger NA. Factors affecting topotecan-induced programmed cell death: adhesion protects cells from apoptosis and impairs cleavage of poly(ADP-ribose)polymerase. Cancer Res 1997;57:2157-63.

84. Ye J, Ding M, Leonard SS, et al. Vanadate induces apoptosis in epidermal JB6 P+ cells via hydrogen peroxide-mediated reactions. Mol Cell Biochem 1999;202:9-17.

85. Simizu S, Imoto M, Masuda N, Takada M, Umezawa K. Involvement of hydrogen peroxide production in erbstatin-induced apoptosis in human small cell lung carcinoma cells. Cancer Res 1996;56:4978-82.

86. Simizu S, Takada M, Umezawa K, Imoto M. Requirement of caspase-3(-like) protease-mediated hydrogen peroxide production for apoptosis induced by various anticancer drugs. J Biol Chem 1998;273:26900-7.

87. Martinvalet D, Dykxhoorn DM, Ferrini R, Lieberman J. Granzyme A cleaves a mitochondrial complex I protein to initiate caspase-independent cell death. Cell 2008;133:681-92.

88. Parreno M, Vaque JP, Casanova I, et al. Novel triiodophenol derivatives induce caspase-independent mitochondrial cell death in leukemia cells inhibited by Myc. Mol Cancer Ther 2006;5:1166-75.

89. Rudolf E, Rudolf K, Cervinka M. Selenium activates p53 and p38 pathways and induces caspase-independent cell death in cervical cancer cells. Cell Biol Toxicol 2008;24:123-41.

90. Watrach AM, Milner JA, Watrach MA, Poirier KA. Inhibition of human breast cancer cells by selenium. Cancer Lett 1984;25:41-7.

91. Pozo-Guisado E, Merino JM, Mulero-Navarro S, et al. Resveratrol-induced apoptosis in MCF-7 human breast cancer cells involves a caspase-independent mechanism with downregulation of Bcl-2 and NF-kappaB. Int J Cancer 2005;115:74-84.

92. Bey EA, Bentle MS, Reinicke KE, et al. An NQO1- and PARP-1-mediated cell death pathway induced in non-small-cell lung cancer cells by beta-lapachone. Proc Natl Acad Sci U S A 2007;104:11832-7.

93. Dragovich T, Gordon M, Mendelson D, et al. Phase I trial of imexon in patients with advanced malignancy. J Clin Oncol 2007;25:1779-84.

94. Maeda H, Hori S, Ohizumi H, et al. Effective treatment of advanced solid tumors by the combination of arsenic trioxide and L-buthionine-sulfoximine. Cell Death Differ 2004;11:737-46.

95. Magda D, Miller RA. Motexafin gadolinium: a novel redox active drug for cancer therapy. Semin Cancer Biol 2006;16:466-76.

96. Trachootham D, Zhou Y, Zhang H, et al. Selective killing of oncogenically transformed cells through a ROS-mediated mechanism by beta-phenylethyl isothiocyanate. Cancer Cell 2006;10:241-52.

97. Guppy M. The hypoxic core: a possible answer to the cancer paradox. Biochem Biophys Res Commun 2002;299:676-80.

98. Bjorkman U, Ekholm R. Hydrogen peroxide degradation and glutathione peroxidase activity in cultures of thyroid cells. Mol Cell Endocrinol 1995;111:99-107.

99. Ferrington DA, Sun H, Murray KK, et al. Selective degradation of oxidized calmodulin by the 20 S proteasome. J Biol Chem 2001;276:937-43.

100. Leclerc GM, Boockfor FR, Faught WJ, Frawley LS. Development of a destabilized firefly luciferase enzyme for measurement of gene expression. Biotechniques 2000;29:590-1, 4-6, 8 passim.

101. Sommer JM, Cheng QL, Keller GA, Wang CC. In vivo import of firefly luciferase into the glycosomes of Trypanosoma brucei and mutational analysis of the C-terminal targeting signal. Mol Biol Cell 1992;3:749-59.

102. Gould SG, Keller GA, Subramani S. Identification of a peroxisomal targeting signal at the carboxy terminus of firefly luciferase. J Cell Biol 1987;105:2923-31.

103. Loening AM, Wu AM, Gambhir SS. Red-shifted Renilla reniformis luciferase variants for imaging in living subjects. Nat Methods 2007;4:641-3.